Experimental optimization of *Cynara cardunculus* L. and sewage sludge pyrolysis in a fluidized bed reactor

by

Andrés Morato Godino

A dissertation submitted by in partial fulfillment of the requirements for the degree of Doctor of Philosophy in

Mechanical Engineering and Industrial Organization

Universidad Carlos III de Madrid

Advisors:

Antonio Soria Verdugo

Sergio Sánchez Delgado

January 2020

A mis padres, por su amor,
esfuerzo y sacrificio.

La verdadera ciencia enseña, por encima de todo, a dudar y a ser ignorante.

Miguel de Unamuno

Agradecimientos

Una vez alguien me dijo: "Siempre debes rodearte de personas de las cuales puedas aprender. Cuando veas que esto ya no es así, sabrás que ha llegado el momento de cambiar de aires". Me enorgullece saber que durante tres años tuve la oportunidad de seguir este consejo gracias a mi estancia en el departamento de Ingeniería Térmica y Fluidos de la Universidad Carlos III de Madrid. Allí no solo me rodeé de grandes profesionales, sino que conocí a un grupo humano extraordinario. Cada día fue una oportunidad para aprender tanto en lo profesional como en lo personal. Por ello, quiero dar las gracias a todo el grupo y aprovecho esta sección para nombrar a aquellos con los que pude tener más relación.

En primer lugar, me gustaría dar las gracias a Antonio y a Sergio, mis tutores de esta tesis. Gracias por darme la oportunidad de vivir esta experiencia y, sobre todo, por animarme a culminarla. Si bien es cierto que vuestra ayuda y tutela durante todos estos años han sido esenciales para la realización de esta tesis, mención especial merece vuestro apoyo emocional en mis momentos personales más duros. Quiero que sepáis que es algo que nunca olvidaré.

Este párrafo va dedicado a esos compañeros de despacho que he tenido durante esta etapa. María, la máquina con mayor rendimiento conocido, gracias por compartir agobios y risas casi a partes iguales. Pedro, gracias por nuestras largas charlas y reflexiones. Supiste quitarle hierro a situaciones cotidianas

con tus extrañas comparaciones. Rafa, la alegría y locura hecha persona. Gracias por tus bromas y carácter desenfadado. Me enseñaste que el tramo final de la tesis puede ser más ameno si se combina con tus temazos de YouTube. Marta, gracias por aguantar esos temazos y, sobre todo, por aguantarnos a nosotros. Como te he dicho muchas veces, tienes el cielo ganado.

Sigo con los compañeros de pasillo. Fer y Luismi, gracias por los buenos ratos y por vuestros consejos para afrontar tanto la tesis como la docencia. Espero que hayáis podido aprender algo de mí, como, por ejemplo, a sacar el balón jugado desde atrás. Dani, gracias por formarme para ser un digno sucesor en el cargo de 'LabMan'. Espero que te hayas sentido orgulloso de tu aprendiz. Patri, gracias por tus clemas, bridas, estaño, etc., y por nuestras acaloradas conversaciones de sobremesa. Edu, gracias simplemente por ser como eres, un gran tío al que no hace falta que se lo recuerden. Néstor, gracias por esos buenos ratos de laboratorio y por recordarme tantas veces lo bien que me quedan los pantalones estrechos. Acosta, gracias por todo lo aprendido y por aguantar mis reuniones con Soria. Cristina, gracias por tus enseñanzas y consejos en lo personal, pero sobre todo gracias de corazón por escucharme cuando más lo necesitaba. Fuiste un apoyo importante durante mi estancia en el departamento.

Las siguientes líneas van para Manolo, David e Isra. Gracias por estar siempre dispuestos a echarme una mano en todo lo necesario para sacar las instalaciones adelante. Agradeceros

también vuestro trato en lo personal. Sois un gran equipo y mejores personas.

No puedo dejar fuera de esta sección a mi otra familia. Luis, Mari Loli y Laura, gracias por estar a mi lado durante todos estos años, mostrando interés en todo lo que hacía y aconsejándome en los momentos de mayores dudas. Siempre me habéis recordado que terminar la tesis era algo necesario a pesar de estar trabajando en la industria. Finalmente, os hice caso y esto también es gracias a vosotros.

Cristina, gracias por ser mi compañera en todo el camino, viviendo mis alegrías, ilusiones, tristezas y agobios. Te agradezco todo tu apoyo, cariño y sinceras escuchas. Estoy seguro de que, tras todo lo que te he contado acerca de mis ensayos, tú misma habrías podido escribir parte de esta tesis, la cual considero también tuya.

Por último, gracias a mis padres. Sois un ejemplo a seguir, tanto en lo personal como en lo profesional. Admiro vuestra fuerza y dedicación, y os agradezco de corazón todo vuestro sacrificio para brindarme la posibilidad de formarme y llegar donde estoy hoy día. Sois el mejor referente que un hijo puede tener.

Acknowledgments

I would like to thank Prof. Dr. Leena Hupa and Dr. Oskar Karlström for allowing me to develop part of this thesis at the Inorganic Chemistry Department of Åbo Akademi University. My sincere thanks also go to Dr. Atte Aho for letting me use part of his laboratory material to perform my experiments and for his valuable guidance in their execution. I am also grateful to Luis Becerra for his help at the laboratory and our long conversations about football. Finally, thanks to the Board of the Johan Gadolin Process at Åbo Akademi University for considering me worthy of their scholarship to join again the Inorganic Chemistry Department. I wish my personal situation would have been different at that time so I could have enjoyed the mentioned scholarship and worked again in that fantastic group.

Published and Submitted Content

The results of this PhD thesis have been published in the following papers:

- Soria-Verdugo A., Goos E., Morato-Godino A., N. García-Hernando, Riedel U. Pyrolysis of biofuels of the future: Sewage sludge and microalgae - Thermogravimetric analysis and modelling of the pyrolysis under different temperature conditions. Energy Conversion and Management 2017; 138:261-272.

  DOI: 10.1016/j.enconman.2017.01.059.

  The material from this suorce is presented in chapter 2 of this dissertation.

  The material from this source included in this thesis is not singled out with typographic means and references.

- Soria-Verdugo A., Morato-Godino A., García-Gutiérrez L.M., García-Hernando N. Pyrolysis of sewage sludge in a fixed and a bubbling fluidized bed - Estimation and experimental validation of the pyrolysis time. Energy Conversion and Management 2017; 144:235-242.

  DOI: 10.1016/j.enconman.2017.04.062.

  The material from this suorce is included in chapter 3 of this dissertation.

  The material from this source included in this thesis is not singled out with typographic means and references.

- Morato-Godino A., Sánchez-Delgado S., García-Hernando N., Soria-Verdugo A. Pyrolysis of *Cynara cardunculus* L. samples – Effect of operating conditions and bed stage on the evolution of the conversion. Chemical Engineering Journal 2018; 351:371-38.

  DOI: 10.1016/j.cej.2018.06.114.

  The material from this suorce is included in chapter 4 of this dissertation.

  The material from this source included in this thesis is not singled out with typographic means and references.

The following conference paper is also an outcome of the thesis:

- Soria-Verdugo A., Morato-Godino A., García-Gutiérrez L.M., García-Hernando N. Pyrolysis of sewage sludge in a bubbling fluidized bed: determination of the reaction rate, In: 12th International conference on fluidized bed technology (CFB 12), Krakow, Poland; 2017.

  URL: http://www.cfb12.org/wp-content/uploads/2018/01/art83-PYROLYSIS-OF-SEWAGE-SLUDGE.pdf

  The material from this suorce is included in chapter 3 and 4 of this dissertation.

  Whenever material from this source is included in this thesis, it is single out with typographic means and an explicit reference.

Resumen

La presente tesis doctoral recoge un estudio experimental acerca de la pirólisis de lodos de depuradora y de *Cynara cardunculus* L. en reactores de lecho fluido. La composición de ambas biomasas fue determinada con un analizador elemental, mientras la cinética química de sus reacciones de pirólisis se estudió por medio de ensayos no isotermos realizados en un analizador termogravimétrico.

Se empleó una novedosa técnica de medida para investigar el proceso de pirólisis tanto de lodos de depuradora como de *C. cardunculus* L. Dicha técnica de medida consistió en colocar un reactor de lecho fluido a escala de laboratorio, dentro del cual se movía libremente la muestra de biomasa a convertir, para detectar la masa liberada durante el proceso de pirólisis. Por medio de la señal monitorizada por la balanza, se obtuvieron medidas precisas de la evolución temporal de la conversión de las muestras para distintas condiciones de operación. De este modo, se investigaron los efectos de la temperatura del lecho y la velocidad del gas inerte, y por lo tanto, el régimen del lecho, sobre el proceso de pirolisis para ambos biocombustibles. La influencia del tamaño de partícula en el proceso de pirólisis también se cuantificó para los ensayos en los que se emplearon muestras de *C. cardunculus* L. Además, se desarrolló un modelo de cinética química aparente capaz de estimar la evolución del grado de conversión durante el proceso de conversión para los casos en que los efectos de transferencia de calor son despreciables, es decir, aquellos

casos en los que la pirólisis se lleva a cabo para pequeñas partículas de biomasa en un lecho fluido burbujeante.

La pirólisis de *C. cardunculus* L. fue estudiada también mediante ensayos en una nueva instalación experimental, diseñada para obtener y analizar todos los productos provenientes del proceso de pirólisis. Los productos sólidos y líquidos se recogieron tras cada ensayo, mientras la cantidad y composición de los gases no condensables se determinó en tiempo real mediante analizadores de gases permanentes. El líquido obtenido se sometió a posteriores análisis para determinar su porcentaje de bio-oil y agua, la cual fue generada en su totalidad a través del proceso de pirólisis. Los efectos de la temperatura del lecho, la velocidad del gas inerte y el régimen del lecho sobre los productos de la pirólisis de *C. cardunculus* L. fueron evaluados. Además, los porcentajes de retención de carbono, oxígeno y azufre en los gases permanentes se determinaron para todas las condiciones de operación empleadas.

Abstract

In this PhD thesis the pyrolysis of sewage sludge and *Cynara cardunculus* L. in fluidized bed reactors is investigated experimentally. The composition of both biomass species was determined using an elemental analyzer and their pyrolysis kinetics was studied by means of non-isothermal pyrolysis measurements conducted in a thermogravimetric analyzer.

A novel experimental technique was used to analyze the pyrolysis of sewage sludge and *C. cardunculus* L. The procedure consisted in placing a lab-scale fluidized bed over a scale capable of detecting the mass released during the pyrolysis of a batch sample of biomass, while moving freely inside the bed. Based on the evolution of the mass monitored by the scale, accurate measurements of the time evolution of the pyrolysis conversion were obtained as a function of the operating conditions. The effect of bed temperature, inert gas velocity, and therefore the bed regime, on the pyrolysis process of both biomasses was evaluated. In the case of the *C. cardunculus* L. samples, the particle size was also varied to quantify its effect on the pyrolysis performance in the bed. An apparent kinetic model was also used to estimate the evolution of the reacted fraction during pyrolysis for the cases where heat transfer effects are negligible, i.e., for the pyrolysis of small biomass particles in a bubbling fluidized bed.

The pyrolysis of *C. cardunculus* L. was also analyzed using a different experimental facility where the products obtained

from the pyrolysis process can be collected and analyzed. The solid and liquid yields were collected, whereas the composition of the non-condensable gases was determined by online permanent gas analyzers. The liquid yield was further analyzed to distinguish between the bio-oil and the water generated during pyrolysis. The effect of bed temperature, inert gas velocity, and bed regime on the yields obtained from *C. cardunculus* L. pyrolysis was evaluated. The retention percentages of C, O, and S in the permanent gases were also measured for all the operating conditions tested.

Contents

List of Figures

List of Tables

CHAPTER
ONE

Introduction

Contents

1.1. Biomass as an energy source

The existence of human beings depends directly on the existence of solar energy. Without this energy source, life on Earth would not be possible. The energy produced by the Sun is the origin of the different renewable energy sources: solar energy, wind energy, hydroelectric, biomass, and others. The renewable energy resources are enough to satisfy the current world energy demand, without compromising the energy availability of future generations. However, human beings have used fossil fuels as the main energy source in the last century, consuming in 100 years a resource that needs tens of thousands of years to be regenerated. Therefore, it is only a question of political will and technological development turning towards new energy sources to preserve the balance on the planet and ensure future sustainability.

Biomass can be considered as one of the main actors in the pull of renewable energies, capable of reducing the consumption of fossil fuels and producing high-quality sustainable energy. The development of incipient technologies has several challenges associated that should be identified, evaluated, and overcome: scientific, technological, economic, and social. In addition, it should be considered that the rate of plant growth is limited by photosynthesis itself. In fact, only 0.023% of the solar energy incident on Earth is converted into biomass (Nogués et al., 2010). There is also a food sovereignty conflict when lands are used for energy crops instead of food production, which contributes to reduce

the famine at certain regions of the planet. Therefore, it is essential to focus the attention on the biomass produced as a waste of forest, agricultural, and industrial processes, obtaining a new energy source from waste recovery, while respecting the environment and human development.

Biomass refers to organic matter originated in a biological process, spontaneous or induced, usable as an energy source. Depending on its origin, biomass can be classified as follows: primary biomass, obtained directly from land for energetical purposes (e.g., *Cynara cardunculus* L., reed canary gross, etc.); secondary biomass, derived from a human activity and, thus, considered as residues (e.g., sewage sludge, black liquor from paper mills, agricultural and forest residues, etc.); and tertiary biomass, involving organic matter processed to improve their conversion to energy (e.g., bio-gas, bio-diesel, pellets, etc.).

1.2. Biomass conversion

Several procedures can be employed to convert biomass, such as physico-chemical, biochemical, and thermochemical processes (McKendry, 2002). Physico-chemical processes include the conversion of oleaginous biomass into vegetable oil by mechanical pressing, using either a hydraulic or a screw press. In contrast, bacteria or enzymes are employed in biochemical processes, such as digestion and fermentation, to break the bonds of biomass molecules during its conversion. Thermochemical processes consist in the chemical reaction of biomass at high temperature to generate useful end products. Temperature and the atmosphere surrounding the biomass

during the reaction play a relevant role in thermochemical processes. Depending on these parameters, thermochemical processes can be divided into six categories: combustion, co-firing, gasification, pyrolysis, torrefaction, and liquefaction (Patel et al., 2016).

Combustion is the exothermal chemical reaction of a fuel in an atmosphere rich in oxygen. The products obtained from combustion are useful heat and a solid mineral residue, corresponding to the fuel ash content. Combustion of solid fuels, and specifically biomass, is a complex process involving several subprocesses: drying of the wet material, devolatilization of the solid biomass, oxidation of the volatile gases released, and oxidation of the solid char produced (Williams et al., 2012). The applicability of biomass for combustion in industrial scale is limited by the biomass availability. Thus, co-firing of biomass with coal is normally selected for industrial applications to reduce the requirement of the biomass feedstock, meanwhile the combustion properties of pure coal are improved, for instance reducing the net carbon dioxide emissions associated with combustion or increasing the reactivity of the fuel (Sahu et al., 2014).

Gasification is the conversion of a solid fuel into a useful gaseous fuel by thermal reaction in an atmosphere poor in oxygen. The main product of gasification is the gaseous fuel, called syngas, which is mainly composed by carbon monoxide, hydrogen, and methane (Higman and van der Burgt, 2003). However, a solid residue and some condensable hydrocarbons are also obtained from biomass gasification. In

fact, tars should be removed from the gas flow rate if the syngas is to be used directly as a fuel in engines or turbines (Morin et al., 2018).

Pyrolysis consists in the reaction of a solid fuel taking place in an atmosphere free of oxygen. When temperature is increased in an inert atmosphere, thermal degradation of solid biomass occurs, releasing a gaseous flow, named pyrolysis vapors, and producing a solid residue, known as char (Bridgwater and Peacocke, 2000). The pyrolysis vapors released are composed of condensable and non-condensable gases, so that, a liquid bio-fuel can be generated from condensation of the non-permanent pyrolysis vapors.

Torrefaction of biomass is a special case of pyrolysis reaction, i.e., occurring in an oxygen-free atmosphere, carried out at a low temperature, ranging from 200 and 300 °C (Bates and Ghoniem, 2012). Torrefaction is focused on obtaining a high-quality solid fuel as a product. Thus, during the reaction at low temperature, only moisture and superfluous volatiles are released, generating a dry and homogeneous solid fuel called torrefied biomass. When operating with harmful biomasses, e.g., sewage sludge, torrefaction can be employed to erase the biological activity of the feedstock (Isemin et al., 2019).

Liquefaction involves the disintegration of the organic matter contained in biomass via decomposition of the solid in water at high temperature (Gollakota et al., 2018). Even biomass with high moisture contents can be converted by liquefaction, in contrast to the rest of thermochemical conversion

processes. Liquid bio-fuels are obtained as a main product of biomass liquefaction, after subjecting the feedstock to several sub-processes, including solvolysis, depolymerization, decarboxylation, hydrogenolysis, and hydrogenation (Demirbas, 2009).

1.3. Biomass pyrolysis

Among the thermochemical processes available to convert biomass, pyrolysis is a promising technology due to several benefits, such as counting on a reduced amount of pollutant emission associated with the conversion, using moderate temperatures between 300 and 600 °C, and obtaining high-quality products from the thermal degradation of the biomass.

1.3.1. Pyrolysis products

During pyrolysis, biomass particles are subjected to a heating process in an inert atmosphere. As a result, the chemical bonds conforming the solid fuel are dissociated by the action of thermal power, producing a mixture of gaseous compounds, named pyrolysis vapors, comprising a wide variety of molecules. In addition to the vapors, biomass pyrolysis also generates a solid residue, called char, which concentrates mainly the fixed carbon and ash contents of the original biomass. The way in which the biomass molecules fragment during pyrolysis depends on the kind of chemical bonds present in biomass and on the operating conditions under which the process occurs (Wampler, 1995). Pyrolysis

vapors can be cold down to condensate the non-permanent species, generating a liquid fuel, known as bio-oil, and a flow of permanent gases. Therefore, three different yields can be obtained from biomass pyrolysis: solid, liquid, and gas yields, comprising the biochar, bio-oil, and permanent gases, respectively. The amount and quality of each yield obtained from biomass pyrolysis are strongly affected by the operating conditions under which the thermal degradation process occurs (Guedes et al., 2018).

1.3.2. Effect of operating conditions on pyrolysis

Biomass composition and the pyrolysis reactor operating conditions affect both the distribution of the yields obtained after the thermal degradation of biomass and the quality of the biochar, bio-oil, and permanent gases generated. The main operating parameters affecting the yields, in addition to biomass composition, are reactor temperature, biomass heating rate, pyrolysis vapors residence time, biomass particle size, biomass feeding rate, and reaction time (Guedes et al., 2018).

Reactor temperature controls the thermal energy available to decompose biomass, affecting strongly the yields obtained from pyrolysis. The solid yield is reduced for increasing reactor temperatures, as a consequence of the extra thermal power existing to beak solid biomass bonds (Luo et al., 2004). However, the formation of permanent gases is enhanced for high temperatures, whereas the maximum generation of bio-

oil is obtained for moderate temperatures between 450 and 550 °C (Guedes et al., 2018). For reactor temperatures above 600 °C, secondary cracking reactions of the condensable molecules in the pyrolysis vapors occur, reducing the liquid yield obtained in favor of the permanent gas production (Pütung et al., 2002). The optimal reactor temperature for which bio-oil production is maximized may depend on the biomass composition and other operating conditions (Fonts et al., 2008).

Regarding the heating rates of biomass particles, the release of pyrolysis vapors is promoted by high heating rates due to a fast thermal decomposition of biomass (Akhtar and Amin, 2012). High heating rates enhance also the production of liquid bio-oil by limiting the time available for secondary cracking reactions of the condensable molecules contained in pyrolysis vapors (Strezov et al., 2003). In addition, the water content of the liquid yield obtained after condensation of the pyrolysis vapors is also reduced for fast heating rates, contributing to improve the quality of the bio-oil generated (Ozbay et al., 2006). However, the effect of the heating rate on the pyrolysis yields is also influenced by biomass composition (Bridgwater, 2012).

Residence time of pyrolysis vapors in the high temperature zone of the reactor is a relevant parameter controlling the amount of bio-oil and permanent gases generated. The production of bio-oil is enhanced by short residence time, which limits the occurrence of secondary reactions, such as thermal cracking and repolymerization, for the condensable

species of the pyrolysis vapors (Olukcu et al., 2002). In fact, residence time of pyrolysis vapors indicates the pyrolysis method employed. High biomass heating rates and short residence times of pyrolysis vapors of around 1-5 s are usually employed in fast pyrolysis processes (Bridgwater, 2012), whereas residence times of approximately 5-30 min are used in conventional pyrolysis (Yan et al., 2011). Therefore, regarding the bio-oil generation, fast pyrolysis is a more convenient conversion method than conventional pyrolysis.

Heat transfer effects inside biomass particles affect the yields obtained from pyrolysis. Therefore, biomass particle size is an important parameter for biomass pyrolysis, especially considering the low thermal conductivity typical of biomass. Small biomass particle size is preferred to guarantee a fast and uniform heating, deriving in fast heating rates that promotes the generation of bio-oil (Guedes et al., 2018). However, obtaining fine biomass particles may involve high costs of grinding and may even promote their own removal from the reactor by the inert gas (Stammbach et al., 1989). In contrast, coarse biomass particles would be subjected to uneven heating due to conduction heat transfer inside the particles.

In continuous pyrolysis applications, biomass feeding rate also affects the yields obtained. Depending on the reactor configuration, biomass feeding rate can affect the residence time of biomass and pyrolysis vapors, and the catalytic effect of the char generated from pyrolysis (Fonts et al., 2012). The generation of bio-oil is enhanced by fast feeding rates, due to an increase of the pyrolysis vapors released, which reduces

their residence time (Guedes et al., 2018). In contrast, low feeding rates promote the formation of permanent gases as a result of the secondary cracking reactions to which the condensable fraction of the pyrolysis vapors are subjected due to longer residence times.

The residence time of biomass particles in the reactor controls the pyrolysis reaction time. This is a critical factor in reactor´s design and it could vary substantially for different reactor configuration (Guedes et al., 2018). The generation of bio-oil from biomass pyrolysis can be diminished by long reaction times due to the existence of secondary reactions for the pyrolysis vapors (Bartoli et al., 2016). However, the optimal reaction time to maximize the production of bio-oil depends on the composition of the biomass pyrolyzed (Tsai et al., 2007; Açikalin et al., 2012).

The composition of biomass may vary significantly for different species, and this composition also affects the pyrolysis process and the products obtained. Lignocellulosic biomass is mainly composed of hemicellulose, cellulose, lignin, and small fractions of inorganic matter, in concentrations depending on the biomass considered. Compared to hemicellulose and cellulose, lignin is characterized by lower pyrolysis conversion rates, resulting in larger solid yields (Akhtar and Amin, 2012). For non-lignocellulosic biomass, such as sewage sludge, the composition is even more heterogeneous and may depend on the purification treatments employed and wastewater origin (Fonts et al., 2009).

1.3.3. Pyrolysis reactors

A broad variety of reactors can be used to hold biomass pyrolysis reactions. Each reactor technology has advantages and drawbacks considering the control and range of variability of pyrolysis operating parameters.

Fixed bed reactors are composed by a bed of small particles through which an inert gas at low velocity percolates in the vertical direction. The presence of a large number of small solid particles implies a high thermal inertia and great heat transfer surface for these reactors; however, the static character of the solid particles involves a limited heating rate for biomass particles (Chen et al., 2014a). In contrast, by increasing the gas velocity, the small solid particles conforming the bed can be fluidized and bubbles appear in the bed, resulting in a bubbling fluidized bed reactor. The presence of bubbles in the reactor increases substantially the mixing, resulting in high heating rates to the biomass particles in addition to the high thermal inertia and heat transfer surface of fixed bed reactor (Kunii and Levenspiel, 1969). Another variety of bed reactor is the conical spouted bed reactor, where a shallow bed of broader particles is fluidized forming a spout-annulus interface and a fountain of particles at center of the bed surface. A lower segregation of biomass particles is attained in a conical spouted bed reactor compared to fixed and fluidized beds (Olazar et al., 2009).

In rotating cone reactors, the centrifugal force generated by the vessel rotation is used to impose an ascending spiral

motion to biomass particles fed at the bottom of the reactor. These reactors are characterized by fast heating rates and short biomass and vapors residence times, allowing the operation even without carrier gas to reduce costs and increase the concentration of the pyrolysis products (Wagenaar et al., 1994).

Ablative reactors consist in a hot surface over which biomass is heated, typically by the action of pressure and a relative motion between biomass and the hot surface. The surface temperature, relative velocity biomass-surface, and pressure exerted on the biomass play an important role in ablative pyrolysis of biomass. In fact, the heating rate of biomass particles is not limited by heat transfer in these reactors due to the pressure applied on the biomass particles against the hot surface (Bridgwater, 2012).

A hot steel cylinder into which biomass is fed is used in rotary kiln reactors, which may be slightly inclined to control the residence time of biomass. Slow rotation is induced to the cylinder to improve biomass mixing. The main advantage of rotary kiln reactors is the possibility to pyrolyze heterogeneous biomass, reducing the pre-treatment costs of the feedstock; however, low heating rates are attained in these reactors (Chen et al., 2014a). A different alternative to cylindrical reactor is an auger or screw reactor, where biomass is transported along a hot cylinder by a rotating screw. The rotation of the screw improves biomass mixing and heat transfer from the walls, permitting also an accurate control of biomass residence time (Dhyani and Bhaskar, 2018).

Nevertheless, biomass heating rates are still low in auger/screw reactors compared to other technologies.

Drop tubes or free-fall reactors are a simple design of pyrolysis reactor. They consist only in a hot vertical tube into which biomass is fed to the top and falls freely inside. The simple design, with no moving parts, facilitates the operation of these reactors, which is reliable and robust (Ellens and Brown, 2012). The residence time of biomass is controlled by the length of the tube; however, low biomass particle size is required for these reactors.

Some recent designs of pyrolysis reactors allowing rapid heating rates and/or accurate operating temperature of biomass particles comprise microwave, vacuum, plasma, and Curie-point reactors. In microwave reactors, biomass is heated up in a microwave cavity, typically mixed with a highly microwave absorbent material such as particulate carbon. An efficient heating of the biomass in short reaction times is attained in microwave reactors (Baghurst and Mingos, 1992). Vacuum reactors heat biomass particles by direct contact with hot surfaces in a vacuum chamber, where the residence time of pyrolysis vapors is very low to prevent secondary cracking reactions (Roy et al., 1999). Plasma reactors use electricity to produce plasma around the biomass particles to be pyrolyzed. The energy consumption of these reactors is high, but they produced high-quality permanent gases due to the elevated temperature and high energy density generated in plasma pyrolysis (Yaman, 2004). In contrast, Curie-point reactors offer a very accurate

temperature of operation based on heating a ferromagnetic material by eddy currents induced by radio frequency up to its Curie temperature. High heating rates and very accurate and reliable temperature control are the main advantages of Curie-point reactors (Fan and He, 2016).

Compared to other reactors, the cost of operation and operating conditions provided by fluidized bed reactors are optimal for bio-oil production from biomass pyrolysis.

1.4. Fluidization technology

Fluidized bed reactors have been widely used in the last decades in many industrial applications including thermochemical conversion, catalytic reactions, solids coating, or solids drying due to their high solid mixing and heating rates (Adánez et al., 2018; Li et al., 2018; Haron et al., 2017). However, the phenomenon of fluidization is a complex process that has been described and deeply studied in the last century by many researchers. In this thesis, the description of the fluidization phenomenon and its applications made by Davidson and Harrison (1963), Davidson and Harrison (1971), and Kunii and Levenspiel (1969) have been used as the reference works.

When a low gas flow is forced to cross upwards through a bed of static particles, a pressure loss is generated across the bed. At this moment, two main forces appear over the particles: the drag force caused by the upwards moving gas and the weight of the particles. When the gas velocity increases, the pressure

drop across the bed also increases, reaching a maximum when the pressure loss can support the weight of the particles. At this moment, the bed is at *incipient fluidization* or at *minimum fluidization*, being the velocity of the gas the minimum fluidization velocity, one of the most important operation parameters in fluidized beds. Any further increase of the gas velocity promotes a vertical expansion of the bed.

The use of fluidized beds can be extended to multiple disciplines due to their good operating properties in terms of temperature control, heat transfer, continuous operation, and catalytic reactions. These favourable characteristics, such as high solid mixing rate and homogeneous temperature, present fluidized beds as an excellent technology for heat transfer applications between the gas phase and the solid phase (Kunii and Levenspiel, 1969). The high heat transfer coefficients provided by fluidized beds allow also their use to hold reactions of solid fuels, where heat transfer between the bed and the fuel particles immersed in it is relevant. In addition, fluidized beds are also suitable for large scale operation.

However, fluidized bed reactors have some disadvantages, which should be considered to ensure a proper operation of the reactor. First, the homogeneous temperature inside the reactor limits the use of fluidized bed for processes where temperature gradients are required. Secondly, the quality of fluidization of the particles conforming the fluidized bed is strongly influenced by the type of particles and on the changes promoted over them during the operation. The

vigorous movement of the particles within the fluidized bed may cause the breakage and the attrition of the particles, promoting changes in the particle size and their sphericity, which may affect the fluidization quality (Zhang et al., 2016). Besides, some processes can promote the agglomeration of the particles within the bed. This agglomeration process affects the fluidization quality and can also produce the defluidization of the reactor (Gómez-Hernández et al., 2012). Finally, the generation of different types of bubbles inside the reactor, depending on the excess of gas and the type of particles, can cause problems of operation due to the circulation of gas through the bed without interaction with the solid particles (Villanueva-Chávez and Bizzo, 2019).

One of the most important challenges in fluidized bed reactors is the fluidization quality, closely related to the type of particles and the excess gas inside the reactor. The quality of fluidization is influenced by the size and density of the solid particles, as well as by the particles size distribution. In general, fine particles are difficult to fluidize and even more if they are sticky particles. In these cases, vibration can be induced to the bed to guarantee proper fluidization conditions (Kaliyaperumal et al., 2011). In addition, higher gas velocities and the kinetic energy contained in the gas inlet jets can help to keep the fluidization of the reactor with this type of particles. At the opposite extreme, fluidization of large particles is also complex. The bumping, spouting, and slugging effects can cause structural damages in large reactors. The quality of the fluidization with this type of

particles can be substantially improved by adding a low number of small particles (Estiati et al., 2019).

As stated above, the type of particles used as bed material in the fluidized bed reactor affects the quality of the fluidization. Geldart (1973) established a classification of particles according to their size and density, as shown in Figure 1.1.

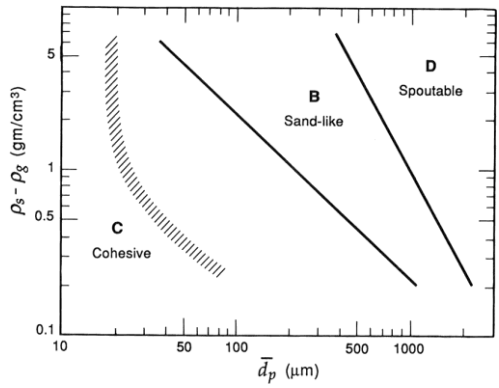

Figure 1.1. Geldart particle classification (adapted from Geldart, 1973).

The main characteristics of the fluidization of each particle type are:

- Geldart C particles: the finest and the most cohesive particles, with high values of inter-particles attraction forces, what makes their fluidization extremely difficult.
- Geldart A particles: particles of small size and low density. The fluidization of these particles is reasonably simple and can be initiated at low gas velocities. The generated bubbles are small even at high values of excess gas.

- Geldart B particles: larger particles than Geldart A. The fluidization of these particles is not complex, generating large bubbles that grow with the excess gas velocity and with the distance to the distributor. For this type of particles, bubbles appear once the minimum fluidization state is reached.
- Geldart D particles: large and very dense particles, quite difficult to fluidize. The fluidization generates large exploding bubbles and severed channelling or spouted beds when the gas distribution is not homogeneous along the distributor.

In most applications of fluidized beds, the particles used are Geldart B particles. This type of particles shows a different behaviour in the fluidized bed depending on the gas velocity. Figure 1.2 represents a schematic of the bed behaviour at different excess gas velocities.

- Fixed bed: state of the bed when gas with a low velocity is circulated through the dense phase and merely percolates through the voids of the statics particles.
- Incipient fluidization or minimum fluidization bed: state in which the drag force generated by the gas velocity counteracts the gravitational force acting on the particles, which are suspended by the upward flowing gas.
- Bubbling fluidized bed: state of the bed in which the excess of the gas over the minimum fluidization generates bubbles, promoting a vigorous movement of solids inside the bed. At this regime, the volume of the

expanded bed is only slightly larger than the volume of the bed at incipient fluidization.

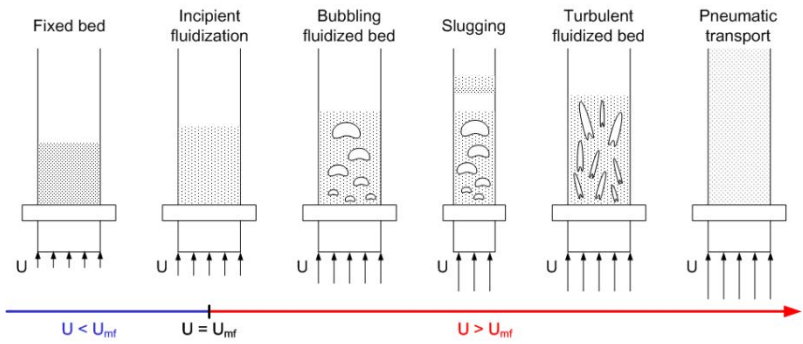

Figure 1.2. Different bed regimes for Geldart B particles as a function of the gas velocity (adapted from Kunii and Levenspiel, 1969).

- Slugging: this is a special case of bubbling fluidized bed, where for deep enough beds of small diameter, the bubbles coalescence generates large bubbles compared to the bed diameter. Bubbles occupy almost the whole reactor section.
- Turbulent fluidized bed: when the gas velocity exceeds a certain value, the terminal velocity of the particles is overcome. At this time, the upper surface of the bed disappears and groups of particles and voids of gas of different sizes can be observed.
- Pneumatic transport: even higher values of excess gas promote the transport of particles outside the bed, generating a diluted distribution of particles inside the reactor.

1.5. Scope of the Thesis

This PhD thesis presents an experimental work on the pyrolysis of two biomasses: sewage sludge and *Cynara cardunculus* L. The thesis has been organized in six chapters. The introduction of the work is provided in Chapter 1. The results of the dissertation are presented from Chapter 2 to Chapter 5 as independent works with their own abstract, introduction, and nomenclature. Chapter 6 summarizes the conclusions of the thesis.

Chapter 2 shows the characterization of sewage sludge and *C. cardunculus* L. samples. Compositional and kinetic analyses were conducted in elemental and thermogravimetric analyzers for both fuels. The large volatile content obtained for the two biomass samples justifies their election for pyrolysis research. The kinetic parameters of the pyrolysis of sewage sludge and *C. cardunculus* L., i.e., the activation energy and pre-exponential factor, obtained from pyrolysis measurements in a TGA were reported.

In Chapter 3, a facility specifically designed for the pyrolysis tests was used to measure the mass remaining in the reactor during the thermochemical conversion of sewage sludge samples. A novel measuring technique consisting in installing the whole reactor over a precision scale was used. Different reactor temperatures, gas velocities, and bed regimes were tested in this first experimental campaign to evaluate the effect of these parameters on the evolution of the conversion, obtaining accurate measurements of the pyrolysis time. In

addition, an apparent kinetics model was proposed and compare to the experimental results. The model was found to predict accurately the pyrolysis time provided that the sewage sludge pyrolysis occurs under the bubbling fluidized bed regime.

Chapter 4 studies the pyrolysis of *C. cardunculus* L. samples using the same facility and experimental technique employed in Chapter 3. The research is focused on the effect of different parameters on the evolution of the conversion. The selected parameters for this experimental campaign were the reactor temperature, gas velocity, bed regime, and biomass particle size. The optimal operating conditions to maximize the pyrolysis conversion were presented, depending on the bed regime selected for the operation. The process was also described by the apparent kinetic model, which is only valid for the small biomass particles pyrolyzing in a bubbling fluidized bed.

Chapter 5 presents an experimental study of *C. cardunculus* L. pyrolysis using a different approach. A different facility was used to collect the mass of each pyrolysis product, i.e., solid residue, liquid, and permanent gases. The experimental campaign was conducted by the PhD candidate in Åbo Akademi University (Turku, Finland) during a 3-months research stay. The influence of reactor temperature, gas velocity, and bed regime on the yields and their composition was evaluated. Liquid phase was subjected to further analysis to distinguish between bio-oil and water generated, and the

retention percentages of C, O, and S in the permanent gases were determined.

Finally, the main conclusions of the thesis are summarized in Chapter 6.

CHAPTER
TWO

Biomass characterization and determination of the pyrolysis kinetic parameters

Contents

Abstract

The biomasses employed in the following chapters of this thesis, namely *Cynara cardunculus* L. and sewage sludge, were characterized performing proximate and ultimate analyses and heating value tests. The pyrolysis process of both biomass species was investigated separately, by means of non-isothermal thermogravimetric analysis. The simplified Distributed Activation Energy Model (DAEM) was employed to obtain the pyrolysis kinetic parameters of the samples, i.e., the activation energy *E* and the pre-exponential factor *A*. Nine different pyrolysis tests at different constant heating rates were conducted for each sample in a thermogravimetric analyzer (TGA) to obtain accurate values of the pyrolysis kinetic parameters when applying simplified DAEM. The accurate values of the kinetic parameters that characterize the pyrolysis reaction of *C. cardunculus* L. and sewage sludge were reported. The activation energy and pre-exponential factor for the *C. cardunculus* L. samples are around 150 kJ/mol and 10^{12} s^{-1} respectively, for most of the pyrolysis conversion, increasing in both cases at the end of the process. In contrast, values ranging from 200 to 400 kJ/mol were obtained for the sewage sludge activation energy, and from 10^{15} to 10^{25} s^{-1} for its pre-exponential factor. From the kinetic parameters obtained, a representative value for the rate coefficient of pyrolysis of both samples was calculated, resulting in a rate coefficient of 4.73 min^{-1} and 2.03 min^{-1} for *C. cardunculus* L. and sewage sludge, respectively.

2.1. Introduction

A continuous growth of the world population has occurred during the last 50 years, resulting in an increase of the primary energy consumption. Currently, more than 80% of the total primary energy consumption is based on fossil fuels, which are responsible for more than 98% of the carbon dioxide emissions to the atmosphere, causing the current global warming problems (Demirbas and Demirbas, 2011). Therefore, there is a need to evaluate the potential of different alternative fuels capable of substituting fossil fuels, with lower associated pollutant emissions. Two of the most promising alternative fuels, due to entirely different reasons, are sewage sludge and *C. cardunculus* L.

Sewage sludge is the residue produced during the treatment of industrial or municipal wastewater. The main ways of disposing of sewage sludge nowadays can be divided into three applications: landfill, agricultural use, and incineration or thermochemical conversion (Fonts et al., 2009). Nevertheless, the European regulations try to limit the amount of sewage sludge employed for landfill. Concerning the agricultural use, sewage sludge contains organic matter, nitrogen, and phosphorus, making them suitable as a fertilizer. However, the sludge may also concentrate heavy metals and pathogens, which could cause significant environmental problems. In contrast, the thermochemical conversion of sewage sludge (Manara and Zabaniotou, 2012) presents several benefits, such as the possibility to recover

energy (Rulkens, 2008), the reduction of the residue volume by 70%, and the thermal destruction of pathogens (Fytili and Zabaniotou, 2008). Furthermore, the population growth in urban areas causes also the problem of an increase in the sewage sludge production. Therefore, the thermochemical conversion of sewage sludge with energy recovery might solve the issue of the increase in residues produced due to the population growth, contributing to a reduction of the dependence on fossil fuels.

Among the potential replacement for fossil fuels, biodiesel is gaining importance in applications such as transport, where other possible substitute fuels count on a limited applicability. The production of biodiesel has been based on different crops, causing social problems as the dilemma regarding the risk of diverting farmland or crops for biofuels production to the detriment of the food supply. Among these crops, *C. cardunculus* L. is a perennial plant growing under hot weather conditions and low rainfall in Mediterranean climates (Gominho et al., 2018). This energy crop permits an excellent biomass production, up to 14-20 $t \cdot yr^{-1} \cdot Ha^{-1}$, with a low cost associated (Fernández, 1998; Shatalov and Pereira, 2011). Based on a thermo-economic study, Torres et al. (2013) concluded that *C. cardunculus* L. is a feasible alternative for biodiesel production, capable of replacing part of the liquid fuel consumed by transport in Southern Europe.

In comparison to other thermochemical conversion processes, such as combustion or gasification, pyrolysis presents the advantage of producing mainly an easy to store and transport

liquid product, in particular for those fuels characterized by high volatile matter and low fixed carbon content, like sewage sludge and *C. cardunculus* L. (Marcilla et al., 2013). Pyrolysis was found to be the optimal thermochemical process for sewage sludge by Samolada and Zabaniotou (2014), due to its favorable energy balance, material recovery, and zero-waste conversion. Several methods have been employed in the literature to model the pyrolysis process of biomass, such as the single step model (Coats and Redfern, 1964), the three pseudo-components model (Li et al., 2008), the sectional approach model (Lin et al., 2013), or the Distributed Activation Energy Model (DAEM) (Vand, 1943). Miura (1995) and Miura and Maki (1998) proposed a simplification for DAEM to easily obtain the activation energy and the pre-exponential factor of a sample from different thermogravimetric analysis (TGA) tests. This simplified DAEM has been employed, achieving a proper agreement with experimental measurements, for a wide variety of samples, such as coal (Günes and Günes, 2008), charcoal (Várghegyi et al., 2002), polymers (Wanjun et al., 2005), oil shale (Wang et al., 2009), medical waste (Yan et al., 2009), sewage sludge (Soria-Verdugo et al., 2013), microalgae (Ceylan and Kazan, 2015; Yang et al., 2014), and several different types of biomass (Hu et al., 2007; Cai and Liu, 2008; Cai et al., 2014; Sonobe and Worasuwannarak, 2008; Shen et al., 2011; Soria-Verdugo et al., 2014).

In this chapter, the pyrolysis of the *C. cardunculus* L. and sewage sludge are investigated separately, by means of non-

isothermal thermogravimetric analysis. Independent TGA tests of both biomasses under different constant heating rates were conducted and the experimental results were employed as input data to apply the simplified Distributed Activation Energy Model. Nine different TGA curves were employed for both the *C. cardunculus* L. and the sewage sludge samples to obtain accurate values of pyrolysis kinetic parameters, i.e., the activation energy and the pre-exponential factor, of the samples when applying simplified DAEM (Soria-Verdugo et al., 2015). The accurate values of the kinetic parameters of the pyrolysis reactions of *C. cardunculus* L. and sewage sludge are reported, and these values are employed to determine representative values for their pyrolysis rate coefficient.

2.2. Mathematical model

The simplified Distributed Activation Energy Model was applied to obtain accurate values of the kinetic parameters of pyrolysis of *C. cardunculus* L. and sewage sludge, i.e., activation energy E and pre-exponential factor A. The activation energy is the energy needed to activate the pyrolysis reactions and the pre-exponential factor expresses the empirical temperature dependence of the reaction rate coefficient k (Soustelle, 2010), which considering the Arrhenius law can be expressed as follows:

$$k = A \cdot \exp\left(-\frac{E}{RT}\right). \tag{2.1}$$

DAEM considers a complex solid fuel as a mixture of components, which decompose following first-order reactions. Thus, a large number of independent irreversible first-order reactions occur simultaneously with different associated activation energies. The reacted fraction V/V^* in a pyrolysis process can be determined as follows (Miura, 1995):

$$1-\frac{V}{V*}=\int_0^{\infty}\exp\left(-A\int_0^t e^{-E/RT}dt\right)f\left(E\right)\cdot dE \tag{2.2}$$

where V is the volatile matter content released at time t, V^* is the total volatile matter content of the sample, A is the pre-exponential factor corresponding to the activation energy E, R is the universal gas constant, and $f(E)$ is the probability density function of the activation energy. The exponential term in Eq. (2.2) is the so-called ϕ function:

$$\phi\left(E,T\right)=\exp\left(-A\int_0^t e^{-E/RT}dt\right) \tag{2.3}$$

which can be written as a function of temperature instead of time considering a constant heating rate, $\beta = \mathrm{d}T/\mathrm{d}t$:

$$\phi\left(E,T\right)=\exp\left(-\frac{A}{\beta}\int_0^T e^{-E/RT}dT\right) \tag{2.4}$$

The ϕ function is typically approximated by a step function at a value of the activation energy $E = E_a$, obtaining for the reacted fraction:

$$\frac{V}{V*} = 1 - \int_{E_a}^{\infty} f(E) \cdot dE = \int_{0}^{E_a} f(E) \cdot dE \tag{2.5}$$

Miura (1995) proposed a value for $\phi(E_a,T) = 0.58$, which has been employed for several different types of mineral carbon and biomass samples, obtaining good agreement with experimental measurements. Using the approximation of Coats and Redfern (Coats and Redfern, 1964) for the temperature integral in the ϕ function, the following expression is obtained:

$$\phi(E,T) \approx \exp\left(-\frac{ART^2}{\beta E} e^{-E/RT} \right) \tag{2.6}$$

and using the value proposed by Miura (1995) of $\phi(E_a,T) = 0.58$, the widely used Arrhenius equation for the pyrolysis of a sample under a constant heating rate β can be derived:

$$\ln\left(\frac{\beta}{T^2} \right) = \ln\left(\frac{AR}{E} \right) + 0.6075 - \frac{E}{R}\frac{1}{T} \tag{2.7}$$

Based on this Arrhenius equation, Miura and Maki (1998) proposed a method to determine the activation energy E and the pre-exponential factor A of a sample from TGA curves of the pyrolysis process obtained for different heating rates β.

2.3. Materials and Methods

The pyrolysis tests were performed in a thermogravimetric analyzer TGA Q500 from TA Instruments. A nitrogen

flowrate of 60 ml/min was supplied to the furnace to guarantee the existence of an inert atmosphere. The temperature profile programmed to the TGA consisted of two processes occurring in series, first a drying process of the sample at 105 °C and then the pyrolysis process taking place when increasing the temperature of the sample in an inert atmosphere up to 800 °C. Nine different pyrolysis tests were carried out, as proposed by Soria-Verdugo et al. (2015), using heating rates of 10, 13, 16, 19, 22, 25, 30, 35, and 40 K/min. These heating rates are low compared to industrial applications, nevertheless, similar results were obtained by Soria-Verdugo et al. (2014) when applying simplified DAEM to TGA curves obtained at higher heating rates, up to 200 K/min.

The sensitivity of the TGA mass measurement is 0.1 μg and the weighing precision is ±0.01%. The dynamic baseline drift during a heating process of an empty platinum pan from 50 to 1000 °C at 20 K/min is lower than 50 μg with no baseline subtraction. The TGA temperature accuracy during an isothermal process is ±1 °C and the temperature precision is ±0.1 °C. A mass of 10.0±0.5 mg of sample, sieved previously under 100 μm, was employed in the pyrolysis measurements in the TGA to reduce heat and mass transfer effects in the sample (Hu et al., 2007; Mani et al., 2010). Each pyrolysis test was conducted three times to guarantee the repeatability of the process, obtaining differences lower than 1%, and a blank experiment was also run for each heating rate to exclude buoyancy effects.

The sewage sludge was obtained from the municipal sewage treatment plant of Loeches (Madrid, Spain) in February 2016. The sludge was taken after the pre-drying process at 80 °C in a fluidized bed in the sewage treatment plant. The *C. cardunculus* L. was obtained from pellets. The samples of *C. cardunculus* L. and sewage sludge were characterized by proximate and elemental analyses. The proximate analysis was performed in the TGA Q500 from TA Instruments to determine the moisture, ash, volatile matter, and fixed carbon contents of the samples. The moisture content was characterized as the mass released by the sample at 105 °C. The ash content was determined as the percentage of mass remaining after a heating of the sample up to 550 °C, supplying the furnace with an oxygen flow rate of 60 ml/min using a heating rate of 10 K/min, followed by an isothermal process at 550 °C until the mass of the sample stabilized. The volatile matter content of the samples was measured as the percentage of mass released by the sample during a heating process at a heating rate of 10 K/min from 105 to 900 °C and an isothermal process at 900 °C in an inert atmosphere, obtained supplying 60 ml/min of nitrogen to the furnace, until the mass of the sample stabilized. Finally, the fixed carbon content was obtained from the difference between these two procedures.

The elemental analysis of the sample was carried out in a LECO TruSpec CHN analyzer, where the carbon and hydrogen contents of the sample are measured using an infrared absorption detector for the exhaust gases obtained

from a complete combustion of the sample. The nitrogen content is determined conducting the exhaust gases through a thermal conductivity cell. The carbon and nitrogen contents are measured with a precision of ±0.5%, while the precision of the measurement of the hydrogen content is ±1%. Heating value tests of the samples were also conducted in an isoperibolic calorimeter Parr 6300 with an instrument precision of 0.1% relative standard deviation. Control limits were based on 99% confidence (3 sigma) values. The calorimeter has a temperature resolution of 0.0001 °C.

The results obtained from the proximate analysis, the ultimate analysis and the heating value tests of the *C. cardunculus* L. and sewage sludge samples are reported in Table 2.1. Table 2.1 shows that the volatile matter content of both *C. cardunculus* L. and sewage sludge is high, and therefore the pyrolysis study of these biofuels is justified. Concerning the elemental analysis, the carbon and hydrogen contents of sewage sludge are higher than those of *C. cardunculus* L. samples, however, due to the high ash content of sewage sludge, the higher heating value of both samples is similar. The nitrogen content of sewage sludge is high, which indicates a high pollution level of NO_x emission if direct combustion of this biomass is selected as the thermochemical conversion method. Therefore, an appropriate NO_x after-treatment system would be required to satisfy EU emission regulations. Additionally, the high ash content, especially in sewage sludge, needs to be considered as it influences the optimal operation and maintenance conditions of pyrolysis,

gasification, and combustion systems. Also, ash compounds like heavy metals should not end up in the environment due to their negative impact on health of humans, animals, plants, and microorganism.

Table 2.1. Results obtained from the characterization of the *C. cardunculus* L. and the sewage sludge samples (d: dry basis, daf: dry ash free, * obtained by difference).

Proximate analysis		
	Cynara cardunculus L.	Sewage sludge
Volatile matter [% d]	74.50	57.11
Fixed carbon* [% d]	12.29	8.23
Ash [% d]	7.49	34.66
Elemental analysis		
	Cynara cardunculus L.	Sewage sludge
C [% daf]	45.36	56.46
H [% daf]	6.63	7.91
N [% daf]	2.65	8.42
O* [% daf]	45.36	27.21
High heating value		
	Cynara cardunculus L.	Sewage sludge
HHV [MJ/kg]	15.09	15.73

The composition of sewage sludge samples is quite heterogeneous. Sewage sludge is a complex mixture of water, organic compounds (such as carbohydrates, lipids, and proteins), microorganisms which can be pathogenic before they are destroyed through heating processes, and inorganic

substances, e.g., silicates and metal containing compounds, which are left over as ash after a high-temperature oxidation process. The composition of sewage sludge depends strongly on the origin of the wastewater and the season, as well as the pretreatment methods used, such as aerobic, anaerobic, chemical or thermal stabilization, dewatering, thickening and drying processes (Bresters et al., 1997). These influences, for instance, the pyrolysis product distribution, as shown by Fonts et al. (2009) for three samples of anaerobically digested sewage sludge obtained from three different urban wastewater treatment plants.

2.4. Results and discussion

The pyrolysis tests using constant heating rates were conducted under a controlled atmosphere in the thermogravimetric analyzer. The procedure described by Soria-Verdugo et al. (2015) was followed to obtain accurate values of the kinetic parameters of the pyrolysis, i.e., the activation energy E and the pre-exponential factor A. Following this procedure, tests using nine different heating rates (β = 10, 13, 16, 19, 22, 25, 30, 35, and 40 K/min) were performed. The evolution of the reacted fraction V/V^*, defined as the percentage of the total volatile matter released by the sample, with temperature T is shown in Figure 2.1 a) for the *C. cardunculus* L. and in Figure 2.1 b) for the sewage sludge sample.

The pyrolysis of both samples was analyzed between 150 and 600 °C. The evolution of the reacted fraction of sewage sludge

with temperature is more progressive than that of the lignocellulosic *C. cardunculus* L. sample, for which the pyrolysis takes place faster for temperatures in the range 250-450 °C. Furthermore, the effect of the heating rate variation on the reacted fraction is higher for the cardoon sample, obtaining a displacement of the curves to higher temperatures when increasing the heating rate, a typical result for non-isothermal pyrolysis reactions (Munir et al., 2009; Tonbul et al., 2009). This effect is slighter for the sewage sludge, resulting in a collapse of the reacted fraction curves for the different heating rates in a narrow zone.

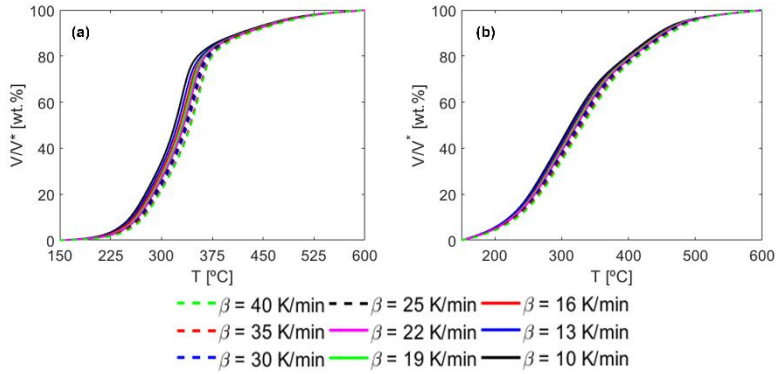

Figure 2.1. Evolution of the reacted fraction, V/V^*, with temperature, T, during the pyrolysis process at constant heating rates. a) *Cynara cardunculus* L., b) Sewage sludge.

The effect of the heating rate can be better appreciated in Figure 2.2, where the reaction rate $\mathrm{d}(V/V^*)/\mathrm{d}t$ is represented as a function of temperature T for both the *C. cardunculus* L. (a) and the sewage sludge (b) pyrolysis. For both samples, the reaction rate increases for higher heating rates. The reaction rate of the *C. cardunculus* L. sample is composed of two

overlapping peaks and a third underlying peak, corresponding to the three typical pseudo-components used to characterize lignocellulosic biomass, namely cellulose, hemicellulose, and lignin. In contrast, for sewage sludge, the reaction rate is lower than for cardoon, as a result of a more distributed conversion of the sample in the whole temperature range, from 150 to 600 °C. In addition, as stated above, the composition of sewage sludge is more complex than that of lignocellulosic biomass and, thus, the reaction rate curve is not composed of only three peaks.

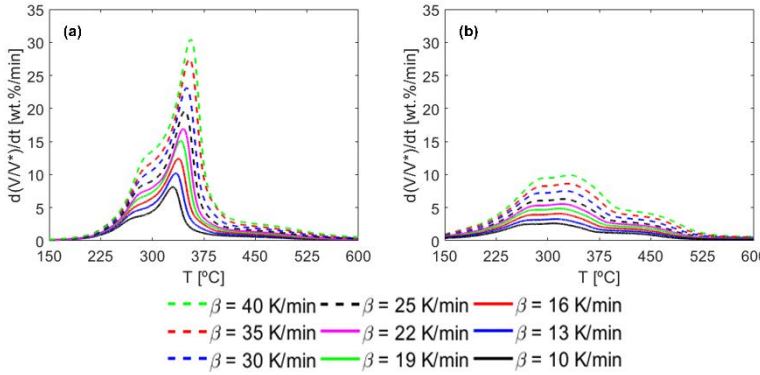

Figure 2.2. Evolution of the reaction rate, d(V/V^*)/dt, with temperature, T, during the pyrolysis process at constant heating rates. a) *Cynara cardunculus* L., b) Sewage sludge.

From the reacted fraction curves shown in Figure 2.1, and considering the Arrhenius equation, Eq. (2.7), the Arrhenius plot can be built by plotting $\ln(\beta/T^2)$ as a function of $1/T$ for different values of the reacted fraction V/V^*. Even though all calculations within this chapter were carried out using intervals of 1% for the reacted fraction, Figure 2.3 shows the

Arrhenius plots of the *C. cardunculus* L. (a) and the sewage sludge (b), built using reacted fraction intervals of 5 wt.% to improve data visualization. The Arrhenius plot of sewage sludge is wider because of the more progressive evolution of the reacted fraction with temperature observed in Figure 2.1 and 2.2 b).

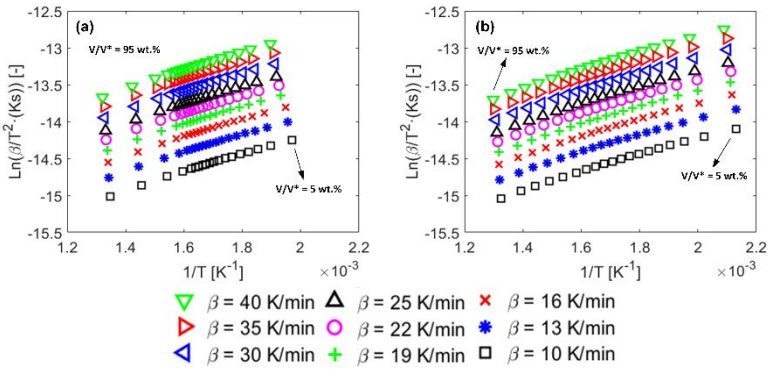

Figure 2.3. Arrhenius plot obtained using reacted fraction intervals of 5 wt.%. a) *Cynara cardunculus* L., b) Sewage sludge.

The data represented in the Arrhenius plots can be employed to determine the activation energy E and the pre-exponential factor A of the samples by linearizing the points obtained for the different values of the reacted fraction V/V^*. Both for the cardoon and the sludge samples, the points in the Arrhenius plot present a high linearity. To quantify the linearity of the Arrhenius plots, the determination coefficient of the linear fitting of the points, R^2, was calculated. The results can be observed in Figure 2.4, both for the *C. cardunculus* L. and the sewage sludge. A high linearity, i.e., high values of R^2, can be observed for a wide range of reacted fractions between 20 and

80 wt.% in both cases, whereas the values of the determination coefficient of the fitting decrease for low and high reacted fractions, where the slope of the curves $V/V^*–T$ is smooth, as shown in Figure 2.1. These high values of R^2 prove the reliability of the experimental measurements conducted (Anca-Couce, 2016).

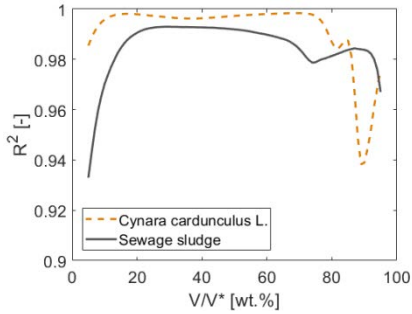

Figure 2.4. Determination coefficient of the linear fitting of the Arrhenius plot data.

Considering the Arrhenius equation for constant heating rates, Eq. (2.7), the kinetic parameters of the pyrolysis reaction, i.e., the activation energy E and the pre-exponential factor A, can be obtained for each reacted fraction from the linear fitting of the values of the Arrhenius plot ($ln(\beta/T^2) = m \cdot (1/T) + n$). Equaling terms of Eq. (2.7) with the linear fitting, the activation energy E and the pre-exponential factor A of the samples can be calculated from the slope m and the intercept n of the linear fitting as follows:

$$E = -m \cdot R \tag{2.8}$$

$$A = -m \cdot \exp(n - 0.6075) \tag{2.9}$$

Accurate values of the activation energy E and the pre-exponential factor A can be calculated using the nine different heating rate curves shown in Figure 2.1, obtained for different constant heating rates, as stated by Soria-Verdugo et al. (2015). The accurate values of E and A for the *C. cardunculus* L. and the sewage sludge are shown in Figure 2.5. The activation energy of the *C. cardunculus* L. is around 150 kJ/mol for most of the pyrolysis process, increasing up to 450 kJ/mol at the end of the process. A similar tendency is detected for the pre-exponential factor of cardoon, varying in a narrow range from 10^{12} to 10^{13} s^{-1}, with a sudden increase to 10^{30} s^{-1} at the end of the pyrolysis process. In contrast, higher average values for both E, ranging from 200 and 400 kJ/mol, and A, varying between 10^{15} and 10^{25} s^{-1}, were obtained for sewage sludge. These values of the kinetic parameters for sewage sludge are in accordance with the measurements of different authors (Liu et al., 2015; Lin et al., 2016; Huang et al., 2016; Wang et al., 2016a; Urych and Smolinski, 2016). In a previous work by Soria-Verdugo et al. (2013), slightly lower values were obtained for the activation energy and pre-exponential factor of sewage sludge. Nonetheless, it should be noticed that the sewage sludge analyzed in Soria-Verdugo et al. (2013) was obtained from a different municipal sewage treatment plant, La China (Madrid, Spain), and were collected in 2012.

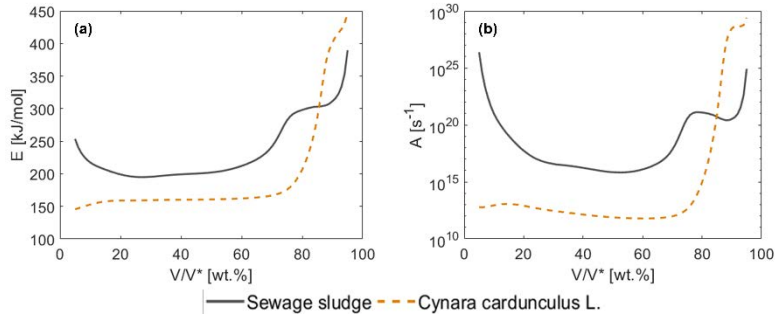

Figure 2.5. Kinetic parameters of the pyrolysis process: a) activation energy and b) pre-exponential factor.

From the kinetic parameters reported in Figure 2.5, an average value of the rate coefficient k can be obtained considering the Arrhenius expression, Eq. (2.1). Assuming a conversion temperature of 325 °C for both biomasses, in accordance to Figure 2.1, and considering activation energies and pre-exponential factors of E = 150 kJ/mol and A = 10^{12} s^{-1} for *C. cardunculus* L. and E = 200 kJ/mol and A = 10^{16} s^{-1} for sewage sludge, a representative value of the rate coefficient of 4.73 min^{-1} and 2.03 min^{-1} is obtained for *C. cardunculus* L. and sewage sludge, respectively.

2.5. Conclusions

Non-isothermal thermogravimetric analysis was employed to characterize the pyrolysis of *C. cardunculus* L. and sewage sludge. The simplified Distributed Activation Energy Model

was applied to simulate the pyrolysis of the samples, obtaining the activation energy and the pre-exponential factor of *C. cardunculus* L. and sewage sludge. The activation energies of *C. cardunculus* L. is around 150 kJ/mol and its pre-exponential factor is approximately 10^{12} s^{-1} for most of the pyrolysis conversion, whereas for the sewage sludge the activation energies range between 200 and 400 kJ/mol and pre-exponential factors vary from 10^{15} to 10^{20} s^{-1}. Considering the kinetic parameters of the pyrolysis conversion of both biomass samples analyzed, representative values of their pyrolysis rate coefficients were calculated, obtaining a rate coefficient of 4.73 min^{-1} for *C. cardunculus* L. and 2.03 min^{-1} for sewage sludge.

Nomenclature

A	Pre-exponential factor [s^{-1}].
E	Activation energy [kJ mol^{-1}].
$f(E)$	Probability density function of E [mol kJ^{-1}].
k	Reaction rate coefficient [s^{-1}].
R	Universal gas constant [J $mol^{-1}K^{-1}$].
t	Time [s].
T	Temperature [K].
V/V^*	Reacted fraction [%].
β	Heating rate [K min^{-1}].
ϕ	ϕ function [-].

CHAPTER
THREE

Pyrolysis of sewage sludge in a fixed and a bubbling fluidized bed – Estimation and experimental validation of the pyrolysis time

Contents

Abstract

Pyrolysis of sewage sludge was studied experimentally in a stainless-steel reactor operated as a fixed or fluidized bed. A novel measuring technique, consisting of measuring the mass of the whole reactor and the sample on a scale, was applied. The scale was capable of measuring the whole mass of the reactor with enough accuracy to detect the mass released by the sewage sludge sample during its pyrolysis. This original measuring technique employed permits the measurement of the time evolution of the mass of sewage sludge supplied to the bed in batch during its pyrolysis while moving freely in the bed. From the measurement of the mass of the solid residue remaining in the reactor, the pyrolysis time of the sewage sludge sample can be obtained accurately for each operating condition. Different operating conditions were selected to analyze the time evolution of the sample mass during the pyrolysis process, including variations of the bed temperature and the velocity of the nitrogen used as inert gas. An increase of the velocity of nitrogen from that of a fixed bed, $0.8U_{mf}$, to that of a low velocity bubbling fluidized bed, $2.5U_{mf}$, accelerates remarkably the pyrolysis process, i.e., reduces the pyrolysis time. However, increasing the nitrogen velocity further has a slight effect on the characteristic velocity of the pyrolysis process. The pyrolysis process of sewage sludge can also be accelerated by increasing the bed temperature, even though the effect of temperature is lower than that of the nitrogen velocity. Furthermore, a mathematical model based on a first order apparent kinetics for the pyrolysis of sewage

sludge was proposed. The model was employed to estimate the pyrolysis time for each operating condition, obtaining a proper agreement with the experimental measurements.

3.1. Introduction

Sewage sludge is the solid residue produced during the treatment of municipal and industrial wastewater. The rapid development of urbanization and industrialization has contributed to the dramatic increase of sewage sludge production over the last decades (Wang et al., 2016b), causing a critical problem of waste management. The ways of disposing sewage sludge can be divided into three main applications: landfill, agricultural use, and incineration or thermochemical conversion (Fonts et al., 2012). Nonetheless, the European regulations limit the use of sewage sludge for landfilling due to environmental problems, while the use for agricultural purposes has been also restricted because of the harmful components of sewage sludge, such as heavy metals, polyaromatic hydrocarbons, and polychlorinated biphenyls (Kaminsky and Kummer, 1989). In contrast, sewage sludge thermochemical conversion permits to recover energy, reduces the volume of the residue by 70% and thermally destructs the pathogens (Fytili and Zabaniotou, 2008).

Among the different thermochemical conversion processes, pyrolysis is considered to be a promising sewage sludge disposal technology due to its advantages, such as residue volume reduction, concentration of heavy metals, and

stabilization of waste (Sun et al., 2015). Pyrolysis processes can be divided into conventional or fast pyrolysis, depending mainly on the pyrolysis vapors residence time in the reactor. In conventional pyrolysis, vapor residence times can vary between 5 and 30 min, whereas in fast pyrolysis processes, typical vapor residence times are around 1-5 s (Yan et al., 2011). Fast pyrolysis of biomass is usually employed for fuel liquid production because of the high yield of bio-oil generated (Bridgwater, 2012). Even though fast pyrolysis of biomass has achieved a commercial status (Bridgwater and Peacoke, 2000), many aspects are still empirical, requiring further study to improve the efficiency and reliability of the process, and the final product characteristics (Bridgwater et al., 1999).

Despite the numerous studies published focusing on thermochemical conversion of sewage sludge, most of them work with dry sludge due to the significant reduction of the efficiency and the operating problems derived from the conversion of wet sewage sludge. In this way, fluidized bed reactors permit both the thermochemical conversion and the drying processes to be carried out in the same reactor, avoiding a significant decrease in efficiency. Fluidized beds are employed as industrial chemical reactors due to their ability to convert low quality solid fuels, even wet sewage sludge, with a high efficiency and with an associated low emission of pollutants. The homogeneous and low reaction temperature of fluidized beds limits the emissions of NO_x, whereas sorbent bed materials can be used for in-bed capture

of SO_x emissions. The technology of bubbling fluidized beds is adequate for the conversion of highly volatile fuels such as biomass and organic waste, for which the conversion can occur in the bubbling bed at low temperatures without the need of in-bed heat exchangers (Leckner, 2016). The performance and emission level of bubbling fluidized beds are influenced by fuel mixing (Leckner, 1998), which can be improved by increasing the fluidizing gas velocity (Soria-Verdugo et al., 2011a; Soria-Verdugo et al., 2011b; Soria-Verdugo et al., 2011c; Lundberg et al., 2017).

The products obtained from the pyrolysis of biomass in a fluidized bed are affected by the operating conditions, including fuel particle diameter, pyrolysis vapors residence time, and reactor temperature. The bed temperature is considered to be the most influential parameter and, thus, several authors have focused their research on analyzing its effect on the liquid yield (Park et al., 2008; Park et al., 2010; Arazo et al., 2017). In these works, the bed temperature that maximizes the liquid yield is studied. For low reactor temperatures, the energy supplied to the fuel particles is limited and then the total amount of volatile matter is not released from the solid fuel. In contrast, for high reactor temperatures, the pyrolysis vapors generated may suffer secondary cracking reactions, resulting in an increase of non-condensable gases, decreasing the liquid yield. Therefore, the optimal reactor temperature to produce liquid fuel from a pyrolysis process is a moderate temperature. Concerning the maximum bio-oil yield produced from the pyrolysis of

sewage sludge in fluidized bed reactors, Jaramillo-Arango et al. (2016) obtained a liquid production of 40 wt.% for a temperature of 600 °C; the maximum liquid yield reached by Alvarez et al. (2015) was 48 wt.% for a bed temperature of 500 °C; and Fonts et al. (2008) reached a maximum liquid production of 40 wt.% at a temperature of 550 °C. Sun et al. (2013) studied the pyrolysis of sewage sludge in a wide range of temperatures between 300 and 900 °C, concluding that the maximum liquid production from the condensation of the pyrolysis vapors was obtained at moderate temperatures of around 550 °C. In fact, in a following study conducted by Sun et al. (2015), they focused the analysis of sewage sludge pyrolysis on a narrow temperature range of 400-600 °C. Moreover, for temperatures above 650 °C the char generated during the pyrolysis process may react with the water vapor produced (Reschmeier et al., 2014).

The secondary thermal cracking of the pyrolysis vapors depends also on their residence time inside the reactor. To avoid the thermal cracking of the product gas, which promotes the formation of non-condensable gases and diminishes the formation of liquid yield, the residence time of the pyrolysis vapors at high temperatures should be limited. The effect of this parameter on the bio-oil production has been studied by several authors, showing an increase in the liquid yield produced during the pyrolysis of sewage sludge when decreasing the residence time (Piskorz et al., 1986; Shen and Zhang, 2003).

In this work, a novel measurement technique is employed to analyze the evolution of the pyrolysis process of sewage sludge in a lab-scale bed reactor. The reactor was installed over a precision scale capable of measuring the mass released by the sewage sludge sample during its pyrolysis process, moving freely inside the reactor. This original measurement technique permits the study of the pyrolysis process to be focused on the solid fuel instead of analyzing only the liquid and/or the gas produced. The measurement obtained from the scale permitted the measurement of the time evolution of the mass released by the sample for various operating conditions. The pyrolysis of sewage sludge was analyzed for six different nitrogen velocities, from a velocity lower than the minimum fluidization velocity, corresponding to a fixed bed, to a velocity three times faster than the minimum fluidization velocity, which induces a bubbling fluidized bed. For each gas velocity, two different bed temperatures, 500 and 600 °C, in the range for which the liquid fuel production from pyrolysis is maximized, were tested. The pyrolysis time was obtained from the experimental measurements, and a mathematical model based on a first order apparent kinetics was proposed. The pyrolysis time estimated by the model was compared to the experimental results, obtaining a fairly good agreement.

3.2. Theory

Pyrolysis is a complex process in which a huge amount of chemical reactions occur simultaneously or consecutively. The parallel reactions taking place are in competition to each

other and depend mainly on the pyrolysis conditions. A simplified approach permits the variation of the sample mass with time, dm/dt, to be determined as a function of the remaining volatile matter in the sample, m_{vol}, and an apparent rate constant, k, for a determined reaction order, n, (Reschmeier et al., 2014) as:

$$\frac{\mathrm{d}m}{\mathrm{d}t} = -k \cdot m_{vol}{}^{n} \tag{3.1}$$

The mass of the sample, m, at each time, t, can be determined as the summation of the volatile matter remaining in the sample, m_{vol}, and the solid residue, m_{res}.

$$m = m_{vol} + m_{res} \tag{3.2}$$

Considering a first order reaction, n = 1, which is the simplest and most generally used case, the integration of Eq. (3.1) reads:

$$m = m_{vol0} \cdot \exp\left(-k \cdot t\right) + m_{res} \tag{3.3}$$

where m_{vol0} is the initial mass of volatiles in the sample. Dividing Eq. (3.3) by the initial mass of the sample, m_0, the evolution of the percentage of mass of the sample, X, with time, t, can be estimated as a function of the initial percentage of volatile content, X_{vol}, the percentage of solid residue, X_{res}, and the apparent rate constant, k. Notice that the percentage of solid residue is related to the initial volatile content of the sample as X_{res} = 100 - X_{vol}.

$$X = X_{vol} \cdot \exp\left(-k \cdot t\right) + X_{res} \tag{3.4}$$

3.3. Materials and methods

3.3.1. Experimental facility

The pyrolysis experiments were conducted in a cylindrical reactor made of stainless steel, with an inner diameter, d_i, of 4.7 cm and a height, h, of 50 cm, operating at atmospheric pressure. The energy required to reach the desired pyrolysis temperature was supplied by three electric resistors, surrounding the reactor, capable of supplying a maximum thermal power of 1.2 kWt.

The absence of oxygen required for the pyrolysis reaction was ensured using nitrogen as fluidization agent. The nitrogen flowrate was measured by a flowmeter PFM750-F01-F from SMC, with a measurement range from 1 to 50 l/min. The reactor was placed on a precision scale PS 6000 R2 from RADWAG. The weight measurements conducted during the pyrolysis tests were below the minimum weighting requirement of the scale for all the cases analyzed. Furthermore, the accuracy of the weight measurements registered by the scale met the accuracy requirements during the pyrolysis tests. Figure 3.1 shows a schematic of the facility, further details of the system can be found in (Soria-Verdugo et al., 2017a).

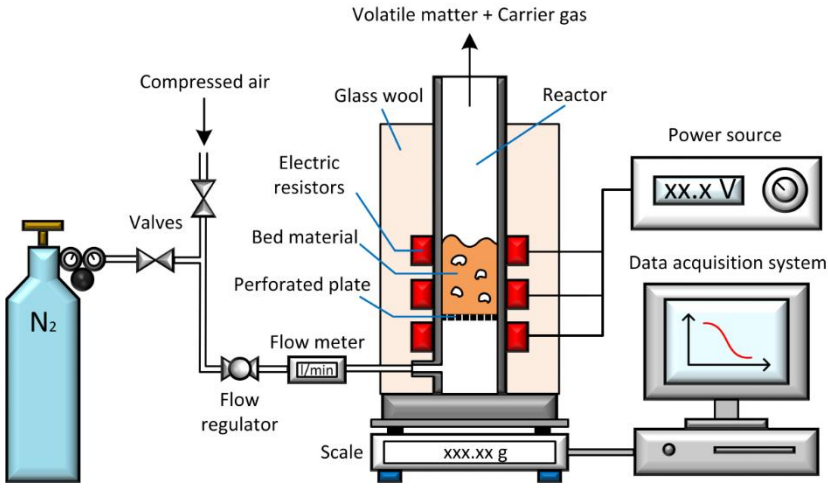

Figure 3.1. Schematic of the experimental facility.

The reactor temperature was measured by a type-k thermocouple immersed in the bed until reaching the desired temperature. Once the desired temperature was attained, the thermocouple was removed to prevent the perturbation of the signal registered by the scale, and the flowrate of nitrogen was adjusted with a value corresponding to a specific excess gas velocity. Finally, the sewage sludge was introduced in the reactor, the pyrolysis occurred, and the vapors released were absorbed by a fume extractor placed above the reactor.

3.3.2. Bed material characterization

Silica sand was employed as bed material since it is known to be inert, not affecting the reaction rate during the thermochemical decomposition of biomass (Koppatz et al., 2011). The silica sand particle diameter, d_{bm}, was in the range of 425-600 μm and the particle density, ρ_{bm}, was 2600 kg/m^3. A

mass of 240 g of sand was used in each test to reach a fixed bed height, h_b, of 9.4 cm (bed aspect ratio h_b/d_i = 2), corresponding to a void fraction, ε, of 0.44.

The variation of the gas density, ρ_g, with temperature was considered to determine the minimum fluidization velocity, U_{mf}, as described in Sánchez-Prieto et al. (2014). The gas density at the reactor temperature was calculated considering the ideal gas law:

$$\rho_g = \rho_{g0} \frac{T_0}{T} \tag{3.5}$$

where ρ_g is the nitrogen density at temperature T and ρ_{g0} is the nitrogen density at the reference temperature T_0. The reference temperature was selected as T_0 = 300 K and the nitrogen density at this temperature is ρ_{g0} = 1.14 kg/m3.

The minimum fluidization velocity can be estimated as a function of the reactor temperature using the correlation of Carman-Kozeny (Carman, 1937):

$$U_{mf} = \frac{\left(\phi d_{bm}\right)^2 \left(\rho_{bm} - \rho_g\right) g}{180 \mu_g} \frac{\varepsilon^3}{1-\varepsilon} \tag{3.6}$$

where U_{mf} is the minimum fluidization velocity, ϕ is the sphericity of the dense phase particles, ε is the void fraction, g is the gravity acceleration, d_{bm} is the diameter of the bed material particles, ρ_{bm} is the density of the bed material particles, ρ_g is the density of nitrogen at the reactor temperature, and μ_g is the dynamic viscosity of nitrogen at the

bed temperature. The variation of the dynamic viscosity of nitrogen with the reactor temperature, T, can be determined by the potential law:

$$\mu_g = \mu_{g0}\left(\frac{T}{T_0}\right)^{2/3} \tag{3.7}$$

where the dynamic viscosity of nitrogen at the reference temperature (T_0 = 300 K) is $\mu_{g0} = 1.78 \cdot 10^{-5}$ kg/(m·s).

3.4. Results and discussion

3.4.1. Minimum fluidization velocity

The minimum fluidization velocity of the silica sand particles was measured as a function of the bed temperature. Figure 3.2 shows the experimental results of the minimum fluidization velocity, U_{mf}, together with the estimation from the Carman-Kozeny correlation, Eq. (3.6), as a function of the reactor temperature, T. An average particle diameter of silica sand of d_{bm} = 512.5 μm and a sphericity of ϕ = 0.8 were selected for the Carman-Kozeny correlation. As can be seen in Figure 3.2, the estimation of the Carman-Kozeny correlation properly describes the variation of the minimum fluidization velocity measured experimentally.

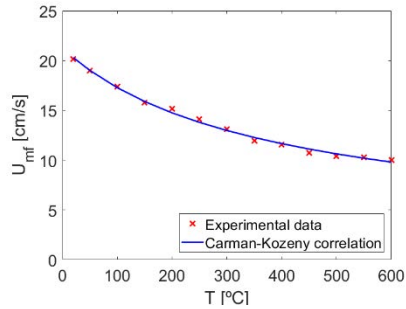

Figure 3.2. Variation of the minimum fluidization velocity with the reactor temperature.

3.4.2. Pyrolysis experimental measurements

The sewage sludge pyrolysis experiments consisted in recording the mass signal measured by the scale while the pyrolysis process of the sewage sludge sample was taking place inside the reactor. Therefore, the mass released during the pyrolysis of the sampled could be determined. First, the reactor, filled with the sand particles that conformed the bed, was heated up by the resistors to the desired reactor temperature, T, while an air flowrate was used as fluidizing agent. Once the reactor temperature of the test was reached, the fluidizing gas was switched to nitrogen, and the flowrate was adjusted. When the operating conditions of the bed, i.e., reactor temperature and nitrogen flowrate, were selected, the scale, on which the reactor rested, was tared and a batch of around 10 g of dry sewage sludge particles was introduced through the top of the reactor. The particle size of sewage sludge was d_p < 3 mm and they were dried at 105 °C in a universal oven UFE 500 from Memmett for 5 h, after which no

mass variation of the sample was detected. The basic characterization of the sewage sludge particles can be found in Chapter 2. Each experimental measurement was replicated to test the reproducibility of the experimental procedure, obtaining deviations lower than 5%.

The mass signal measured by the scale during the pyrolysis of the sewage sludge registered the vibration induced by the ascension of bubbles when the bed was fluidized. Therefore, the mass signals measured in all cases were filtered using a moving average. Further details of the filtration of the mass signals can be found in a previous work (Soria-Verdugo et al., 2017a). The filtered signals were proved to follow the average behavior of the raw signal measured by the scale in all cases.

Different operating conditions were tested, varying both the reactor temperature and the fluidizing gas velocity. The reactor temperatures analyzed in this chapter are 500 and 600 °C, temperatures for which the production of liquid fuel from the condensation of the sewage sludge pyrolysis vapors is optimal. A thermogravimetric analysis of the pyrolysis of the same sewage sludge studied in this chapter showed that most of the mass released by the samples during the pyrolysis occurs for temperatures below 500 °C (Soria-Verdugo et al., 2017b). Concerning the velocity of the fluidizing gas (nitrogen) during the pyrolysis process, 6 different values were tested for each reactor temperature, U/U_{mf} = 0.8, 1, 1.5, 2, 2.5, and 3, from a velocity lower than U_{mf}, corresponding to a fixed bed reactor, to 3 times U_{mf}, which induces a bubbling fluidized bed regime in the reactor. Gas velocities higher than

$3U_{mf}$ may produce large bubbles in the bed compared to the reactor diameter, leading to a slugging regime, which is not the focus of this study.

3.4.3. Time evolution of the sewage sludge mass

The evolution with time of the mass of the sewage sludge sample during the pyrolysis, measured by the scale, was filtered and divided by the initial mass of the sample, m_0, to obtain the percentage of mass remaining, X. The variation of X with time during the pyrolysis of sewage sludge for each gas velocity analyzed are plotted in Figure 3.3 a) for a reactor temperature of 500 °C and in Figure 3.3 b) for a bed temperature of 600 °C. The pyrolysis process is accelerated when increasing the fluidizing gas velocity for the two reactor temperatures tested. This fact can be attributed to the increase of the heating rate of the sewage sludge particles (Bridgwater et al., 1999; Scott and Piskorz, 1984) caused by the higher axial fuel mixing obtained when the fluidizing gas velocity is increased (Soria-Verdugo et al., 2011c; Lundberg et al, 2017). Comparing the experimental measurements obtained for both reactor temperatures, a slight effect of the temperature can be observed, accelerating scarcely the pyrolysis process when increasing the reactor temperature from 500 to 600 °C. Nevertheless, the effect of the reactor temperature on the pyrolysis process is lower in comparison to the significant effect of increasing the fluidization velocity.

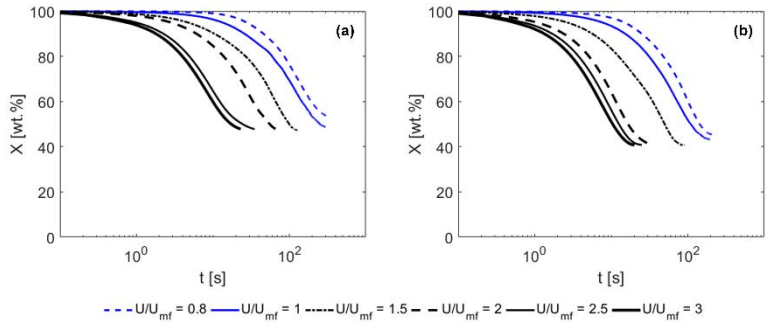

Figure 3.3. Time evolution of the percentage of mass of the sewage sludge sample remaining in the reactor for a bed temperature of a) 500 °C and b) 600 °C.

To facilitate the analysis of the effect of the reactor temperature on the pyrolysis process, the derivative of the percentage of mass remaining in the reactor is plotted as a function of time in Figure 3.4. The derivative of the percentage of mass is clearly increased for both reactor temperatures when increasing the fluidization velocity, accelerating the pyrolysis of the samples as stated above. Comparing the results plotted in Figure 3.4 a) for a reactor temperature of 500 °C with those in Figure 3.4 b) obtained for a bed temperature of 600 °C, the increase of the dX/dt with temperature can be observed. Therefore, the pyrolysis reaction of sewage sludge can be accelerated by increasing the gas velocity and/or the reactor temperature.

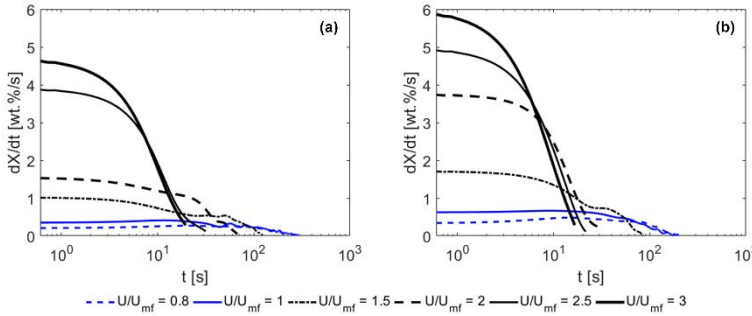

Figure 3.4. Time evolution of the derivative of the percentage of mass of the sewage sludge sample remaining in the reactor for a bed temperature of a) 500 °C and b) 600 °C.

The percentage of mass remaining after the pyrolysis process, X_{res}, can be determined as the percentage of mass at the end of the tests shown in Figure 3.3. It can be observed in Figure 3.3 that this percentage of mass remaining, X_{res}, depends on the operating conditions. To analyze the effect of both the reactor temperature and the nitrogen velocity on the mass remaining after the pyrolysis, X_{res}, Figure 3.5 shows the percentage of mass of volatiles released by the sample during the complete pyrolysis process, X_{vol}, defined as X_{vol} = 100 - X_{res}. Thermogravimetric analysis (TGA) tests of the pyrolysis of sewage sludge samples were also carried out for comparison to the pyrolysis tests in the reactor. The TGA tests were conducted in the TGA Q500 from TA Instruments and consisted in measuring the evolution of an initial mass of 10 mg of sewage sludge in a nitrogen atmosphere at temperatures of 500 and 600 °C. The percentage of volatile matter released by the sewage sludge during the pyrolysis in the TGA is also included in Figure 3.5 as dotted (T = 500 °C)

and dashed (T = 600 °C) lines for comparison, although the nitrogen flow rate for all the TGA tests was maintained constant at 60 ml/min.

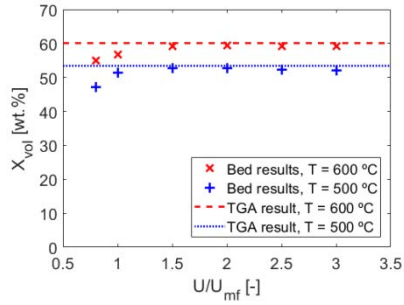

Figure 3.5. Total volatile matter released by the sewage sludge sample.

The percentage of volatile matter released by the samples during the pyrolysis process in the reactor is very similar to that obtained in the TGA, provided that the nitrogen velocity is sufficient to induce a proper fluidization of the bed ($U/U_{mf} \geq 1.5$). However, when the pyrolysis occurs in a fixed bed ($U/U_{mf} = 0.8$) or in a bed at minimum fluidization velocity ($U/U_{mf} = 1$), the value of X_{vol} obtained in the reactor is lower than that of the TGA. This can be attributed to heat transfer effects inside the sample when no bubbles are present in the bed ($U/U_{mf} \leq 1$) and the fuel particles accumulate on the bed surface after being supplied as a batch through the bed top and, thus, the low conduction of heat inside this accumulation of fuel particles in the surface is relevant. When the gas velocity is increased above the minimum fluidization velocity ($U/U_{mf} > 1$), bubbles appear in the bed and induce the motion of fuel particles, breaking the typical accumulation of fuel

found in fixed beds, and enhancing the axial dispersion of fuel inside the bed (Soria-Verdugo et al., 2011c; Lundberg et al., 2017). Therefore, in the case of fluidized beds, the fuel particles are separated from each other due to the higher dispersion of fuel induced by the presence of bubbles, hence the effect of heat transfer inside the sample is reduced, and the heating rate is increased.

The values of the percentage of volatile matter released during the pyrolysis of sewage sludge, X_{vol}, shown in Figure 3.5 are in accordance with those reported by different authors in the literature. Regarding the pyrolysis of sewage slugde in a fixed bed, Wang et al. (2016b) obtained values of X_{vol} = 50.9 wt.% and X_{vol} = 55 wt.% for reactor temperatures of 500 and 600 °C respectively, whereas Atienza-Martínez et al. (2015) reached X_{vol} = 51 wt.% for a bed temperature of 530 °C. Despite the great heterogeneity in the composition of sewage sludge, these values are quite close to those obtained in our work, X_{vol} = 47.2 wt.% for T = 500 °C and X_{vol} = 55.1 wt.% for T = 600 °C. Concerning the pyrolysis of sewage sludge in a fluidized bed, Shen and Zhang (2003) obtained percentages of volatile matter of X_{vol} = 55.2 wt.% and X_{vol} = 57.4 wt.% for fluidized bed temperatures of 500 and 600 °C, respectively, which are comparable to those obtained in this work X_{vol} = 53.4 wt.% (T = 500 °C) and X_{vol} = 60.1 wt.% (T = 600 °C) in the TGA tests. Furthermore, several authors informed of a reduction of the solid residue produced during the pyrolysis of biomass for higher heating rates (Bridgwater et al., 1999; Reschmeier et al., 2014; Damartzis et al, 2011) and pyrolysis temperatures (Yan

et al., 2011; Park et al., 2008; Jaramillo-Arango et al., 2016; Alvarez et al., 2015; Shen and Zhang, 2003).

3.4.4. Pyrolysis time

The effect of the different volatile matter released for each operating condition can be removed by re-scaling the evolution of the percentage of sewage sludge mass remaining in the reactor, *X*, shown in Figure 3.3, to calculate the reacted fraction, *V*/*V**. The reacted fraction, *V*/*V**, is defined as the ratio of the volatile matter released at a determined time to the total volatile matter released after the complete pyrolysis process, thus *V*/*V** = 0 wt.% at the beginning of the pyrolysis process and *V*/*V** = 100 wt.% when the process ends. The results obtained for the reacted fraction, *V*/*V**, are shown in Figure 3.6, where a very similar shape of the curves obtained for the different gas velocities and reactor temperatures can be observed. The increase of either the gas velocity or the bed temperature produces a displacement of the curves to shorter times, reducing the time needed for the pyrolysis of the sample.

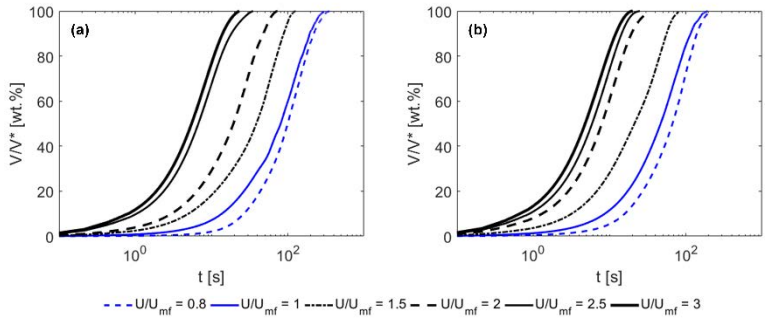

Figure 3.6. Time evolution of the reacted fraction of sewage sludge with time for reactor temperatures of a) 500 °C and b) 600 °C.

The pyrolysis time, t_{pyr}, can be calculated as the time needed to reach a determined value of the reacted fraction. In this work, a value of V/V^* = 95 wt.% is selected to determine the pyrolysis time. Figure 3.7 shows the pyrolysis time of sewage sludge as a function of the nitrogen velocity for the two different reactor temperatures studied. A substantial reduction of the pyrolysis time can be obtained by raising the fluidization velocity. The reduction of the pyrolysis time between a fixed or minimum fluidization bed ($U/U_{mf} \leq 1$) and a bubbling fluidized bed reactor ($U/U_{mf} \geq 1.5$) is significant, due to the higher heating rate characteristic of fluidized beds (Piskorz et al, 1986). A clear reduction of the pyrolysis time with the reactor temperature can be also observed for low gas velocities ($U/U_{mf} < 2.5$). However, these differences are negligible when further increasing the nitrogen velocity ($U/U_{mf} \geq 2.5$).

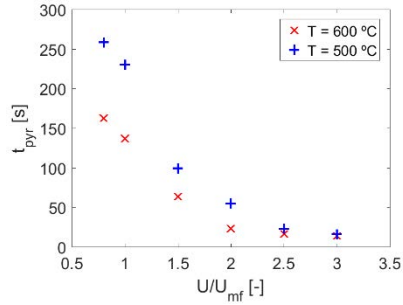

Figure 3.7. Pyrolysis time of sewage sludge for reactor temperatures of a) 500 °C and b) 600 °C.

The reduction of the pyrolysis time produced by fluidized bed reactors is of central importance for industrial reactors since a lower pyrolysis time, i.e., faster pyrolysis reaction rate permits the increase of the fuel feeding rate and, thus, the production of liquid fuel from the condensation of the pyrolysis vapors is enhanced. Furthermore, a higher fluidizing gas velocity reduces the pyrolysis vapors residence time in the reactor, promoting a higher content of condensable gases in the pyrolysis vapors, which further improves the production of liquid fuel from the pyrolysis of the sample (Bridgwater et al., 1999; Park et al., 2010; Shen and Zhang, 2003).

3.4.5. Modelling of the pyrolysis process

In this section, a mathematical procedure to estimate the pyrolysis time of sewage sludge as a function of the operating conditions of the reactor is presented. The procedure is based on determining the apparent rate constant, *k*, for the different gas velocities and reactor temperatures studied experimentally. The apparent rate constant, *k*, can be

determined by fitting the experimental curves of the time evolution of the percentage of mass of the sample, X, shown in Figure 3.3, to an exponential decay function in the form of Eq. (3.4). The fitting of the experimental curves $X - t$ was carried out only for nitrogen velocities high enough to properly fluidize the bed, i.e., $U/U_{mf} \geq 1.5$, causing a negligible effect of heat transfer inside the sample. For the pyrolysis tests of high gas velocities ($U/U_{mf} \geq 1.5$), the percentage of volatile matter released by the sewage sludge can be considered to be an exclusive function of temperature, being X_{vol} = 53.4 wt.% for a reactor temperature of 500 °C and X_{vol} = 60.1 wt.% for a bed temperature of 600 °C (see Figure 3.5). Therefore, the only free parameter on the fitting of the evolution of X with time to Eq. (3.4) is the apparent rate coefficient, k. The values obtained for the apparent rate coefficient, k, for each operating condition are included in Table 3.1, together with the determination coefficient, R^2, of the fitting. These values are similar to the average rate coefficient obtained in Chapter 2 for the pyrolysis of sewage sludge in the TGA. As can be observed in Table 3.1, the determination coefficient, R^2, is higher than 0.98 in all the cases analyzed, thus, the experimental data of the variation of the percentage of mass of sewage sludge during the pyrolysis in the bubbling fluidized bed reactor can be said to follow a first order apparent kinetics.

Table 3.1. Values of the apparent rate coeffient and determination coefficient of the fitting for different gas velocities and reactor temperatures.

	T = 500 °C		T = 600 °C	
U/U_{mf} [-]	k [min^{-1}]	R^2 [-]	k [min^{-1}]	R^2 [-]
1.5	1.25	0.981	2.07	0.986
2	2.43	0.983	5.88	0.985
2.5	6.48	0.996	7.89	0.984
3	8.18	0.991	9.61	0.987

The values obtained for the apparent rate constant, included in Table 3.1, are depicted in Figure 3.8 as a function of the dimensionless gas velocity, U/U_{mf}, for both reactor temperatures, along with a linear fitting of the data.

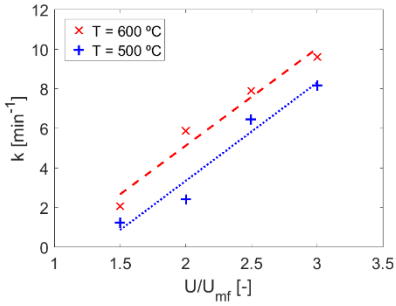

Figure 3.8. Apparent rate constant obtained from the fitting as a function of the gas velocity.

The variation of the apparent rate coefficient, k, with the dimensionless gas velocity, U/U_{mf}, was fitted to a linear equation, obtaining the slopes and intercepts presented in Eq. (3.8) and Eq. (3.9) for T = 500 °C and T = 600 °C, respectively. The increase of the apparent rate coefficient with the gas velocity is similar for the two reactor temperatures analyzed,

as can be observed from the similar values of the slopes in Eqs. (3.8) and (3.9). The reactor temperature affects only the intercept of the linear fitting of the apparent rate coefficient with the dimensionless gas velocity.

$$k_{500} = 4.97\left(U / U_{mf}\right) - 6.59 \tag{3.8}$$

$$k_{600} = 4.92\left(U / U_{mf}\right) - 4.71 \tag{3.9}$$

The pyrolysis time can be estimated, t_{mod}, using the first order kinetic model described in section 3.2, as an only function of the apparent rate coefficient obtained for each bed temperature and gas velocity. Eqs. (4.8) and (4.9) can be used to estimate the value of the apparent rate coefficient for the pyrolysis of sewage sludge in a bubbling fluidized bed as a function of the gas velocity, for reactor temperatures of 500 and 600 °C, respectively. The estimated values of the apparent reaction velocities, k_{500} and k_{600}, can be introduced in Eq. (3.4) to estimate numerically the evolution of the percentage of mass of the sewage sludge sample, X, with time during the pyrolysis process. This numerical estimation of the evolution of X with time can be rescaled to obtain a numerical reacted fraction, V/V^*, that can be employed to calculate the estimated pyrolysis time, t_{mod}, as the time for which the numerical reacted fraction reaches 95 wt.%. The results obtained for the estimation of the pyrolysis time, t_{mod}, are presented in Table 3.2 together with the experimental results, t_{pyr}, for comparison. The relative error, ε_t, between the estimated and the experimental pyrolysis time is also included in Table 3.2 for

each operating condition of the fluidized bed reactor. The results presented in Table 3.2 show a good agreement between the prediction of the pyrolysis time by the model and the experimental results, obtaining relative errors around 10%.

Table 3.2. Comparison between the estimated and experimental pyrolysis times for different gas velocities and reactor temperatures.

	T = 500 °C			T = 600 °C		
U/U_{mf} [-]	t_{pyr} [s]	t_{mod} [s]	ε_t [%]	t_{pyr} [s]	t_{mod} [s]	ε_t [%]
1.5	99.9	111.2	11.3	63.7	60.9	4.4
2	55.6	49	11.9	23.7	26.3	11
2.5	23.4	25.8	10.2	17	19.1	12.3
3	16.8	17.5	4.2	14.3	14.9	4.3

3.5. Conclusions

The pyrolysis process of sewage sludge was studied experimentally in a bed reactor, analyzing the evolution of the sample mass with time for different reactor temperatures and gas velocities. For high gas velocities, corresponding to a bubbling fluidized bed regime, $1.5 \leq U/U_{mf} \leq 3$, the pyrolysis process was accelerated due to the higher heating rate of fuel particles in fluidized beds in comparison to fixed bed reactors. The pyrolysis process occurs faster also for higher reactor temperatures, although the effect of the bed temperature is slight compared to that of the gas velocity. The percentage of volatile matter released by the sewage sludge sample during

the pyrolysis in a bubbling fluidized bed reactor was around 53.4 wt.% for a bed temperature of 500 °C and 60.1 wt.% for a temperature of 600 °C. These results are in accordance with the literature, and very similar to those obtained from a thermogravimetric analysis of the samples. The amount of volatile matter released by the

sewage sludge is slightly lower when the pyrolysis process is carried out in a fixed bed reactor.

The pyrolysis time was determined experimentally from the evolution of the reacted fraction of the sewage sludge, showing a significant diminution when the gas velocity increases due to the larger heating rates characteristic of bubbling fluidized beds. The effect of the reactor temperature is significant for low gas velocities, whereas for high gas velocities the influence of the bed temperature is negligible. A mathematical procedure, based on a first order apparent chemical kinetics and capable of predicting the evolution of the complex pyrolysis process, was proposed. The apparent pyrolysis rate coefficient was obtained from a fitting of the experimental data to the first order kinetics equation. The apparent rate constant showed a linear increase with the gas velocity, maintaining a constant slope for the two different bed temperatures studied. Finally, the mathematical model proposed was employed to estimate the pyrolysis time for each operating condition, showing a good agreement with the experimental pyrolysis time, obtaining deviations of around 10% for all the operating conditions analyzed.

Nomenclature

d_{bm} Particle diameter of the bed material [m].

d_i Inner diameter of the reactor [m].

d_p Particle diameter of sewage sludge [m].

g Gravity acceleration [m s^{-2}]

h Height of the reactor [m].

h_b Height of the fixed bed [m].

k Apparent rate constant [min^{-1}].

k_{500} Apparent rate constant for T = 500 °C [s^{-1}].

k_{600} Apparent rate constant for T = 600 °C [s^{-1}].

m Mass of the sample [kg].

m_0 Initial mass of the sample [kg].

m_{vol} Mass of volatiles remaining in the sample [kg].

m_{vol0} Initial mass of volatiles in the sample [kg].

m_{res} Mass of the solid residue in the sample [kg].

n Reaction order [-].

t Time [s].

t_{mod} Estimated pyrolysis time [s].

t_{pyr} Experimental pyrolysis time [s].

T Temperature [K].

T_0 Reference temperature [K].

U Gas velocity [m s^{-1}].

U/U_{mf} Dimensionless gas velocity [-].

U_{mf} Minimum fluidization velocity [m s^{-1}].

V/V* Reacted fraction [%].

X Percentage of mass of the sample [%].

X_{vol} Percentage of total volatile content [%].

X_{res} Percentage of solid residue [%].

ε_t Relative error of the pyrolysis time [%].

ε Void fraction of the bed material [-].

ρ_{bm} Particle density of the bed material [kg m^{-3}].

ρ_g Gas density at bed temperature [kg m^{-3}].

ρ_{g0} Gas density at T_0 [kg m^{-3}].

μ_g Gas dynamic viscosity at bed temperature [kg m^{-1} s^{-1}].

μ_{g0} Gas dynamic viscosity at T_0 [kg m^{-1} s^{-1}].

ϕ Sphericity of the dense phase particles [-].

CHAPTER
FOUR

Pyrolysis of *Cynara cardunculus* L. samples – Effect of operating conditions and bed stage on the evolution of the conversion

Contents

Abstract

The effect of different parameters on the pyrolysis of *Cynara cardunculus* L. was studied through an innovative technique based on a precision scale, capable of measuring the time evolution of the biomass samples mass during their thermochemical conversion process, while moving freely inside a fluidized bed. A silica sand bed reactor, operated under different values of excess gas velocity and reactor temperature, was employed to hold the pyrolysis reaction of cardoon particles of three different size ranges. The pyrolysis was accelerated for higher excess gas velocities, obtaining pyrolysis times as short as 17 s for experiments conducted under bubbling fluidized bed regimes, compared to 186 s required to complete the pyrolysis of the same sample in a fixed bed configuration. Similarly, the effect of increasing the reactor temperature promoted faster heating rates across the fuel samples, especially under fixed bed configurations, for which the pyrolysis time is reduced from 322 s to 132 s when increasing the bed temperature from 450 to 650 °C. Regarding the biomass particle size, small sizes are recommended to minimize the conduction thermal resistance inside the fuel particles and, thus, reduce pyrolysis times and increase volatile yields for the pyrolysis in a bubbling fluidized bed reactor. The opposite result was found when the pyrolysis took place in non-bubbling beds, where the use of larger particles is beneficial to accelerate the biomass pyrolysis reaction.

4.1. Introduction

Pyrolysis, which consists in the thermal decomposition of solid fuels in a non-oxidative atmosphere at elevated temperatures, is a favorable thermochemical process for biomass conversion, since it enhances the production of a brown-dark liquid called bio-oil, with a lower heating value (LHV) around 14-18 MJ/kg (Chen et al., 2014b). This bio-oil can be readily stored and transported, permitting its decentralized usage as a fuel in turbines, boilers, and engines or as a source for chemicals production (Piskorz et al, 1986; Czernik and Bridgwater, 2004). In addition to the bio-oil generated, charcoal and permanent gases are also produced during the pyrolysis of biomass. The physico-chemical properties and the yields of the bio-oil, the permanent gases and the solid residue are strongly affected by the composition of the feedstock, the use of pretreatment techniques for biomass (Chen et al., 2017a; Chen et al., 2015), and the operating conditions selected for the pyrolysis process, i.e., reactor temperature, heating rate, biomass particle size, or pyrolysis vapor residence time (Bridgwater et al, 1999; Chen et al., 2014c).

Temperature is considered the most sensitive parameter for pyrolysis, influencing significantly the production of the different pyrolysis products (Guedes et al., 2018). Previous studies have demonstrated that liquid production can be maximized under certain operating conditions, attaining up

to 75 wt.% on a dry basis for the pyrolysis of wood in a temperature range of 480-520 °C (Bridgwater et al., 1999). Nevertheless, the maximum liquid yield depends not only on the pyrolysis conditions employed, but also on the feedstock. According to the specific literature, the optimal temperature interval to produce liquid fuel from the pyrolysis of different biomass species ranges from 450 to 650 °C (Uzun et al., 2006; Pattiya and Suttibak, 2012; Sharma and Sheth, 2015). Above this temperature range, the released pyrolysis vapors may undergo secondary cracking reactions, decreasing the liquid yield in favor of permanent gas production (Duanguppama et al., 2016). Besides, other research studies have assessed the effect of temperature on the other pyrolysis products, i.e., char and permanent gas. Several authors (Acikgoz et al., 2004; Luo et al., 2004; Xu et al., 2009) have found a reduction of the solid residue remaining after pyrolysis, i.e., an improvement of the conversion, for increasing reactor temperatures due to the higher thermal energy available.

The effect of heating rate of biomass particles on the pyrolysis reaction has also been studied by many researchers (Chen et al., 2014c). It is widely accepted that rapid heating of biomass samples is required to enhance liquid production (Demirbas and Balat, 2007; Bridgwater, 2012; Onay et al., 2001; Chen et al., 2016). Biomass particle size also influences the pyrolysis process due to heat and mass transfer effects inside the solid particle (Isahak et al., 2012). The use of biomass particle sizes under 2 mm was recommended by Bridgwater et al. (1999) to reduce thermal conduction effects inside fuel particles and

enhance bio-oil yields when the pyrolysis occurs in fluidized bed reactors. Regarding experimental works, the most common conclusion is that a decrease in biomass particle size leads to larger conversion degrees and liquid yields (Kang et al., 2006; Shen et al., 2009; Garg et al., 2016).

Considering the effects of the aforementioned parameters on the pyrolysis of lignocellulosic biomass, an accurate control of the operating conditions is required to improve the conversion efficiency and maximize liquid yields. Fluidized beds are widely employed in the thermochemical conversion of biomass since they enable an easy control of the operating conditions of the chemical reactions. This technology provides high heat and mass transfer coefficients due to the contact between fuel particles and bed material (Piskorz et al., 1986). In fact, the convection heat transfer coefficient of a fixed bed increases substantially when the gas velocity is increased above the minimum fluidization velocity (Davidson and Harrison, 1971). In addition, the high thermal inertia of the solid particles that conform fluidized beds permits the isothermal operation, even when holding exothermic or endothermic chemical reactions.

Thermochemical conversion in fluidized bed reactors requires a proper fuel mixing with the bed material to maximize the heat transfer and, thus, increase the efficiency of the process. The effect of the superficial velocity of the fluidizing gas on this mixing has been studied by several authors. Rowe and Nienow (1976), who studied particle mixing and segregation

in fluidized beds, reported a better solid mixing as the excess gas velocity was increased. This conclusion was also attained by Bilbao et al. (1991), who found more homogenous straw/sand mixtures for higher gas velocities. Soria-Verdugo et al. (2011a, 2011b), applying digital image analysis to study the motion of fuel particles in a pseudo 2D fluidized bed, concluded that the axial mixing increased with the gas velocity, obtaining homogeneous mixing for gas velocities around three times the minimum fluidization velocity even for low density fuel particles, for which the buoyancy force obtained is overcome by the increase of the drag force for higher gas velocities. This result was confirmed for lab-scale 3D fluidized beds by Soria-Verdugo et al. (2011c) and Lundberg et al. (2017).

This work investigates the effects of variations in reactor temperature, biomass particle size, and excess gas velocity on the pyrolysis of *C. cardunculus* L. (cardoon) samples in a silica sand bed reactor using an innovative measuring system. The time evolution of the mass of cardoon remaining inside the reactor during the pyrolysis was measured by a precision scale, capable of detecting the mass released by the sample during its conversion while moving freely inside the reactor. The effects of temperature, excess gas velocity, and biomass particle size were studied, analyzing the synergies between the operating parameters and the reactor bed regime. The optimal excess gas velocity for the conversion of cardoon was also determined based on the measured pyrolysis time.

4.2. Materials and methods

4.2.1. Minimum fluidization velocity

The same silica sand particles used in Chapter 3 were employed as bed material for these experiments. However, the particle size selected for the bed material is smaller in this case, d_{bm} = 180 – 600 μm.

The minimum fluidization velocity of silica sand particles was measured in the reactor for temperatures up to 650 °C to evaluate the validity of the correlation of Carman-Kozeny (Carman, 1937). The measurement was performed by visual inspection of the bed surface to detect the presence of bubbles. The minimum bubbling velocity detected coincides with the minimum fluidization velocity for particles type B according to the Geldart classification (Geldart, 1973), such as the sand particles employed as bed material during the pyrolysis experiments (Kunii and Levenspiel, 1969). The measurement was conducted for reducing values of the gas flow rate, from a vigorous bubbling fluidized bed to a fixed bed stage, to prevent the effect of cohesive forces between particles on the minimum fluidization velocity. Figure 4.1 shows the experimental values of the minimum fluidization velocity together with the estimation of the Carman-Kozeny correlation. The correlation shows a high accuracy to estimate the minimum fluidization velocity of silica sand particles, considering a mean particle diameter, d_{bm}, of 390 μm, a porosity, ε, of 0.44, and a sphericity, ϕ, of 0.64, which is a

common value for irregular silica sand particles (Kunii and Levenspiel, 1969). The lower average particle size of the silica sand used in this chapter compared to that employed in Chapter 3 causes a significant reduction of the minimum fluidization velocity of the particles.

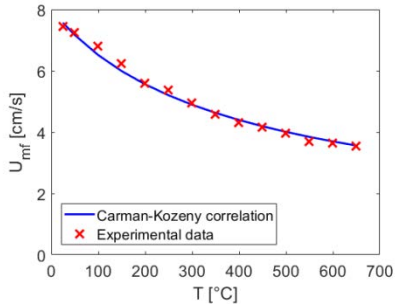

Figure 4.1. Minimum fluidization velocity of the silica sand particles as a function of reactor temperature.

4.2.2. Experimental procedure

The experimental facility described in Chapter 3 was also used to conduct the pyrolysis tests of *C. cardunculus* L. of this chapter. The only difference was the flow meter employed to determine the gas velocity of nitrogen, since the lower minimum fluidization velocity of the smaller silica sand particles used for these tests resulted in a lower nitrogen flow rate required. In this case, the nitrogen flow rate was controlled by a flow regulator and measured by a digital flowmeter PFM710-C6-E from SMC, with a measurement range from 0.2 to 10 l/min.

C. cardunculus L. was used as fuel in this chapter. The basic characteristics of this feedstock are reported in Chapter 2. The samples were previously dried for 5 h at 105 °C in a universal oven UFE 500.

The experiments consisted in recording the mass signal measured by the precision scale on which the reactor rested while the pyrolysis of cardoon occurred inside the bed. The experimental process was composed of two stages: a first one to reach the desired pyrolysis temperature and a second one in which the biomass conversion occurred while the scale monitored and recorded the mass loss. In the former stage, air was used as fluidization agent for the reactor heating with the thermal power supplied by the three electric resistors until the desired temperature for the run was reached. Once the desired temperature was attained, the fluidization flow was switched to nitrogen and the flow was adjusted to a value corresponding to a specific excess gas velocity. After removing the thermocouple from the bed and taring the scale, the recording of the evolution of mass started and a mass of around 10 g of cardoon was introduced at the top of the reactor as a batch.

The influence of three operating parameters, namely gas velocity, bed temperature, and biomass particle size, on the evolution of the mass remaining inside the reactor during the *C. cardunculus* L. pyrolysis was analyzed. The experiments were performed at three different temperatures, T (450, 550, and 650 °C), three biomass particle sizes, and five different

flows for nitrogen, corresponding to five excess gas velocities, U-U_{mf} = -2, 0, 3.5, 7, 10.5 cm/s, and resulting in different regimes: fixed bed, bed at incipent fluidization, and three different regimes of bubbling fluidized bed (Kunii and Levenspiel, 1969). The three biomass particle sizes tested are: small size (0.85 – 1.25 mm), medium size ($L_{pellet} \simeq D_{pellet}$), and large size ($L_{pellet} \simeq 3\ D_{pellet}$), where L_{pellet} and D_{pellet} are the length and the diameter of the cardoon pellets, respectively. The diameter of the cardoon pellets was D_{pellet} = 6 mm in all cases. The same values of the excess gas velocity were used for the different tests to obtain similar bubbles' properties, whose motion induced a similar distribution of biomass particles in the bed.

The combination of these variable operating parameters results in 45 different experimental conditions, shown in Table 4.1. The effects of reactor temperature and biomass particle size on the pyrolysis process were investigated by comparing the cases from different experimental conditions. In contrast, the effect of the excess gas velocity, and thus the effect of the bed regime, was studied comparing the experiments from the same campaign, i.e., maintaining the same reactor temperature and biomass particle size. The pyrolysis experiments corresponding to each operating condition were replicated to evaluate the repeatability of the experimental procedure followed, attaining deviations lower than 5% in all cases.

Table 4.1. Operating conditions used during the pyrolysis experiments.

Experimental campaign	Reactor temperature, T [°C]	Biomass particle size	Excess gas velocity, U-U_{mf} [cm/s]
1	450	Small	-2, 0, 3.5, 7, 10
2		Medium	
3		Large	
4	550	Small	-2, 0, 3.5, 7, 10
5		Medium	
6		Large	
7	650	Small	-2, 0, 3.5, 7, 10
8		Medium	
9		Large	

4.3. Results and discussion

4.3.1. Effect of excess gas velocity

As stated in the introduction, an increase of the excess gas velocity in a bubbling fluidized bed reactor promotes heat transfer by increasing the convection coefficient in the bed (Davidson and Harrison, 1971). Furthermore, a higher visible bubble flow is also obtained when increasing the excess gas velocity (Johnsson et al., 1991) and, thus, larger and more numerous bubbles are found in the bed. These larger bubbles produce a more vigorous fluidization of the bed, which enhances the axial mixing of fuel particles, even for fuel

particles with a different density from the dense bed, for which buoyancy forces appear (Soria-Verdugo et al., 2011c; Lundberg et al., 2017). Therefore, the effect of the excess gas velocity on the heat transfer and on the axial mixing of fuel particles, previously studied in the literature, will affect the reaction rate of biomass during its pyrolysis. To study the effect of the excess gas velocity on the pyrolysis of *C. cardunculus* L., the experimental results obtained for the reactor temperature of 550 °C and the small particle size will be analyzed in this section.

The mass of biomass particles remaining in the reactor during the pyrolysis process, monitored by the scale, was employed to calculate the time evolution of the percentage of fuel mass remaining in the reactor, *X*, as the ratio between the mass at each time over the initial mass of the batch of biomass particles supplied to the reactor. The results for the time evolution of the percentage of mass remaining in the reactor are depicted in Figure 4.2 (a) for the various excess gas velocities tested. The signals corresponding to the bubbling fluidized bed cases were filtered using a moving average filter to remove the vibration induced by the motion of bubbles. The filtered signal fitted the average trend of the raw signals registered by the precision scale. Further details of this filtration process can be found in a previous work (Soria-Verdugo et al., 2017a).

Figure 4.2 (a) shows a rapid decrease of the percentage of mass remaining in the reactor for all the excess gas velocities tested, motivated by the release of pyrolysis vapors, composed of

condensable and permanent gases, during the thermal decomposition of the solid biomass sample. Two different configurations are shown in Figure 4.2 (a) depending on the value of the excess gas velocity: for $U\text{-}U_{mf} \leq 0$ cm/s, i.e., for a fixed bed or an incipient fluidization regime, and for $U\text{-}U_{mf} > 0$ cm/s, corresponding to a bubbling fluidized bed regime. In the former case, when $U\text{-}U_{mf} \leq 0$ cm/s, the batch of biomass particles supplied at the top of the reactor rests stationary over the bed surface, forming a package of biomass particles. In contrast, in the latter case, the presence of bubbles in bubbling fluidized beds, when $U\text{-}U_{mf} > 0$ cm/s, promotes the dispersion of the biomass particles throughout the whole reactor, enhancing the axial mixing of fuel particles in the bed. This difference in the configuration and location of the biomass particles in the bed affects significantly the time evolution of the percentage of mass remaining in the reactor during the pyrolysis reaction, presented in Figure 4.2 (a).

For the fixed bed and incipient fluidization regimes ($U\text{-}U_{mf} \leq 0$ cm/s), shown as blue curves in Figure 4.2 (a), the heating rate of the biomass particles is reduced due to conduction heat transfer effects inside the package of particles resting stationary on the bed surface. These conduction heat transfer inside the package of biomass particles delays the pyrolysis reaction compared to the pyrolysis in a bubbling fluidized bed ($U\text{-}U_{mf} > 0$ cm/s), shown as black curves in Figure 4.2 (a), for which the package of biomass particles is dispersed rapidly in the bed by the action of bubbles, and thus, the effect of conduction heat transfer between sample particles is

negligible. Furthermore, an increase of the excess gas velocity in the bubbling fluidized bed slightly accelerates the pyrolysis process due to the increase of convection heat transfer coefficients (Davidson and Harrison, 1971) and fuel axial mixing reported in the literature (Lundberg et al., 2017).

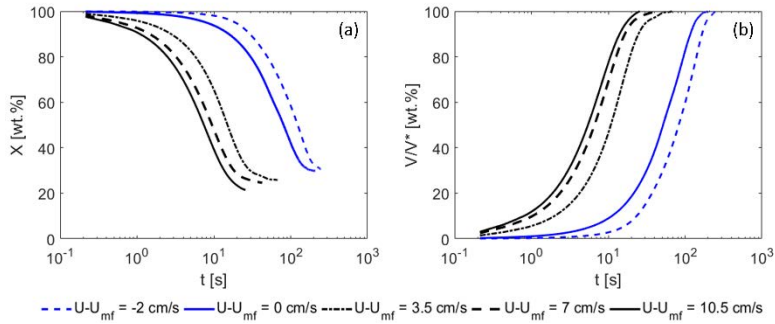

Figure 4.2. (a) Time evolution of the percentage of mass remaining in the reactor and (b) time evolution of the reacted fraction, during the pyrolysis of small particles of *Cynara cardunculus* L. with a bed temperature of 550 °C, for various excess gas velocities.

Figure 4.2 (a) also shows an effect of the excess gas velocity on the percentage of mass remaining in the reactor, X_{res}, once the pyrolysis of the sample is completed. The total volatile matter released during the pyrolysis can be calculated by difference, as $X_{vol} = 100\% - X_{res}$. A decrease of the mass remaining, i.e., an increase of the total volatile matter released, can be observed in Figure 4.2 (a) when increasing the excess gas velocity. The values of the volatile matter released during the complete pyrolysis process, X_{vol}, are reported in Table 4.3 for each excess gas velocity. A variation of X_{vol} between 69.6 wt.% for the fixed bed configuration and 78.6 wt.% for the bubbling fluidized

bed with the maximum excess gas velocity tested was obtained. The increase of the total volatile matter released with the excess gas velocity may be attributed to the higher heating rates of the fuel particles obtained due to the higher convection coefficients and axial mixing rates. The increase of the volatile matter released for higher particle heating rates is in agreement with the findings of Bridgwater et al. (1999) and Yan et al. (2011).

The effect of the different percentage of mass remaining in the reactor for each excess gas velocity can be avoided by calculating the reacted fraction, V/V^*, from the percentage of mass remaining in the reactor, X, to improve the comparison between the curves obtained for each excess gas velocity. Considering the percentage of mass remaining after the pyrolysis process, X_{res}, the reacted fraction is defined as $V/V^* = (100 - X)/(100 - X_{res})$, being 0 wt.% at the beginning of the pyrolysis process and 100 wt.% once the pyrolysis process is completed. The time evolution of the reacted fraction can be found in Figure 4.2 (b) for the various excess gas velocities tested. In this figure, a displacement of the reacted fraction curves to shorter times when increasing the excess gas velocities can be observed, as a result of the higher heating rates of fuel particles. A remarkable effect of the excess gas velocity is observed again between the fixed bed/incipient fluidization and the bubbling fluidized bed regimes, due to the dispersion of fuel particles throughout the whole reactor in the latter case, promoted by the motion of bubbles. A further increase of the excess gas velocity for the bubbling

fluidized bed regime accelerates the pyrolysis process slightly because of the higher convection heat transfer coefficients and axial mixing of biomass particles.

The reacted fraction curves for each excess gas velocity permits the calculation of the pyrolysis time, t_{pyr}, as the time required to attain a specific value for the reacted fraction. Depending on the application, the value of the reacted fraction used to define the pyrolysis time may differ. In this work, a value for the conversion factor equal to 95 wt.% was selected to calculate the pyrolysis time for each operating condition. The values of the pyrolysis time for the pyrolysis of small particles of *C. cardunculus* L. at 550 °C are reported in Table 4.2, where a substantial reduction in the pyrolysis time of 91% can be observed, from 185.9 s for the fixed bed configuration to 17.3 s for the bubbling fluidized bed regime operated at the maximum excess gas velocity tested.

Table 4.2. Total volatile matter released and pyrolysis time for the pyrolysis of small particles of *Cynara cardunculus* L. at 550 °C, as a function of the excess gas velocity.

U-U_{mf} [cm/s]	X_{vol} [wt.%]	t_{pyr} [s]
-2	69.6	185.9
0	70.1	134.0
3.5	74.3	31.1
7	75.4	20.4
10.5	78.6	17.3

The optimal biomass feeding rate for each pyrolysis reactor would be inversely proportional to the pyrolysis time

obtained. Therefore, a significant increase of the feeding rate can be expected for bubbling fluidized bed reactors compared to fixed beds or incipient fluidized beds. Thus, although an increase of the excess gas velocity from a fixed bed to that of a bubbling fluidized bed involves a higher nitrogen consumption and a higher pressure drop for the gas circulating through the bed, this higher operating cost is justified by the significant increase of the biomass feeding rate feasible in a bubbling fluidized bed, which results in a substantial increase of the biomass conversion by pyrolysis. However, once the bed is operated in a bubbling fluidized bed stage, a further increase of the excess gas velocity produces only a slight decrease of the pyrolysis time, i.e., a slight increase of the biomass feeding rate. Hence, the optimal excess gas velocity for the pyrolysis conversion of biomass particles in a bed reactor corresponds to the lowest excess gas velocity for which the bed is operated under a bubbling fluidized bed regime.

The acceleration of the pyrolysis reaction, when increasing the excess gas velocity in a bubbling fluidized bed, was also found for the rest of reactor temperatures and biomass particle sizes. Therefore, an increase of the excess gas velocity accelerates the pyrolysis process of biomass in a bubbling fluidized bed in the range of excess gas velocity tested in this study.

4.3.2. Effect of reactor temperature

Pyrolysis is an endothermic reaction that converts a solid fuel into volatile gases, remaining a carbonaceous solid residue known as char. Several works have investigated the effect of temperature on the pyrolysis process. Generally, a reduction of the solid residue remaining after the pyrolysis reaction is obtained when increasing the temperature and, thus, the conversion yield is improved for higher temperatures (Acikgoz et al., 2004; Luo et al., 2004; Xu et al., 2009). This section focuses on the effect of the reactor temperature on the pyrolysis of *C. cardunculus* L. samples conformed by particles of small size. Pyrolysis tests were conducted for reactor temperatures, T, of 450, 550, and 650 °C, for various excess gas velocities. Since the pyrolysis experiments were conducted under isothermal conditions and for a constant value of the excess gas velocity, no overestimation of the mass measured by the scale, promoted by variations of the gas pressure drop was detected, in contrast to the non-isothermal pyrolysis measurements performed by Samih and Chaouki (2015).

The time evolution of the percentage of mass remaining in the reactor, X, for various excess gas velocities is presented in Figure 4.3 for the three different reactor temperatures, T, tested, i.e., 450, 550, and 650 °C. The end of all the pyrolysis tests is established when the variation of the percentage of mass with time is lower than 0.02 wt.% in 1 s. A similar effect of the increase in excess gas velocity is observed for all the reactor temperatures, accelerating the pyrolysis process in all cases. An effect of temperature on the percentage of solid

residue obtained when the pyrolysis is completed can be observed in Figure 4.3. A reduction of the solid residue, i.e., an increase of the total volatile matter released, was obtained when the pyrolysis of *C. cardunculus* L. was carried out in a reactor operated at a higher temperature, due to the higher thermal energy available in the reactor, as previously stated by several authors (Luo et al., 2004; Demirbas and Balat, 2007; Horne and Williams, 1996; Asadullah et al., 2008; Heo et al., 2010).

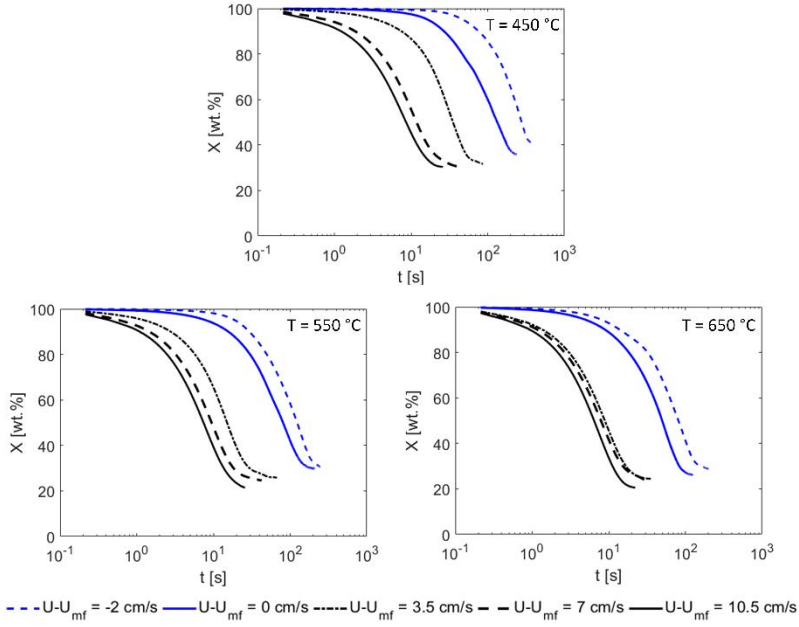

Figure 4.3. Time evolution of the percentage of mass remaining in the reactor during the pyrolysis of small particles of *Cynara cardunculus* L. for various excess gas velocities and bed temperatures.

From the time evolution of the percentage of mass remaining in the reactor, X, shown in Figure 4.3, the reaction rate, dX/dt, was calculated as its derivative with time to improve the comparison of the results obtained for the different reactor temperatures. The time evolution of the reaction rate, dX/dt, is depicted for all excess gas velocities and reactor temperatures in Figure 4.4. For all the reactor temperatures tested, an increase of the excess gas velocity results in a higher reaction rate, and thus, accelerates the pyrolysis process. As stated above, there is also a substantial difference in the reaction rate for the different configurations analyzed, obtaining low reaction rates for the fixed bed and incipient fluidization regimes, for which the biomass particles are accumulated on the bed surface, and remarkably higher values of the reaction rate for the bubbling fluidized bed regime, for which the motion of bubbles promotes the dispersion of biomass particles throughout the whole bed height.

For the bubbling fluidized bed regime, the effect of temperature is more pronounced for the lowest excess gas velocity corresponding to a bubbling fluidized bed regime, $U-U_{mf}$ = 3.5 cm/s, for which the low-density biomass particles supplied at the top of the bed are more prone to be found at the upper part of the bed due to buoyancy effects (Soria-Verdugo et al., 2011c). In this case, the higher thermal energy available in this zone of a reactor operated at a higher temperature promotes a faster pyrolysis reaction of the biomass samples because of a higher heating rate of the fuel

particles. This effect of the reactor temperature is lower when increasing the excess gas velocity, due to the more vigorous fluidization produced in the bed that counteracts the buoyancy effect, enhancing the mixing of biomass particles throughout the whole bed height.

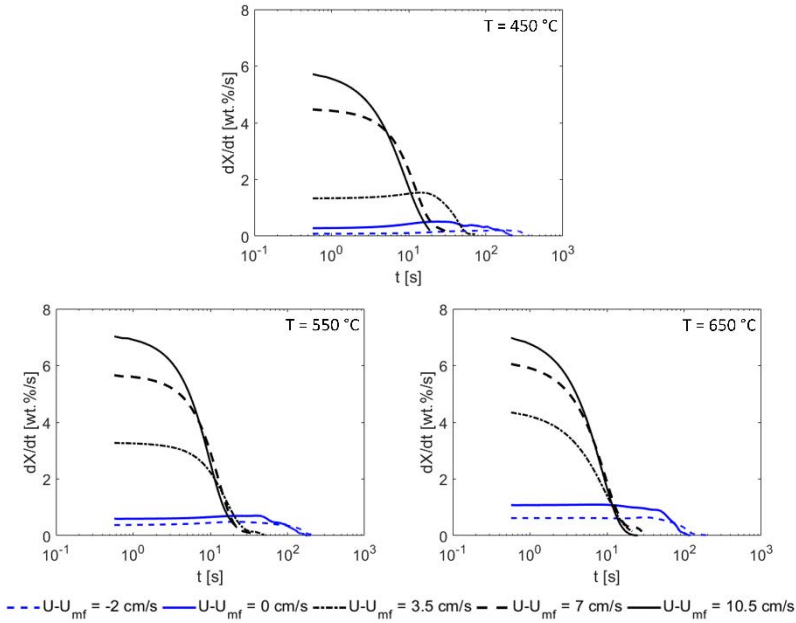

Figure 4.4. Time evolution of the reaction rate during the pyrolysis of small particles of *Cynara cardunculus* L. for various excess gas velocities and bed temperatures.

Figure 4.5 (a) shows the total volatile matter released during the pyrolysis of small particles of *C. cardunculus* L. in a bed operated at 450, 550, and 650 °C, as a function of the excess gas velocity. The total volatile matter released during the pyrolysis process increases with both the excess gas velocity and the reactor temperature. For an excess gas velocity of *U*-

U_{mf} = - 2 cm/s, corresponding to a fixed bed configuration, an increase of 11.8 wt.% in the conversion yield was attained by increasing the reactor temperature from 450 to 650 °C, whereas for an excess gas velocity of U-U_{mf} = 10.5 cm/s, corresponding to a bubbling fluidized bed regime, an increase of 10.1 wt.% in the conversion yield was obtained for the same increase of the reactor temperature. Furthermore, as can be observed in Figure 4.5 (a), the effect of increasing the reactor temperature on the conversion yield, i.e., on the total volatile matter released, is not linear, being stronger for lower reactor temperatures.

The effect of the reactor temperature on the velocity of the pyrolysis process can be observed by calculating the pyrolysis time, as the time required for the reacted fraction, V/V^*, to attain a value of 95 wt.%. The results for the pyrolysis time of small particles of *C. cardunculus* L. are plotted in Figure 4.5 (b) as a function of the excess gas velocity, for the various reactor temperatures tested.

A remarkable effect of the reactor temperature on the pyrolysis time can be observed for the fixed bed and incipient fluidization regimes, i.e., U-$U_{mf} \leq 0$ cm/s, for which the heat transfer from the pyrolysis medium to the biomass particles is limited due to a reduced contact area between the bed material and the fuel, which formed a package of particles resting stationary on the bed surface. Therefore, the higher thermal energy associated with higher temperatures results in an acceleration of the pyrolysis, due to the higher heating rate of the biomass particles enhanced by an increase of the

temperature difference between the reactor and the biomass particles. The effect of the reactor temperature is still visible for the lowest excess gas velocity corresponding to a bubbling fluidized bed regime, U-U_{mf} = 3.5 cm/s, for which buoyancy effects on the biomass particles supplied to the bed are still noticeable due to the smooth fluidization produced in the bed. These buoyancy effects forced the biomass particles to move in a restricted zone of the bed, close to the bed surface and, thus, the higher thermal energy available in this restricted zone when the bed temperature is higher increases the heating rate of the particles, reducing the pyrolysis time. This effect of the reactor temperature on the pyrolysis time is reduced for higher excess gas velocities, for which the large bubbles present in the bed increase the drag force on the biomass particles, reducing significantly the effect of buoyancy forces. Hence, the axial mixing of biomass particles is promoted by the increase in excess gas velocities, and once the biomass particles are distributed throughout the bed height, the thermal energy of the whole bed is used to heat up the biomass particles and the effect of bed temperature is lower. In terms of relative variation, a time reduction of 59.0% (189.7 s) was reached by increasing the reactor temperature from 450 to 650 °C under fixed bed conditions, U-U_{mf} = - 2 cm/s, whereas a time reduction of only 18.2% (3.15 s) was attained for the same temperature increase in a bubbling fluidized bed operated with an excess gas velocity of U-U_{mf} = 10.5 cm/s.

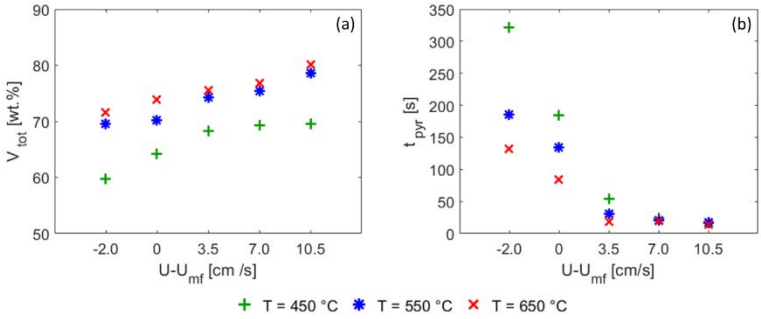

Figure 4.5. (a) Total volatile matter released and (b) pyrolysis time for the pyrolysis of small particles of *Cynara cardunculus* L. as a function of the excess gas velocity for various reactor temperatures.

The total conversion yields obtained for the small particle size of *C. cardunculus* L. in a fixed bed are comparable to those reported by Encinar et al. (2000), while the conversion measured in this chapter for the small cardoon particles in a bubbling fluidized bed are similar to those determined by Coulson and Bridgwater (2004).

The enhancement of the pyrolysis process attributed to the temperature increase was found to be independent of the particle size of the biomass samples, since the same results reported for samples conformed by small particles, i.e., larger conversion yields for all excess gas velocities and acceleration of the process at low gas velocities, were observed for the rest of particles sizes.

4.3.3. Effect of biomass particle size

Previous research on the pyrolysis of lignocellulosic biomass has shown that fuel particle size affects significantly the distribution of the three major products obtained from this conversion process, i.e., solid residue (char), liquid, and permanent gases. The common conclusion among these works is a decrease of the solid residue for the use of fine particles, and thus an increase of the conversion yield due to a reduction of heat and mass transfer effects inside the solid particles (Shen et al., 2009; Garg et al., 2016; Demirbas, 2004; Choi et al., 2012). In this study, the effect of particle size is evaluated comparing results obtained for the pyrolysis of three different particle sizes: small size (0.85 – 1.25 mm), medium size ($L_{pellet} \simeq D_{pellet}$), and large size ($L_{pellet} \simeq 3\ D_{pellet}$).

The time evolution of the reaction rate, dX/dt, is presented for a reactor temperature of 550 °C and for all the excess gas velocities and biomass particle sizes analyzed in Figure 4.6. As in the previous sections, the different configurations of the bed affect significantly the evolution of the reaction rate. Higher reaction rates are attained for bubbling bed configurations (U-$U_{mf} > 0$ cm/s) due to a better axial mixing of the biomass, whereas the static behavior of the samples over the bed material during the pyrolysis for the cases of fixed bed and incipient fluidization regimes (U-$U_{mf} \leq 0$ cm/s) resulted in a decrease of the reaction rates.

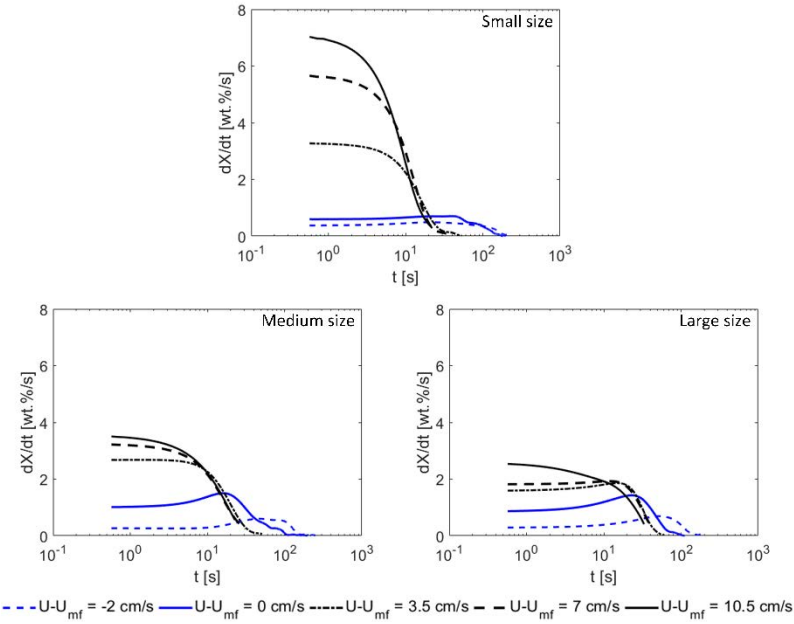

Figure 4.6. Time evolution of the reaction rate during the pyrolysis of *Cynara cardunculus* L. at 550 °C for various excess gas velocities and particle sizes.

Concerning pyrolysis at high gas velocities, in which the fuel particles are dispersed through the whole bed height, $U\text{-}U_{mf} \geq$ 7 cm/s, a reduction in biomass particle size resulted in a significant increase in the reaction rate because of the enhancement of the heating rate of these small particles. In contrast, the effect of reducing particle size was less pronounced when working under the bubbling fluidized bed regime with a lower excess gas velocity, i.e., $U\text{-}U_{mf}$ = 3.5 cm/s. In that case, as previously mentioned, the particles move freely in a restricted zone close to the bed surface due to buoyancy effects and, thus, the heating rate of the particles is limited by the thermal energy available instantaneously in

that zone. Therefore, although reducing particle size has a beneficial effect on the conversion process for a bubbling fluidized bed since the heating rate of the particles is enhanced, the limited external heat transfer for low excess gas velocities leads to slight variations on the reaction rate.

The opposite effect was found for non-bubbling bed operations, where reducing particle size resulted in a decrease of the reaction rate. Under these configurations of the bed, U-$U_{mf} \leq 0$ cm/s, for which the biomass rests stationary over the inert bed material forming a package of biomass particles, the samples compactness depends on their particle size. The compactness of smaller particles tends to be higher than for the large pellets, whose shape enhances the appearance of gaps between the pellets conforming the package of particles, through which the hot inert gas employed can easily percolate. Therefore, the effects of interparticle heat transfer inside the package of small particles is significantly higher, delaying the conversion process and enhancing charring reactions. For the pyrolysis of medium and large size particles, the higher percolation of hot inert gas between particles increases their heating rates, resulting in a higher reaction rate. The time evolution of the reaction rate of medium size particles, i.e., small pellets, in a fixed and an incipient fluidization bed shows an increase to reach a maximum reaction rate close to the end of the pyrolysis process. The appearance of this maximum for the reaction rate may be attributed to a limitation of the particles heating by thermal conduction inside them, which is enhanced by the

lower thermal gradient between the particles' surface and center at low gas velocities due to the lower convection coefficients. The maximum of the reaction rate is observed during the pyrolysis of large pellets for excess gas velocities up to $U\text{-}U_{mf}$ = 3.5 cm/s, due to the higher importance of thermal conduction inside these coarse particles.

The total volatile matter released during the pyrolysis of *C. cardunculus* L. is depicted in Figure 4.7 as a function of the excess gas velocity for each temperature and particle size analyzed. The volatile matter released increases with the excess gas velocity independently of the reactor temperature and biomass particle size. In addition, an increase of the volatile matter released, i.e., larger conversion yields, is also obtained for higher reactor temperatures as a result of the higher thermal energy available in the reactor, especially for the increase from 450 to 550 °C, due to the limited thermal energy available at 450 °C. Regarding the effect of particle size, an enhancement of the conversion yield is found for the use of coarse particles in fixed and incipient fluidization beds due to their higher heating rate promoted by the lower compactness of the package of large particles located on the bed surface. In contrast, the higher compactness of the package of small particles produced for fixed bed and incipient fluidization stages reduces the heating rate of the particles because of the importance of interparticle thermal conduction inside the package, resulting in lower values of the volatile matter released. This effect is evident for temperatures of 450 and 550 °C, whereas at 650 °C similar

values were obtained for the total volatile matter released by small and large particles. In this last case, the heat transfer limitations related to interparticle thermal conduction may be overcome by the larger temperature difference associated with the elevated reactor temperature. The pyrolysis of large particles under fixed bed conditions (U-U_{mf} = - 2 cm/s) resulted in an increase of the volatile matter released of 3.7, 0.6, and 0.2 wt.% compared to the pyrolysis of small particles, for reactor temperatures of 450, 550, and 650 °C, respectively.

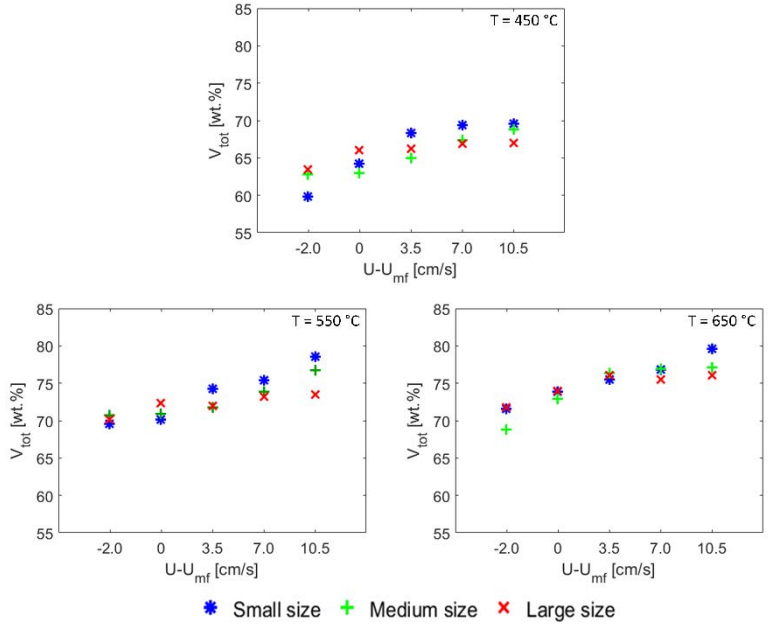

Figure 4.7. Total volatile matter released during the pyrolysis of *Cynara cardunculus* L. as a function of the excess gas velocity for various reactor temperatures and particles sizes.

The use of small particles is beneficial when the pyrolysis of *C. cardunculus* L. occurs in a bubbling fluidized bed, U-U_{mf} > 0

cm/s. At this fluidization stage, for low excess gas velocities, the biomass particles are mixed with the bed material only in the upper part of the bed due to buoyancy effects, however, the external convection on the particles is improved because of a better axial mixing compared to the fixed bed and incipient fluidization configurations. Therefore, in these cases, an increase of the volatile matter production is attained for lower particle sizes, since smaller particles are heated faster and more uniformly, preventing charring reactions.

As the excess gas velocity is increased, the fluidization becomes more vigorous and thus the fuel is more dispersed throughout the whole bed height, attaining larger volatile yields for the pyrolysis of samples consisting of small particles, whereas no significant increase in the solid conversion for samples conformed by larger particles is observed. This is caused by the importance of thermal conduction inside the biomass particles, which, in combination with a significant particle size, limits the biomass conversion, resulting in higher residue yields. Therefore, the use of finer particles is recommended to achieve larger conversion yields during the pyrolysis of biomass in a bubbling fluidized bed. For the pyrolysis of *C. cardunculus* L., the conversion increases associated with the use of the smallest particle size compared to the largest pellets during the pyrolysis in a bubbling fluidized bed operated at the maximum excess gas velocity tested, i.e., U-U_{mf} = 10.5 cm/s, were 2.5, 5.1, and 3.5 wt.% for reactor temperatures of 450, 550, and 650 °C, respectively.

The pyrolysis time for the *C. cardunculus* L. samples is plotted in Figure 4.8 as a function of the excess gas velocity for the different reactor temperatures and particle sizes tested. The effect of the excess gas velocity on the pyrolysis time is similar for all the reactor temperatures and particles sizes studied, obtaining a reduction of the pyrolysis time for higher excess gas velocities as a result of the higher heating rates of the biomass particles motivated by the higher axial mixing and convection coefficients. This time decrease with the excess gas velocity is very significant until reaching the bubbling fluidized bed stage, for which the conduction heat transfer limitations between particles are overcome when the package of biomass particles on the bed surface is broken due to the motion of bubbles inside the bed. Further increases of the excess gas velocity, once the bubbling fluidized bed regime is attained, result only in slight pyrolysis time reductions. The fluidization stage also influences on the effect of the other two parameters, i.e., reactor temperature and particle size, on the time required to complete the pyrolysis process.

Increasing the reactor temperature results in an acceleration of the biomass pyrolysis when the fuel is static forming a package of particles on the bed surface, i.e., for the fixed bed and incipient fluidization regimes, because of the increase of the heating rate of particles motivated by the larger temperature difference between the reactor and the biomass. In addition, larger particles are preferred for the pyrolysis experiments conducted under fixed bed and incipient fluidization configurations, since shorter pyrolysis times are

obtained due to the higher heating rate attributed to the lower compactness of the package conformed by these coarse particles. Time reductions of 39.6% (127.3 s), 20.2% (37.6 s) and 16.4% (21.7 s) were attained for the pyrolysis of the largest pellets in a fixed bed reactor compared to the pyrolysis of the smallest particles for reactor temperatures of 450, 550, and 650 °C, respectively.

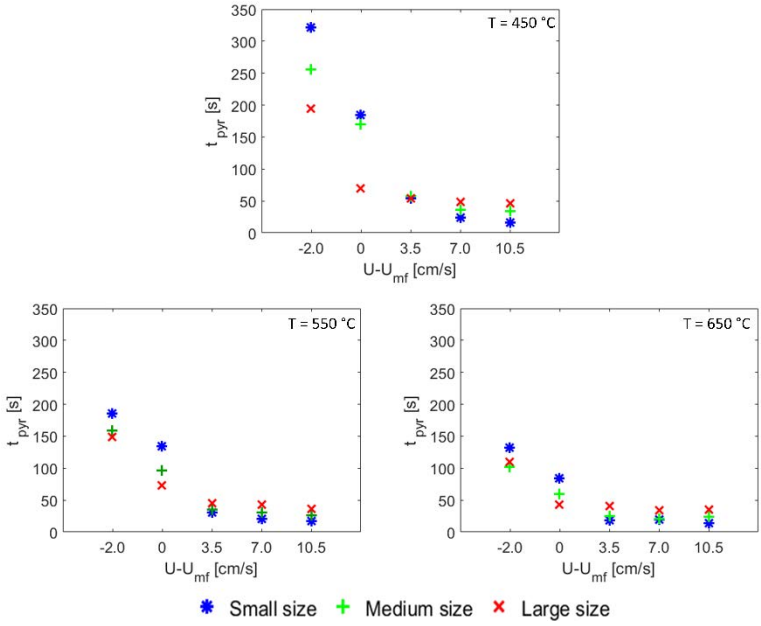

Figure 4.8. Pyrolysis times of *Cynara cardunculus* L. as a function of the excess gas velocity for samples of different particle sizes and bed temperatures of 450, 550, and 650 °C.

In contrast, once the bed is fluidized (U-U_{mf} > 0 cm/s) and the fuel is mixed with the inert material of the bubbling fluidized bed, increasing the reactor temperature leads to no time reductions. In these scenarios, the limiting factor for the biomass heating is the thermal conduction inside the biomass

particles, since the convection at the particle's external surface is enhanced by the fuel mixing with the bed material due to the motion of bubbles and by the higher convection coefficient obtained for higher excess gas velocities. Therefore, the most effective measure to accelerate the pyrolysis of biomass under bubbling fluidized bed regimes is the reduction of particle size, which decreases the effect of thermal conduction, leading to higher heating rates of the biomass particles. The pyrolysis time reductions obtained employing the small particle size instead of the largest pellets were 65.2% (46.4 s), 52.0% (36 s) and 59.3% (34.7 s) for an excess gas velocity of U-U_{mf} = 3.5 cm/s and reactor temperatures of 450, 550, and 650 °C, respectively.

The effect of the particle size on the conversion during the pyrolysis of biomass strongly depends on the fluidization stage under which the pyrolysis is conducted. When the pyrolysis occurs in a fixed or an incipient fluidization bed, where the biomass forms a package of particles resting stationary on the bed surface, the use of large particles accelerates the pyrolysis and results in larger volatile yields because of an enhancement of the biomass particles' heating rate. In contrast, the bubbles' motion characteristic of fluidized beds promotes the axial mixing of the biomass particles with the bed material, enhancing the heating rate of the fuel. When the biomass pyrolysis occurs in a bubbling fluidized bed, the thermal conduction inside the biomass particles is the limiting factor for the thermal degradation process and, thus, a reduction of the biomass particle size results in larger conversion yields and shorter pyrolysis times.

Therefore, the use of large biomass particles is advisable when the pyrolysis occurs in a reactor in which the particles form a stationary package; however, when the biomass particles are dispersed and separated from each other, as in a bubbling fluidized bed, the use of fine particles is recommended to improve the pyrolysis process.

4.3.4. Apparent kinetics of the pyrolysis process

The apparent kinetics model proposed by Reschmeier et al. (2014) and described in Chapter 3 was applied to all the pyrolysis measurements conducted in this work for *C. cardunculus* L. The comparison of the experimental results and the estimations of the apparent kinetics model permits the evaluation of the relevance of heat and mass transfer effects during the pyrolysis process. As stated in Chapter 3, the apparent kinetics model proposed by Reschmeier et al. (2014) is accurate to describe the pyrolysis of biomass, provided that the effects of heat and mass transfer inside the sample are negligible. Therefore, the deviations of the model predictions from the experimental measurements could be attributed to heat and mass transfer effects inside the biomass particles.

The time evolution of the mass percentage measured by the scale, i.e., the experimental X vs t curves, where fitted to the expression obtained from the apparent kinetics model, Eq. (3.4). For the fitting, the experimental value of the total volatile matter released by the sample, shown in Figure 4.8, was used. Thus, the only free fitting parameter was the apparent rate

coefficient, *k*, which was obtained for the pyrolysis of *C. cardunculus* L. under each operating condition. The results obtained for the apparent rate coefficient, *k*, for each case are reported in Table 4.3 together with the determination coefficient of the fitting, R^2, which informs of the accuracy of the apparent kinetics model to describe *C. cardunculus* L. pyrolysis. The values obtained for the apparent rate coefficient are similar to the average rate coefficient obtained in Chapter 2 for the pyrolysis of *C. cardunculus* L. in the TGA.

The low values of the determination coefficient, R^2, for the fixed and incipient fluidization regimes, independently of the biomass particle size, confirm the importance of heat and mass transfer effects inside the package of particles formed over the bed surface in these cases. Furthermore, although the biomass particles are rapidly dispersed throughout the bed in a bubbling fluidized regime, the R^2 values are also low for the pyrolysis of medium and large particles of *C. cardunculus* L. in a bubbling fluidized bed, i.e., U-U_{mf} = 3.5, 7, and 10 cm/s, informing of the relevance of heat and mass transfer effects inside the individual biomass particles. Therefore, the apparent kinetics model proposed is only valid to describe the pyrolysis of small cardoon particles in a bubbling fluidized bed, for which the values of the determination coefficient of the fitting are high (higher than 0.98 in all cases, except for the lower excess gas velocity and lower temperature due to the low energy available in the reactor) as a result of the slight effects of heat and mass transfer inside the small size particles.

Table 4.3. Results of the fitting of the experimental results to the apparent kinetics model.

		450 °C		550 °C		650 °C	
	U-U_{mf} [cm/s]	k [min^{-1}]	R^2 [-]	k [min^{-1}]	R^2 [-]	k [min^{-1}]	R^2 [-]
Small	-2	0.30	0.884	0.60	0.933	0.90	0.958
	0	0.66	0.952	0.96	0.965	1.44	0.956
	3.5	2.22	0.961	4.56	0.981	7.74	0.985
	7	6.42	0.987	7.20	0.989	8.28	0.992
	10.5	8.88	0.988	9.24	0.988	9.84	0.988
Medium	-2	0.42	0.902	0.72	0.917	1.08	0.949
	0	0.72	0.939	1.62	0.962	2.70	0.961
	3.5	1.98	0.915	3.84	0.971	5.34	0.976
	7	3.30	0.950	4.56	0.977	5.88	0.984
	10.5	3.66	0.972	4.98	0.973	7.02	0.982
Large	-2	0.48	0.850	0.78	0.892	1.44	0.971
	0	1.50	0.885	1.68	0.935	2.76	0.943
	3.5	1.80	0.934	2.52	0.935	3.06	0.954
	7	1.98	0.902	2.70	0.934	3.36	0.963
	10.5	2.28	0.916	3.60	0.971	4.20	0.989

4.4. Conclusions

The pyrolysis process was significantly influenced by the excess gas velocity, especially when different configurations of the bed were obtained. For the fixed and incipient fluidization beds, the biomass particles form a package that

rests stationary on the bed surface, whereas in a bubbling fluidized bed the fuel particles are dispersed and mixed with the bed material due to the motion of bubbles, enhancing the heating rate of the fuel, and thus its conversion. An increase of the reactor temperature also affects the pyrolysis, resulting in a faster process with a larger conversion yield, as an effect of the increase of the biomass heating rate because of the higher difference in temperature between the fuel and the reactor, which leads to a higher thermal power transferred from the reactor to the fuel particles.

Concerning the biomass particle size, the results were influenced by the fluidization regime under which the conversion process occurred. Larger particles sizes are preferred for reactors where the biomass forms stationary packages of particles, since the lower compactness of packages conformed by coarse particles permits a better contact between the particles surface and the hot percolating gas. However, for reactors in which the particles are rapidly dispersed, such as in bubbling fluidized bed reactors, small particle size is recommended to avoid the limiting effect of the thermal conduction inside the individual particles on their heating rate. The effects of heat and mass transfer on the pyrolysis reactions were quantified by comparing the estimations of a first-order apparent kinetics model to the experimental results. The model was found to be valid to describe the pyrolysis of small particles of *C. cardunculus* L. in a bubbling fluidized bed, where heat and mass transfer effects are negligible. However, for larger particles and/or lower

excess gas velocities corresponding to a fixed or an incipient fluidization bed, discrepancies were found between the model predictions and the experimental measurements due to heat and mass transfer inside or between the biomass particles.

Nomenclature

d_{bm} Particle diameter of the bed material [m].

D_{pellet} Diameter of *Cynara cardunculus* L. pellets [m].

k Apparent rate coefficient [s^{-1}].

L_{pellet} Length of *Cynara cardunculus* L. pellets [m].

t Time [s].

t_{pyr} Pyrolysis time [s].

T Reactor temperature [K].

U Gas velocity [m/s].

U_{mf} Minimum fluidization velocity [m/s].

V/V^* Reacted fraction [%].

X Percentage of mass of the sample [%].

X_{res} Percentage of solid residue [%].

X_{vol} Percentage of total volatile content released [%].

ε Void fraction of the bed material [–].

ϕ Sphericity of the dense phase particles [–].

CHAPTER
FIVE

Pyrolysis of *Cynara cardunculus* L. samples – Effect of operating conditions and bed stage on the yields obtained

Contents

Abstract

This chapter presents an experimental study on pyrolysis of *Cynara cardunculus* L. samples in a reactor operated as a fixed and a bubbling fluidized bed. Silica sand was employed as bed material and the influence of reactor temperature and bed regime on the conversion products obtained from pyrolysis is investigated. The pyrolysis temperatures tested were 450, 550, and 650 °C; whereas fixed bed and fluidized bed regimes were imposed to conduct the experiments by adjusting the gas excess over minimum fluidization velocity, U-U_{mf}, to -2 and 7 cm/s, respectively. The results showed that bed configuration has a strong effect on product yields. A fluidized bed operation induces a decrease in solid residues and gas yields due to the better axial mixing caused by bubbles motion, what results in an enhancement of the heat transfer and the prevention of secondary cracking reactions for the pyrolysis vapors released. Therefore, the liquid production was enlarged when pyrolysis occurred under the fluidized bed regime for all the bed temperatures tested. An increase of bed temperature for a specific bed stage causes larger conversions, i.e., decreases the solid residues, and gas yields. Concerning the liquid yield, the operation of the bed under a bubbling fluidized bed promotes the generation of liquid from condensation of the pyrolysis vapors, as a consequence of the faster heating rate of the biomass particles for this bed regime. Further analysis of the liquid phase revealed that the bio-oil fraction reached a maximum of 33.5 wt.% for a reactor

temperature of 450 °C and the bubbling fluidized bed configuration.

5.1. Introduction

The increasing demand of global energy requires sustainable alternatives to fossil fuels, capable of reducing the emission of greenhouse gases associated with energy conversion. Biomass is a promising source of energy which can be converted into valuable fuels through several processes (Demirbas, 2001; Panwar et al., 2012). Among these conversion technologies, pyrolysis is a thermochemical process consisting in the degradation of a solid fuel subjected to a temperature increase in an inert atmosphere. The products obtained from the pyrolysis of a solid fuel are bio-char, bio-oil, and permanent or non-condensable gases. The quality and quantity of each of these products are strongly affected by both the conditions employed during the pyrolysis process and the characteristics of the feedstock (Bridgwater et al., 1999). The most valuable product is the liquid bio-oil because of its ease handling, storage, and transportation to wherever the energy is required.

The bio-oil production is maximized for fast pyrolysis processes, which involves high heating rates, moderate temperatures (450-650 °C), reduced vapor residence times (below 2 s), and rapid cooling of the condensable gases (Bridgwater and Peacocke, 2000). Fast pyrolysis processes can lead to liquid yields up to 70-80% on dry basis, provided that the pyrolysis process occurs under the aforementioned

conditions (Demirbas and Balat, 2007; Bridgwater, 2012; Xiu and Shahbazi, 2012). Concerning the high heating rates, fluidized bed reactors are widely used due to the high solid-solid contact between fuel particles and bed material (Bridgwater, 1999). In addition, fluidized bed reactors present other characteristics which make them optimum to hold solid fuels pyrolysis reactions, such as a high thermal inertia, a homogeneous bed temperature, and an easy operating control (Kunii and Levenspiel, 1969). In terms of rapid condensation of the non-permanent gases, direct contact of the gas flow with a cold liquid is a common option in literature (Becidan et al., 2007; Gauthier et al., 2013; Duanguppama et al., 2016; Chen et al., 2017b; Guizani et al., 2017; Jia et al., 2017; Tan et al., 2017). In contrast, indirect contact between the gas flow and cold liquids, which is known as dry-condensation, was also employed in several works (Chang et al., 2013; Jeong et al., 2015; Farag et al., 2016; Kim, 2016). This condensation technique allows an easy recuperation of the liquid phase product with no solvent separation post-process since the liquid phases are not in direct contact at any point.

Several researchers have carried out pyrolysis studies of solid fuels under different conditions, from varying particle fuel diameter to changing the inert gas velocity, analyzing the effect on the pyrolysis products (González et al., 2001; Becidan et al., 2007; Angin, 2013; Beneroso et al., 2015; Zeng et al., 2015). Reactor temperature and residence time of the pyrolysis vapors are the most common parameters studied due to their strong effect on the pyrolysis products obtained.

The latter is commonly varied in fluidized bed reactors by adjusting the fluidization gas flow (Gerçel, 2002). However, the variation of the fluidization gas velocity affects not only the pyrolysis vapors residence time, but also the heating rate of the solid fuel particles, since a higher fluidization velocity produces a more vigorous fluidization of the bed, caused by the motion of bigger bubbles, which contributes to increase the mixing of fuel particles and bed material and thus enhances the heating rate (Soria-Verdugo et al., 2017c; Morato-Godino et al., 2018).

In this study, the effect of pyrolysis temperature and heating rate of *C. cardunculus* L. particles in a fluidized bed reactor on the product distribution is analyzed. The quantity of the three products is reported for different temperatures and fluidization regimes, which control the solid particles heating rate as stated above. In terms of liquid production, a dry-condensation system was employed for an easy collection of the liquid. Water content in the produced liquid was obtained for all the experiments, so that a distinction was made between bio-oil, which is the useful liquid phase, and generated water. Concerning the gas phase, the composition of permanent gases and its variation with the studied parameters were also reported in this chapter.

5.2. Materials and methods

5.2.1. Pyrolysis facility

Pyrolysis of *C. cardunculus* L. samples was conducted in a cylindrical fluidized bed reactor. A schematic of the experimental setup is shown in Figure 5.1. Five main parts are identified in the facility: the feeding system, the stainless-steel reactor, the condensation system, the combustion reactor, and the gas analyzers.

The feeding system was composed of a hopper, where the biomass was stored at the beginning of each experiment, and a screw, which introduced the biomass directly into the bed at a velocity controlled by an electric motor. The biomass was weighted prior to the experiment and at the end, to quantify the amount of biomass introduced in the reactor in each experiment. Before the experiment, the entire system was purged by a low flow of nitrogen to maintain an inert atmosphere in the whole feeding system. As a safety measure, a water column with a height of around 1 m ($\Delta p \approx 0.1$ bar) was connected to the feeder, to facilitate the gas exhaust in the event of an excessive pressure inside the system.

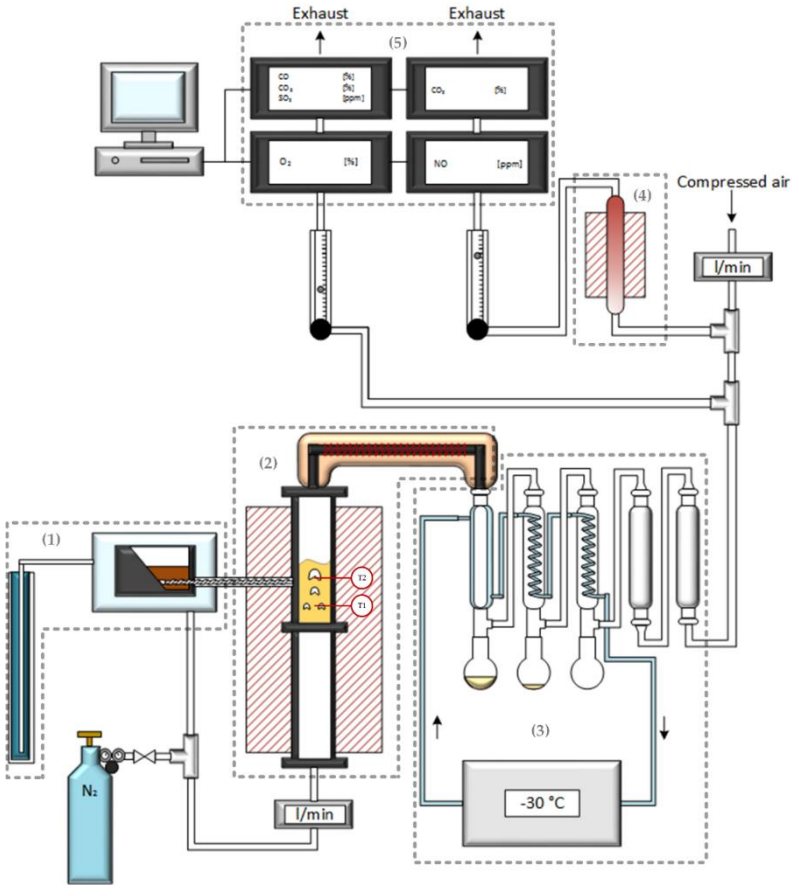

Figure 5.1. Schematic of the pyrolysis facility. (1) Feeding system, (2) Stainless-steel bed reactor, (3) Condensation system, (4) Combustion reactor, (5) Gas analyzers.

The cylindrical stainless-steel reactor had a height, h, of 50 cm and an inner diameter, d_i, of 3.7 cm, and it was surrounded by an electric furnace to keep the desire temperature for each experiment. Two thermocouples type-k, namely T_1 and T_2, were located at the middle part of the reactor to measure the bed temperature during the process. A metallic mesh with a pore size of 45 μm was located at the exit of the reactor as a

filter to prevent the pneumatic transportation of char and bed material into the bio-oil collectors.

The transfer line was constructed from a stainless-steel pipe with an inner diameter of 1 cm and a total length of 50 cm. It was surrounded by an electric resistor to maintain a minimum temperature of 250 °C to prevent the condensation of tars and its eventual blockage during the experiments.

As shown in Figure 5.1, once the gas produced during the pyrolysis process leaves the transfer line, it flows through the condensation system. First, the tars contained in the pyrolysis vapors condensate into three cooling systems. The first condenser was a glass tube surrounded by a jacket through which the refrigerant, methanol in this case, flowed. The other two condensers had an inner spiral through which the refrigerant was pumped. The liquid products from the condensers were collected in flasks placed right after each condenser. The temperature of the refrigerant was set at -30 °C by a chiller. Finally, the gas stream flowed through two cotton filters to protect the gas analyzers from the condensable compounds generated during the conversion process.

The combustion reactor consists of a quartz tube surrounded by a ceramic furnace. The desired temperature for the combustion was reached by means of an electric resistor located inside of the ceramic material. A thermocouple type-k was placed at the wall of the ceramic furnace to measure the reactor temperature. This reactor helped to consider indirectly

the unmeasured gases as it forced the complete combustion of a fraction of the gas stream, obtaining the total carbon of the produced gases.

The gas analyzers employed in this work were different depending on the composition of the gas to be measured. The evolved gases were conducted through a non-dispersive infrared (NDIR) analyzer for CO and CO_2 detection; SO_2 concentration was measured by means of an infrared analyzer; and a chemiluminiscence analyzer was employed for NO detection. Further details of both the combustion reactor and the analyzers are reported in Giuntoli et al. (2010).

5.2.2. Bed material

In this chapter, silica sand was also employed as bed material for all the experiments. A mass of 165 g of silica sand particles was introduced into the reactor to obtain a height of the fixed bed, h_b, of 10 cm. The relation between fixed bed height and the fluidized bed diameter, h_b/d_i, was 2.7, a similar value to previous experiments presented in Chapter 4. The silica sand employed as bed material is the same as in Chapter 4, with an average diameter, d_p, of 390 μm, corresponding to particles type B according to Geldar's classification (Geldart, 1973). The minimum fluidization velocity of the silica sand employed can be observed in Figure 4.2 as a function of the bed temperature.

5.2.3. Mass balance

During the pyrolysis process, three main products are obtained: solid residue or char, liquid fraction consisting of bio-oil and water, and permanent gases. The char yield was calculated as the sum of the solid mass collected from the reactor and the transfer line, subtracting the initial mass of silica sand. The liquid yield was determined weighting the condensation system before and after each experiment. The fractions collected in the flasks were subjected to further analysis to determine the water content, since using acetone was not required to recuperate this fraction. The gas yield was calculated as the time integral of the signal reported by the analyzers. The commercial analyzers employed in this research were only able to measure CO, CO_2, SO_2, and NO. The rest of the permanent gases formed during the pyrolysis process, such as H_2, CH_4, and other hydrocarbons, were undetected and, thus, may be a source of error in the mass balance calculation. To minimize the error committed, the final flow was split in two streams and one part was combusted with air in excess in a combustion reactor to quantify the total carbon of the undetected gases.

5.2.4. Variables of interest

This work investigates the influence of reactor temperature and bed regime on the product distribution obtained from the pyrolysis of *C. cardunculus* L. samples. Experiments were conducted under different combinations of reactor

temperature and bed regime. The selected values for temperature, T, were 450, 550, and 650 °C; whereas the bed regimes tested were fixed and fluidized bed configurations. In the cases of fixed bed, the flow rate of nitrogen supplied to the reactor was adjusted to obtain an excess gas velocity, U-U_{mf}, of -2 cm/s for all the temperatures; while for the fluidized bed configuration, this value was set to 7 cm/s. These values for the excess gas velocity were also studied in the previous chapter, where the conversion rate of *C. cardunculus* L. samples was obtained for different gas velocities, temperatures, and biomass particle sizes. Therefore, it was decided to maintain these values, together with those of reactor temperature, to link both experimental campaigns and investigate the effect of the same parameters on the gas and liquid formation. Concerning the biomass particle size, no variation of this parameter was studied in this chapter due to limitations related to the screw feeder, which was only able to introduce biomass within a very narrow particle range. Consequently, the small particle size studied in Chapter 4, d_p = 0.85 – 1.25 mm, was selected for the experiments in this chapter, since this size was adequate for the feeding system. Therefore, a total of six different cases were studied. For all the cases, an analysis of the product yields, water content in liquid product, and permanent gases composition was carried out.

5.3. Results and discussion

5.3.1. Product yields

The mass balance of each experiment was carried out to quantify the mass losses during the experiment. Table 5.1 shows the mass balance closures for all the experiments conducted.

Table 5.1. Mass closure percentage as a function of reactor temperature and bed regime.

T [°C]	Fixed bed [wt.%]	Fluidized bed [wt.%]
450	91.4	85.0
550	90.4	83.2
650	79.4	81.7

The mass balance was always closed between 79.4 and 91.4 wt.% (dry basis). An increase of the mass lost with the reactor temperature can be observed for both the fixed and the fluidized bed regimes. This increase of mass lost with temperature may be attributed to the generation of permanent gases undetectable for the gas analyzers employed. However, the carbon content from these non-detected permanent gases was also considered through their total combustion.

The pyrolysis products for all the experiments were quantified to determine the produced amount of char, liquid, and gas. Figure 5.2 shows the variation of the pyrolysis

products with temperature for the different bed stages. These results, and all the results reported in this chapter, are corrected considering the mass balance closures of each experiment, included in Table 5.1, to facilitate the comparison of the results obtained for different operating conditions.

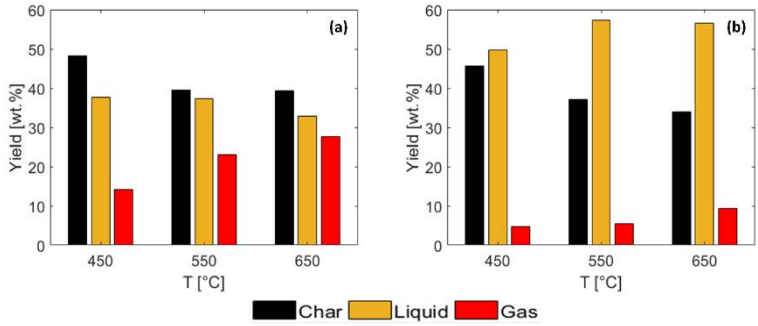

Figure 5.2. Product distribution as a function of temperature for (a) fixed bed and (b) fluidized bed regimes.

Figure 5.2 shows that an increase in the reactor temperature resulted in a reduction in the final solid residue at the two reactor configurations, due to a higher amount of thermal energy available in the reactor (Luo et al., 2004; Xu et al., 2009). This effect is more significant in the fluidized bed stage, as a consequence of the better mixing of the bed material and biomass, promoting a better heat transfer to the *C. cardunculus* L. particles (Soria-Verdugo et al., 2017c; Morato-Godino et al., 2018). Besides, the reason for this enhancement of the conversion yield with temperature may be a combination of a more extensive primary degradation of the biomass and a higher thermal decomposition of the char. This result agrees with other works from literature (Encinar et al., 2000;

Demirbas, 2004; Sharma and Sheth, 2015). The results of the solid residue are in agreement with those obtained in Chapter 4, where a significant decrease of the solid residue when increasing the bed temperature from 450 to 550 °C was also detected for the fixed and fluidized bed regimes, whereas only a slight reduction of the char generated when the bed temperature was further increased from 550 to 650 °C was obtained.

The permanent gas yield increased as reactor temperature was raised due to secondary cracking reactions suffered by the released pyrolysis vapors (Commandré et al., 2011). In contrast, the effect of temperature on the liquid production was different depending on the bed configuration selected for the process. Under fixed bed regime, an increase of the reactor temperature resulted in a reduction of the liquid yield. The reason for this decrease may be the secondary cracking reactions of the condensable species of the pyrolysis vapors to generate permanent compounds with lower molecular weight. However, rising temperature for the fluidized bed operation promoted an increase of the liquid yield, reaching a maximum at a reactor temperature of 550 °C. Nevertheless, further temperature increases over 550 °C resulted in a reduction of the liquid production in favor of the permanent gas formation due to the aforementioned thermal cracking reactions (Mohan et al., 2006).

The bed configuration influences not only the effect of temperature on the product distribution, but also the produced percentage of each product. Employing a fluidized

bed instead of a fixed bed resulted in decreasing solid residues by 2.6, 2.5, and 5.4 wt.% for reactor temperatures of 450, 550, and 650 °C, respectively. Similarly, the permanent gas yield was found to decrease by 9.4, 17.6, and 18.3 wt.% with the use of the fluidized bed configuration for the mentioned temperatures. In contrast, considering these three reactor temperatures, the liquid production experienced increases by 11.9, 20.1, and 23.6 wt.% under a bubbling bed regime with respect to the fixed bed stage. The reason for these variations in the pyrolysis products may be related to the differences in the heat transfer to the biomass samples depending on the bed configuration, as stated in Chapter 4.

For all cases, the feeding system introduced the biomass in the same zone of the reactor. In cases of fixed bed, the compactness of the bed restricted the biomass location, since it kept static in a certain region of the bed over the surface. Therefore, the endothermic process of the pyrolysis generated a decrease of the local temperature of the bed in this zone, delaying the conversion process. However, when operating under a bubbling fluidized bed regime, the motion of bubbles characteristic of the fluidized bed induces a better mixing of the fuel with the bed material, enhancing the dispersion of the fuel particles in the bed. This mixing effect accelerates the thermal degradation of the biomass samples, which occurs in the whole bed for a vigorous bubbling stage.

Another aspect accounting for the larger fuel conversion and liquid production found in the fluidized bed operation is the enhancement of the convective heat transfer coefficient due to

the higher carrier gas velocity employed, resulting in faster heating rates of the fuel particles (Akhtar and Amin, 2012; Demirbas and Balat, 2007). In addition, this higher carrier flow permits the rapid removal of the vapor from the reactor, as previously mentioned, reducing the residence time of the vapors and, thus, minimizing the probability of suffering secondary reactions (Olukcu et al., 2002; Bridgwater, 2012), what enlarges the liquid production at the expense of permanent gas formation.

5.3.2. Water content in liquid product

The liquid product reported in this work was formed by two components: organic compounds (bio-oil) and water. The water collected after each experiment was completely generated through the pyrolysis reactions since the samples were dried prior to the experiments. Therefore, the original water derived from biomass is not considered in the analysis. While the previous section reported the total liquid yield for different reactor temperatures and bed configuration, in this section the variations of the different components in the liquid fraction are discussed. Figure 5.3 shows the yields of water and liquid organic compounds as a function of temperature, for fixed and fluidized bed regimes.

As discussed in the previous section, an increase of the reactor temperature under fixed bed conditions promotes a diminution of the total liquid produced, reaching the minimum production for the highest temperature. However,

operating under the fluidized bed configuration generated higher amounts of liquid at higher temperatures, reaching the highest liquid production for an intermediate temperature of 550 °C. Nevertheless, the optimum pyrolysis conditions are not those for which largest quantities of liquid are produced, but those for which the largest bio-oil yield with the minimum amount of water is generated, since water reduces the heating value of the bio-oil.

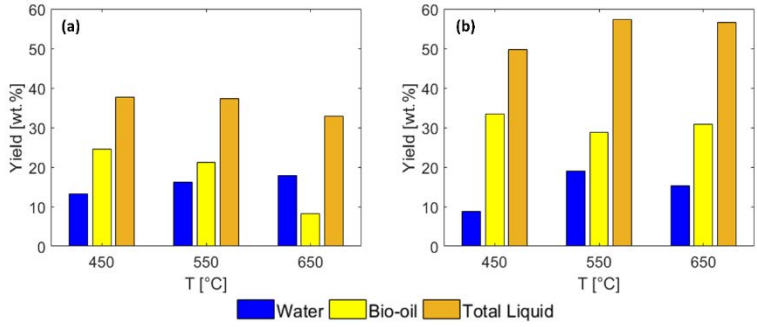

Figure 5.3. Liquid phases distribution as a function of temperature for (a) fixed bed and (b) fluidized bed regimes.

For a fixed bed configuration, the water yield increases slightly with temperature, presenting a value of around 16 wt.% for all the reactor temperatures tested. Nonetheless, a notable reduction of the oil produced is observed when temperature increases. Reductions in the bio-oil yield of 3.4 and 13.0 wt.% were obtained as temperature was increased from 450 to 550 °C and from 550 to 650 °C, respectively. These reductions of bio-oil yield with temperature may be attributed to secondary cracking of tars, promoted by high bed temperatures and high pyrolysis vapors residence times, due

to the low gas velocity in the fixed bed regime (Pütün et al., 2002; Olukcu et al., 2002).

In contrast, for a fluidized bed configuration, no clear effect of the temperature in the water or bio-oil produced is observed. The pyrolysis process generates much larger bio-oil yields compared to the fixed bed cases, reaching a maximum of 33.5 wt.% at a reactor temperature of 450 °C. In addition, at this temperature the lowest water yield was obtained, corresponding to 8.7 wt.%. The better mixing of the fuel particles and bed material inside the reactor in the fluidized bed stage resulted in an enhanced heat transfer, promoting higher conversion rates. Furthermore, the higher gas velocity in the fluidized bed causes a reduction of the residence time of pyrolysis vapors, preventing secondary reactions of the condensable molecules (Olukcu et al., 2002; Bridgwater, 2012).

5.3.3. Permanent gases

The analyzers employed in this research measured the concentration of CO, CO_2, SO_2, and NO in the permanent gases released from the pyrolysis process. However, the concentration of NO was found to be negligibly low in all cases and, thus, NO concentration is not reported in this section. As previously mentioned, the product gas was divided into two flows for the complete combustion of a fraction of the stream. Thereby, the total carbon contained in the product gas was obtained and the unmeasured gases, i.e., H_2, CH_4 and other hydrocarbons, were indirectly quantified.

Figure 5.4. shows the distribution of the compounds which were found in the permanent gases, not considering the CO_2 obtained from the post-combustion process.

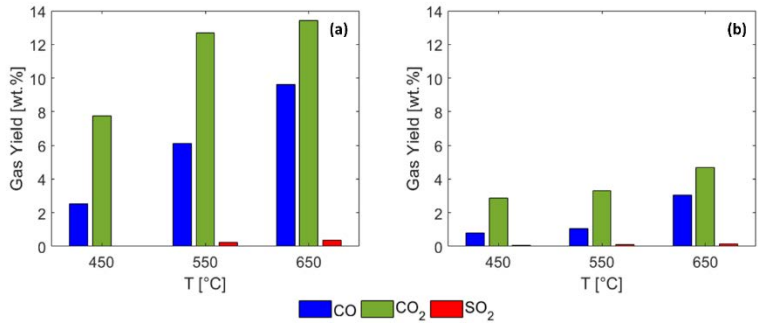

Figure 5.4. Permanent gases distribution for different temperatures under (a) fixed bed and (b) fluidized bed regimes.

The formation of permanent gases was more significant for the fixed bed than for the fluidized bed pyrolysis, since the combination of a lower heating rate of the biomass particles and the larger residence time of the pyrolysis vapors in the hot zone increased the secondary thermal cracking reactions, reducing the liquid fraction in favor of the gas formation (Akhtar and Amin, 2012; Demirbas and Balat, 2007). This explanation is also consistent with the liquid decrease reported in the previous sections for the fixed bed experiments. CO_2 was the main component of the permanent gases for all the temperatures and bed configurations. The maximum yields obtained for this compound correspond to a temperature of 650 °C for both the fixed bed and the fluidized bed configuration, respectively. The lower increase observed

as temperature was raised from 550 to 650 °C under a fixed bed regime, compared to the increase between 450 and 550 °C, may be attributed to the cracking reactions of the pyrolysis vapors due to the long residence time and temperature, resulting in a diminution of CO_2 in favor of the CO formation. CO was the gas with the second largest yield, attaining maximum values of 9.6 and 3.0 wt.% for a temperature of 650 °C under fixed bed and fluidized bed configuration, respectively. SO_2 increased slightly with temperature at the two bed regimes, obtaining a maximum concentration of 0.36 wt.% for the fixed bed and 0.16 wt.% for the fluidized bed, operated in both cases at 650 °C.

This work also presents the total retention of C, O, and S in the permanent gases for all the configurations studied. Figure 5.5 shows the retention of the three elements analyzed in the permanent gases, for the different temperatures employed, under the fixed bed and fluidized bed regimes. These retention percentages were calculated considering the concentration of the different components of the permanent gases generated and the feeding rate and elemental composition of the *C. cardunculus* L. employed as fuel.

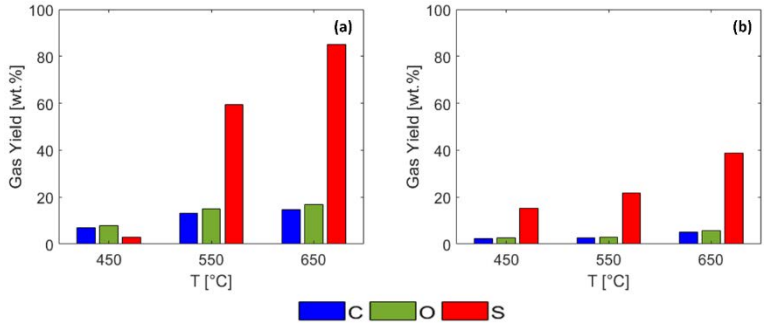

Figure 5.5. Retention percentage of C, O, and S in permanent gases for different temperatures under (a) fixed bed and (b) fluidized bed regimes.

An increase in reactor temperature resulted in larger quantities of C, O, and S in the produced gas for the two bed configurations. This is consistent with the results shown in Figure 5.4, where larger gas yields were attained as temperature increased. The operation of the bed under a bubbling fluidized regime was found to promote the retention of sulfur in the solid and/or liquid yield instead of in the permanent gases, preventing eventual environmental problems derived from the emission of this pollutant. Similarly, lower retention of carbon and oxygen were found when the pyrolysis of biomass occurred under a bubbling fluidized bed regime, since the total gas yield was decreased for this bed configuration.

5.4. Conclusions

In this chapter, the pyrolysis of *C. cardunculus* L. was conducted under different reactor temperatures and bed

configurations to study the effect of these two parameters on the product distribution. The temperature values tested were 450, 550, and 650 °C; whereas the bed configurations under which the conversion took place were fixed and fluidized bed. The results of the mass balance closures were higher than 79 wt.% in all cases, which are proper values compared to those reported in literature. Temperature increases resulted in a diminution of the solid residue (char) and an increase of the permanent gas production, regardless the selected bed configuration, fixed or fluidized bed. However, the tendencies observed for temperature increases in terms of liquid production were different depending on the bed regime employed. A reduction of the total liquid production, i.e., water and bio-oil, was observed under the fixed bed stage as temperature increased. In contrast, a maximum total liquid production was attained at an intermediate temperature of 550 °C for the fluidized bed configuration. Nevertheless, further analysis of the liquid phase showed that the optimum conditions for bio-oil production were operating at a reactor temperature of 450 °C under both a fixed and a fluidized bed configuration, since under these conditions the organic phase was maximized, and the water content was minimum.

Concerning the bed configuration influence on the product distribution, the results showed that employing a bubbling fluidized bed configuration resulted in a slight reduction of the solid residue and a drastic diminution of the gas produced in favor of the generation of the liquid yield for all the temperature values tested. The reason for this enhancement of

the liquid production was a better mixing between biomass particles and bed material inside the fluidized bed, which promotes a better heat transfer from the solid bed material to the fuel, attaining higher solid conversions and preventing secondary reactions of the pyrolysis vapors released. In addition, employing a fluidized bed to convert the biomass promoted a beneficial effect regarding environmental issues, since the sulfur content of the permanent gases was reduced compared to that obtained from the operation with the fixed bed configuration.

Nomenclature

d_{bm} Particle diameter of the bed material [m].

d_i Inner diameter of the reactor [m].

d_p Diameter of *Cynara cardunculus* L. [m].

h Height of the reactor [m].

h_b Height of the fixed bed [m].

T Reactor temperature [K].

U Gas velocity [m/s].

U_{mf} Minimum fluidization velocity [m/s].

Δp Pressure drop [Pa].

CHAPTER
SIX

Conclusions

In this PhD. Thesis, experimental measurements of *Cynara cardunculus* L. and sewage sludge pyrolysis were performed in fluidized bed reactors, to identify the effect of various operational parameters on the performance of the process. *C. cardunculus* L. was selected as biomass feedstock due to its advantages as an energy crop, such as low water requirement and growth on non-arable land for food. In contrast, sewage sludge was selected to study their potential for pyrolysis in a fluidized bed reactor as a way of disposal and energetic valuation of this residue.

A basic characterization of the *C. cardunculus* L. and sewage sludge was accomplished to determine their composition. In addition, simplified DAEM was applied to derive the kinetic parameters of the pyrolysis of these feedstocks from TGA measurements. *C. cardunculus* L. samples presented activation energy values ranging from 150 to 450 kJ/mol and pre-exponential factor values from 10^{12} to 10^{13} s^{-1}, whereas for sewage sludge samples variations between 200 and 400 kJ/mol and between 10^{15} and 10^{25} s^{-1} were obtained for the activation energy and the pre-exponential factor, respectively.A first experimental campaign was conducted in a fluidized bed reactor to investigate the effect of reactor

temperature, bed regime, and gas velocity, on the sewage sludge pyrolysis process. A novel experimental technique was employed for the study, consisting in installing the reactor over a precision scale capable of detecting the mass released by the sample during pyrolysis, while moving freely in the bed. Based on the mass measurement monitored by the scale, the time evolution of the reacted fraction and the pyrolysis time during the sewage sludge thermal degradation was obtained as a function of the operating parameters. The experimental results were used to validate a simple apparent kinetics model that enables the prediction of the pyrolysis time of sewage sludge particles in a bubbling fluidized bed reactor depending on the operating conditions.

The same experimental facility and measurement technique was employed to evaluate the pyrolysis of *C. cardunculus* L. in a fluidized bed. In addition to bed temperature, bed regime, and gas velocity, the effect of the particle size of *C. cardunculus* L. was also quantified. The effect of the biomass particle size on the pyrolysis process was found to be strongly affected by the bed regime. For an operation under a bubbling fluidized bed stage, where biomass particles are rapidly dispersed throughout the whole bed by the action of ascending bubbles, small particle size is recommended to accelerate the pyrolysis process as a result of a faster heating of fine particles. However, when the bed is operated under a fixed bed regime, the biomass supplied to the bed as a batch forms a package of particles whose compactness depends on the particle size, obtaining a faster pyrolysis process for coarser particles.

The validity of the apparent kinetics model to describe the pyrolysis of *C. cardunculus* L. was also tested, finding that the model is valid provided that the effect of heat transfer is limited, i.e., for the pyrolysis of small *C. cardunculus* L. particles in a bubbling fluidized bed.

Finally, a different approach was considered to study the pyrolysis of *C. cardunculus* L. samples, using a new fluidized bed reactor facility, where the products of pyrolysis can be collected and analyzed. In this new experimental campaign, the effect of bed temperature and bed regime on the solid, liquid and gas yields obtained from *C. cardunculus* L. pyrolysis was evaluated. The bio-oil generation from the condensation of *C. cardunculus* L. pyrolysis vapors was found to be enhanced for the operation of the bed as a bubbling fluidized bed for all the temperatures tested, due to the lower residence time of the vapors in the reactor, which limits secondary cracking reactions of tars.

References

Açikalin K., Karaca F., Bolat E. Pyrolysis of pistachio shell: effects of pyrolysis conditions and analysis of products. Fuel 2012; 95:169-177.

Acikgoz C., Onay O., Kockar O.M. Fast pyrolysis of linseed-product yields and compositions. Journal of Analytical and Applied Pyrolysis. 2004; 71:417-429.

Adánez J., Abad A., Mendiara T., Gayán P, de Diego L.F., García-Labiano F. Chemical looping combustion of solid fuels. Progress in Energy and Combustion Science 2018; 65:6-66.

Akhtar J., Amin N.S. A review on operating parameters for optimum liquid oil yield in biomass pyrolysis. Renewable and Sustainable Energy Reviews 2012; 16:5101-5109.

Alvarez J., Amutio M., Lopez G., Barbarias I., Bilbao J., Olazar M. Sewage sludge valorization by flash pyrolysis in a conical spouted bed reactor. Chemical Engineering Journal 2015; 273:173-183.

Anca-Couce A. Reaction mechanisms and multi-scale modelling of lignocellulosic biomass pyrolysis. Progress in Energy and Combustion Science 2016; 53:41-7.

Angin D. Effect of pyrolysis temperature and heating rate on biochar obtained from pyrolysis of safflower seed press cake. Bioresource Technology 2013; 128:593-597.

Arazo R.O., Genuino D.A.D., de Luna M.D.G., Capareda S.C. Bio-oil production from dry sewage sludge by fast pyrolysis in an electrically-heated fluidized bed reactor. Sustainable Environmental Research 2017; 27:7-14.

Asadullah M., Rahman M.A., Ali M.M., Motin M.A., Sultan M.B., Alam M.R., Rahman M.S. Jute stick pyrolysis for bio-oil production in fluidized bed reactor. Bioresource Technology 2008; 99:44-50.

Atienza-Martínez M., Fonts I., Lázaro L., Ceamanos J., Gea G. Fast pyrolysis of torrefied sewage sludge in a fluidized bed reactor. Chemical Engineering Journal 2015; 259:467-480.

Baghurst D.R., Mingos D.M.P. Superheating effects associated with microwave dielectric heating. Journal of the Chemical Society, Chemical Communications 1992; 9:674-677.

Bartoli M., Rosi L., Giovannelli A., Frediani P., Frediani M. Production of bio-oils and bio-char from Arundo donax through microwave assisted pyrolysis in a multimode batch reactor. Journal of Analytical and Applied Pyrolysis 2016; 122:479-489.

Bates R.B., Ghoniem A.F. Biomass torrefaction: Modeling of volatile and solid product evolution kinetics. Bioresource Technology 2012; 124:460-469.

Becidan M., Skreiberg O., Hustad J.E. Products distribution and gas release in pyrolysis of thermally thick biomass residues samples. Journal of Analytical and Applied Pyrolysis 2007; 78:207-213.

Beneroso D., Bermúdez J.M., Arenillas A., Menéndez J.A. Influence of carrier gas on microwave-induced pyrolysis. Journal of Analytical and Applied Pyrolysis 2015; 113:153-157.

Bilbao R., Lezaun J., Menéndez M., Izquierdo M.T. Segregation of straw/sand mixtures in fluidized beds in non-steady state. Powder Technology 1991; 68:31-35.

Bresters A.R., Coulomb I., Deak B., Matter B., Saabye A., Spinosa L., Utvik A.Ø., Uhre L., Meozzi P. Sludge Treatment and Disposal - Management Approaches and Experiences. Environmental Issues Series no. 7, 1-53, 1997 ISWA, European Environment Agency.

Bridgwater A.V. Principles and practice of biomass fast pyrolysis processes for liquids. Journal of Analytical and Applied Pyrolysis 1999; 51:3-22.

Bridgwater A.V. Review of fast pyrolysis of biomass and product upgrading. Biomass and Bioenergy 2012; 38:68-94.

Bridgwater A.V., Meier D., Radlein D. An overview of fast pyrolysis of biomass. Organic Geochemistry 1999; 30:1479-1493.

Bridgwater A.V., Peacocke G.V.C. Fast pyrolysis processes for biomass. Renewable and Sustainable Energy Reviews 2000; 4:1-73.

Cai J., Liu R. New distributed activation energy model: Numerical solution and application to pyrolysis kinetics of some types of biomass. Bioresource Technology 2008; 99:2795-2799.

Cai J., Wu W., Liu R. An overview of distributed activation energy model and its application in the pyrolysis of lignocellulosic biomass. Renewable and Sustainable Energy Reviews 2014; 36:236–246.

Carman P.C. Fluid flow through granular beds. Transactions of the Institution of Chemical Engineers 1937; 15:150-166.

Ceylan S., Kazan D. Pyrolysis kinetics and thermal characteristics of microalgae Nannochloropsis oculata and Tetraselmis sp. Bioresource Technology 2015; 187:1-5.

Chang S., Zhao Z., Zheng A., Li X., Wang W., Huang Z., He F., Li H. Effect of hydrothermal pretreatment on properties of bio-oil produced from fast pyrolysis of eucalyptus wood in a fluidized bed reactor. Bioresource Technology 2013; 138:321–328.

Chen D., Li Y., Cen K., Luo M., Li H., Lu B. Pyrolysis polygeneration of poplar wood: Effect of heating rate and pyrolysis temperature. Bioresource Technology 2016; 218:780-788.

Chen D., Mei J., Li H., Li Y., Lu M., Ma T., Ma Z. Combined pretreatment with torrefaction and washing using torrefaction liquid products to yield upgraded biomass and pyrolysis products. Bioresource Technology 2017a; 228:62-68.

Chen L., Wang S., Meng H., Wu Z., Zhao J. Study on gas products distributions during fast co-pyrolysis of Paulownia wood and PET at high temperature. Energy Procedia 2017b; 105:391-397.

Chen D., Yin L., Wang H., He P. Pyrolysis technologies for municipal solid waste: A review. Waste Management 2014a; 34:2466-2486.

Chen D., Zheng Z., Fu K., Zeng Z., Wang J., Lu M. Torrefaction of biomass stalk and its effect on the yield and quality of pyrolysis products. Fuel 2015; 159:27-32.

Chen D., Zhou J., Zhang Q. Effects of heating rate on slow pyrolysis behavior, kinetic parameters and products properties of moso bamboo. Bioresource Technology 2014c; 169:313-319.

Chen D., Zhou J., Zhang Q., Zhu X. Evaluation methods and research progresses in bio-oil storage stability. Renewable and Sustainable Energy Reviews 2014b; 40:69-79.

Choi H.S., Choi Y.S., Park H.C. Fast pyrolysis characteristics of lignocellulosic biomass with varying reaction conditions. Renewable Energy 2012; 42:131-135.

Coats A.W., Redfern J.P. Kinetic parameters from thermogravimetric data. Nature 1964; 201, 68-69.

Commandré J.M., Lahmidi H., Salvador S., Dupassieux N. Pyrolysis of wood at high temperature: The influence of experimental parameters on gaseous products. Fuel Processing Technology 2011; 92:837-844.

Coulson M., Bridgwater A.V. Fast pyrolysis of annually harvested crops for bioenergy applications. Proceeding of the 2nd World Conference on Biomass, vol. I, 2004, p. 1098.

Czernik S., Bridgwater A.V. Overview of Applications of Biomass Fast Pyrolysis Oil. Energy and Fuels 2004; 18:590-598.

Damartzis T.H., Vamvuka D., Sfakiotakis S., Zabaniotou A. Thermal degradation studies and kinetic modeling of cardoon (*Cynara cardunculus*) pyrolysis using thermogravimetric analysis (TGA). Bioresource Technology 2011; 102:6230-6238.

Davidson J.F., Harrison D. Fluidised particles. Cambridge University Press. 1963.

Davidson J.F., Harrison D. Fluidization. Academic Press Inc. 1971.

Demirbas A. Biomass resource facilities and biomass conversion processing for fuels and chemicals. Energy Conversion and Management 2001; 42:1357-78.

Demirbas A. Effects of temperature and particle size on bio-char yield from pyrolysis of agricultural residues. Journal of Analytical and Applied Pyrolysis 2004; 72:243-248.

Demirbas A., Demirbas M.F. Importance of algae oil as a source of biodiesel. Energy Conversion and Management 2011; 52:163-170.

Demirbas M.F. Biorefineries for biofuel upgrading: A critical review. Applied Energy 2009; 86: 151-161.

Demirbas M.F., Balat M. Biomass pyrolysis for liquid fuels and chemicals: A review. Journal of Scientific and Industrial Research 2007; 66:797-804.

Dhyani V., Bhaskar T. A comprehensive review on the pyrolysis of lignocellulosic biomass. Renewable Energy 2018; 129:695-716.

Duanguppama K., Suwapaet N., Pattiya A. Fast pyrolysis of contaminated sawdust in a circulating fluidised bed reactor. Journal of Analytical and Applied Pyrolysis 2016; 118:63-74.

Ellens C.J., Brown R.C. Optimization of a free-fall reactor for the production of fast pyrolysis bio-oil. Bioresource Technology 2012; 103:374-380.

Encinar J.M., González J.F., González J. Fixed bed pyrolysis of *Cynara cardunculus* L. Product yields and compositions. Fuel Processing Technology 2000; 68:209-222.

Estiati I., Tellabide M., Saldarriaga J.F., Altzibar H., Olazar M. Fine particle entrainment in fountain confined conical spouted beds. Powder Technology 2019; 344: 278-285

Fan H., He K. Fast Pyrolysis of Sewage Sludge in a Curie-Point Pyrolyzer: The Case of Sludge in the City of Shanghai, China. Energy and Fuels 2016; 30:1020-1026.

Farag S., Mudraboyina B.P., Jessop P.G., Chaouki J. Impact of the heating mechanism on the yield and composition of bio-oil from pyrolysis of kraft lignin. Biomass and Bioenergy 2016; 95:344-353.

Fernández J. Cardoon. Energy Plants Species. James James Sci. Publ. Ltd., 1998, London, pp. 113-117.

Fonts I., Azuara M., Gea G., Murillo M.B. Study of the pyrolysis liquids obtained from different sewage sludge. Journal of Analytical and Applied Pyrolysis 2009; 85:184-191.

Fonts I., Gea G., Azuara M., Ábrego J., Arauzo J. Sewage sludge pyrolysis for liquid production: A review. Renewable and Sustainable Energy Reviews 2012; 16:2781-2805.

Fonts I., Juan A., Gea G., Murillo M.B., Sánchez J.L. Sewage sludge pyrolysis in fluidized bed, 1: Influence of operational conditions on the product distribution. Industrial and Engineering Chemistry Research 2008; 47:5376-5385.

Fytili D., Zabaniotou A. Utilization of sewage sludge in EU application of old and new methods - A review. Renewable and Sustainable Energy Reviews 2008; 12:116–140.

Garg R., Anand N., Kumar D. Pyrolysis of babool seeds (Acacia nilotica) in a fixed bed reactor and bio-oil characterization. Renewable Energy 2016; 96:167-171.

Gauthier G., Melkior T., Grateau M., Thiery S., Salvador S. Pyrolysis of centimetre-scale wood particles: New experimental developments and results. Journal of Analytical and Applied Pyrolysis 2013; 104:521-530.

Geldart D. Types of gas fluidization. Powder Technology 1973; 7:285-292.

Gerçel H.F. The production and evaluation of bio-oils from pyrolysis of sunflower-oil cake. Biomass and Bioenergy 2002; 23:307-314.

Giuntoli J., de Jong W., Verkooijen A.H.M., Piotrowska P., Zevenhoven M., Hupa M. Combustion Characteristics of Biomass Residues and Biowastes: Fate of Fuel Nitrogen. Energy and Fuels 2010; 24:5309-5319.

Gollakota A.R.K., Kishore N., Gu S. A review on hydrothermal liquefaction of biomass. Renewable and Sustainable Energy Reviews 2018; 81:1378-1392.

Gómez-Hernández J., Soria-Verdugo A., Villa Briongos J., Santana D. Fluidized bed with a rotating distributor operated

under defluidization conditions. Chemical Engineering Journal 2012; 195-196:198-207.

Gominho J., Curt M.D., Lourenço A., Fernández J., Pereira H. Cynara cardunculus L. as a biomass and multi-purpose crop: A review of 30 years of research. Biomass and Bioenergy 2018; 109:257-275.

González J.F., Encinar J.M., Canito J.L., Rodríguez J.J. Pyrolysis of automobile tyre waste. Influence of operating variables and kinetics study. Journal of Analytical and Applied Pyrolysis 2001; 58-59:667-683.

Guedes R.E., Luna A.S., Rodrigues Torres A. Operating parameters for bio-oil production in biomass pyrolysis: A review. Journal of Analytical and Applied Pyrolysis 2018; 129:134-149.

Guizani C., Valin S., Billaud J., Peyrot M., Salvador S. Biomass fast pyrolysis in a drop tube reactor for bio oil production: Experiment and modeling. Fuel 2017; 207:71-84.

Günes M., Günes S.K. Distributed activation energy model parameters of some Turkish coals. Energy Sources Part A - Recovery Utilization and Environmental Effects 2008; 30:1460-1472.

Haron N.S., Zakaria J.H., Mohideen Batcha M.F. Recent advances in fluidized bed drying. IOP Conference Series: Materials Science and Engineering 2017

Heo H.S., Park H.J., Park Y.K., Ryu C., Suh D.J., Suh Y.W., Yim J.H., Kim S.S. Bio-oil production from fast pyrolysis of waste furniture sawdust in a fluidized bed. Bioresource Technology 2010; 101:91-96.

Higman C., van der Burgt M. Gasification. Gulf Professional Publishing, 1st Ed. 2003.

Horne P.A., Williams P.T. Influence of temperature on the products from the flash pyrolysis of biomass. Fuel 1996; 78:1051-1059.

Hu S., Jess A., Xu M. Kinetic study of Chinese biomass slow pyrolysis: Comparison of different kinetic models. Fuel 2007; 86:2778-2788.

Huang L., Liu J., He Y., Sun S., Chen J., Sun J., Chang K., Kuo J., Ning X. Thermodynamics and kinetics parameters of co-combustion between sewage sludge and water hyacinth in CO_2/O_2 atmosphere as biomass to solid biofuel. Bioresource Technology 2016; 218:631-642.

Isahak W.N.R.W., Hisham M. W.M., Yarmo M.A., Hin T.Y. A review on bio-oil production from biomass by using pyrolysis method. Renewable and Sustainable Energy Reviews 2012; 16:5910-5923.

Isemin R., Klimov D., Larina O., Sytchev G., Zaichenko V., Milovanov O. Application of torrefaction for recycling bio-waste formed during anaerobic digestion. Fuel 2019; 243:230-239.

Jaramillo-Arango A., Fonts I., Chejne F., Arauzo J. Product compositions from sewage sludge pyrolysis in a fluidized bed and correlations with temperature. Journal of Analytical and Applied Pyrolysis 2016; 121:287-296.

Jeong Y.W., Choi S.K., Choi Y.S., Kim S.J. Production of biocrude-oil from swine manure by fast pyrolysis and analysis of its characteristics. Renewable Energy 2015; 79:14-19.

Jia L., Dufour A., Brech Y.L., Authier O., Mauviel G. On-line analysis of primary tars from biomass pyrolysis by single photoionization mass spectrometry: Experiments and detailed modelling. Chemical Engineering Journal 2017; 313:270-282.

Johnsson F., Andersson S., Leckner B. Expansion of a freely bubbling fluidized bed. Powder Technology 1991; 68:117-123.

Kaliyaperumal S., Barghi S., Briens L., Rohani S., Zhu J. Fluidization of nano and sub-micron powders using mechanical vibration. Particuology 2011; 9: 279-287.

Kaminsky W., Kummer A.B. Fluidized bed pyrolysis of digested sewage sludge. Journal of Analytical and Applied Pyrolysis 1989; 16:27-35.

Kang B., Lee K.H., Park H.J., Park Y., Kim J. Fast pyrolysis of radiate pine in a bench scale plant with a fluidized bed: Influence of a char separation system and reaction conditions

on the production of bio-oil. Journal of Analytical and Applied Pyrolysis 2006; 76:32-37.

Kim S.W. Pyrolysis conditions of biomass in fluidized beds for production of bio-oil compatible with petroleum refinery. Journal of Analytical and Applied Pyrolysis 2016; 117:220-227.

Koppatz M., Pfeifer C., Hofbauer H. Comparison of the performance behavior of silica sand and olivine in a dual fluidized bed reactor system for steam gasification of biomass as a pilot plant scale. Chemical Engineering Journal 2011; 175:468-483.

Kunii D., Levenspiel O. Fluidization Engineering. Wiley, New York, 1969.

Leckner B. Developments in fluidized bed conversion of solid fuels. Thermal Science 2016; 20:S1-S18.

Leckner B. Fluidized bed combustion: Mixing and pollutant limitation. Progress in Energy Combustion Science 1998; 24:31-61.

Li G., Liu Z., Feng R., Jiao W., Fang Y., Wang Z. Conceptual design and analysis of a novel system based on ash agglomerating fluidized bed gasification for co-production of hydrogen and electricity. International Journal of Hydrogen Energy 2018; 43:1980-1988.

Li Z., Zhao W., Meng B., Liu C., Zhu Q., Zhao G. Kinetic study of corn straw pyrolysis: comparison of two different three-

pseudo component models. Bioresource Technology 2008; 99:7616–7622.

Lin T., Goos E., Riedel U. A sectional approach for biomass: Modelling the pyrolysis of cellulose. Fuel Processing Technology 2013; 115:246-253.

Lin Y., Liao Y., Yu Z., Fang S., Lin Y., Fan Y., Peng X., Ma X. Co-pyrolysis kinetics of sewage sludge and oil shale thermal decomposition using TGA-FTIR analysis. Energy Conversion and Management 2016, 118:345-352.

Liu G., Song H., Wua J. Thermogravimetric study and kinetic analysis of dried industrial sludge pyrolysis. Waste Management 2015; 41:128–133.

Lundberg L., Soria-Verdugo A., Pallarès D., Johansson R., Thunman H. The role of fuel mixing on char conversion in a fluidized bed. Powder Technology 2017; 316:677-686.

Luo Z., Wang S., Liao Y., Zhou J., Gu Y., Cen K. Research on biomass fast pyrolysis for liquid fuel. Biomass and Bioenergy 2004; 26:455-462.

Manara P., Zabaniotou A. Towards sewage sludge based biofuels via thermochemical conversion - A review. Renewable and Sustainable Energy Reviews 2012; 16:2566-2582.

Mani T., Murugan P., Abedi J., Mahinpey N. Pyrolysis of wheat straw in a thermogravimetric analyzer: effect of particle

size and heating rate on devolatilization and estimation of global kinetics. Chemical Engineering Research and Design 2010; 88:952-958.

Marcilla A., Catalá L., García-Quesada J.C., Valdés F.J., Hernández M.R. A review of thermochemical conversion of microalgae. Renewable and Sustainable Energy Reviews 2013; 27:11-19.

McKendry P. Energy production from biomass (part 2): conversion technologies. Bioresource Technology 2002; 83: 47-54.

Miura K. A new and simple method to estimate f(E) and $k_0(E)$ in the distributed activation energy model from three sets of experimental data. Energy and Fuels 1995; 9:302-307.

Miura K., Maki T. A simple method for estimating f(E) and $k_0(E)$ in the distributed activation energy model. Energy and Fuels 1998; 12:864-869.

Mohan D., Pittman C.U.Jr., Steele P.H. Pyrolysis of Wood/Biomass for Bio-oil: A Critical Review. Energy and Fuels 2006; 20:848-889.

Morato-Godino A., Sánchez-Delgado S., García-Hernando N., Soria-Verdugo A. Pyrolysis of *Cynara cardunculus* L. samples – Effect of operating conditions and bed stage on the evolution of the conversion. Chemical Engineering Journal 2018; 351:371-381.

Morin M., Nitsch X., Hémati M. Interactions between char and tar during the steam gasification in a fluidized bed reactor. Fuel 2018; 224:600-609.

Munir S., Daood S.S., Nimmo W., Cunliffe A.M., Gibbs B.M. Thermal analysis and devolatilization kinetics of cotton stalk, sugar cane bagasse and shea meal under nitrogen and air atmosphere. Bioresource Technology 2009; 100:1413-1418.

Nogués F.S., García-Galindo D., Rezeau A. Energía de la biomasa vol. 1. Prensas Universitarias de Zaragoza 2010.

Olazar M., Lopez G., Amutio M., Elordi G., Aguado R., Bilbao J. Influence of FCC catalyst steaming on HDPE pyrolysis product distribution. Journal of Analytical and Applied Pyrolysis 2009; 85:359-365.

Olukcu N., Yanik J., Saglam M., Yuksel M. Liquefaction of beypazari oil shale by pyrolysis. Journal of Analytical and Applied Pyrolysis 2002; 64:29-41.

Onay Ö., Beis S.H., Koçkar Ö.M. Fast pyrolysis of rape seed in a well-swept fixed-bed reactor. Journal of Analytical and Applied Pyrolysis 2001; 58:995-1007.

Ozbay N., Pütün A.E., Pütün E. Bio-oil production from rapid pyrolysis of cotton seed cake: product yields and compositions. International Journal of Energy Research 2006; 30:501-510.

Panwar N.L., Kothari R., Tyagi V.V. Thermo chemical conversion of biomass - Eco friendly energy routes. Renewable and Sustainable Energy Reviews 2012; 16:1801-1816.

Park E.S., Kang B.S, Kim J.S. Recovery of oils with high caloric value and low contaminant content by pyrolysis of digested and dried sewage sludge containing polymer flocculants. Energy and Fuels 2008; 22:1335-1340.

Park H.J., Heo H.S., Park Y.K., Yim J.H., Jeon J.K., Park J., Ryu C., Kim S.S. Clean bio-oil production from fast pyrolysis of sewage sludge: Effects of reaction conditions and metal oxide catalysts. Bioresource Technology 2010; 101:83-85.

Patel M., Zhang X., Kumar A. Techno-economic and life cycle assessment on lignocellulosic biomass thermochemical conversion technologies: A review. Renewable and Sustainable Energy Reviews 2016; 53:1486-1499.

Pattiya A., Suttibak S. Production of bio-oil via fast pyrolysis of agricultural residues from cassava plantations in a fluidized-bed reactor with a hot vapour filtration unit. Journal of Analytical and Applied Pyrolysis 2012; 95:227-235.

Piskorz J., Scott D.S., Westerberg I.B. Flash Pyrolysis of Sewage Sludge. Industrial and Engineering Chemistry Process Design and Development 1986; 25:265-270.

Pütün A.E., Apaydin E., Pütün E. Bio-oil production from pyrolysis and steam pyrolysis of soybean-cake: product yields and composition. Energy 2002; 27:703-713.

Reschmeier R., Roveda D., Müller D., Karl J. 2014. Pyrolysis kinetics of wood pellets in fluidized beds. Journal of Analytical and Applied Pyrolysis 2014; 108:117-129.

Rowe P.N., Nienow A.W. Particle Mixing and Segregation in Gas Fluidised Beds: A Review. Powder Technology 1976; 15:141-147.

Roy C., Chaala C., Darmstadt H. The vacuum pyrolysis of used tires: end-uses for oil and carbon black products. Journal of Analytical and Applied Pyrolysis 1999; 51:201-221.

Rulkens W. Sewage Sludge as a Biomass Resource for the Production of Energy: Overview and Assessment of the Various Options. Energy and Fuels 2008; 22:9-15.

Sahu S.G., Chakraborty N., Sarkar P. Coal–biomass co-combustion: An overview. Renewable and Sustainable Energy Reviews 2014; 39:575-586.

Samih S., Chaouki J. Development of a fluidized bed thermogravimetric analyzer. AIChE Journal 2015; 61:84-89.

Samolada M.C., Zabaniotou A.A. Comparative assessment of municipal sewage sludge incineration, gasification and pyrolysis for a sustainable sludge-to-energy management in Greece. Waste Management 2014; 34:411-420.

Sánchez-Prieto J., Soria-Verdugo A., Briongos J.V., Santana D. The effect of temperature on the distributor design in bubbling fluidized beds. Powder Technology 2014; 261:176-184.

Scott D.S., Piskorz J. The continuous flash pyrolysis of biomass. Canadian Journal of Chemical Engineering 1984; 62:404-412.

Sharma R., Sheth P.N. Thermo-Chemical Conversion of Jatropha Deoiled Cake: Pyrolysis vs. Gasification. International Journal of Chemical Engineering and Applications 2015; 6:376-380.

Shatalov A.A., Pereira H. Biorefinery of energy crop cardoon (Cynara cardunculus L.)-hydrolytic xylose production as entry point to complex fractionation scheme. Journal of Chemical Engineering Process and Technology 2011; 2:118-125.

Shen D.K., Gu S., Jin B., Fang M.X. Thermal degradation mechanisms of wood under inert and oxidative environments using DAEM methods. Bioresource Technology 2011; 102:2047-2052.

Shen J., Wang X., Garcia-Perez M., Mourant D., Rhodes M. J., Li C. Effect of particle size on the fast pyrolysis of oil mallee woody biomass. Fuel 2009; 88:1810-1817.

Shen L., Zhang D.K. An experimental study of oil recovery from sewage sludge by low-temperature pyrolysis in a fluidized-bed. Fuel 2003; 82:465-472.

Sonobe T., Worasuwannarak N. Kinetic analyses of biomass pyrolysis using the distributed activation energy model. Fuel 2008; 87: 414-421.

Soria-Verdugo A., Garcia-Gutierrez L.M., Blanco-Cano L., Garcia-Gutierrez N., Ruiz-Rivas U. Evaluating the accuracy of the Distributed Activation Energy Model for biomass devolatilization curves obtained at high heating rates. Energy Conversion and Management 2014; 86:1045-1049.

Soria-Verdugo A., García-Gutiérrez L.M., García-Hernando N., Ruiz-Rivas U. Buoyancy effects on objects moving in a bubbling fluidized bed. Chemical Engineering Science 2011a; 66:2833-2841.

Soria-Verdugo A., García-Gutiérrez L.M., Sánchez-Delgado S., Ruiz-Rivas U. Circulation of an object immersed in a bubbling fluidized bed. Chemical Engineering Science 2011b; 66:78-87.

Soria-Verdugo A., García-Hernando N., Almendros-Ibáñez J.A., García-Hernando U. Motion of a large object in a bubbling fluidized bed with a rotating distributor. Chemical Engineering and Processing 2011c; 50, 859-868.

Soria-Verdugo A., Garcia-Hernando N., Garcia-Gutierrez L.M., Ruiz-Rivas U. Analysis of biomass and sewage sludge

devolatilization using the distributed activation energy model. Energy Conversion and Management 2013, 65:239-244.

Soria-Verdugo A., Goos E., Garcia-Hernando N. Effect of the number of TGA curves employed on the biomass pyrolysis kinetics results obtained using the Distributed Activation Energy Model. Fuel Processing Technology 2015; 134:360-371.

Soria-Verdugo A., Goos E., Morato-Godino A., Garcia-Hernando N., Riedel U. Pyrolysis of biofuels of the future: Sewage sludge and microalgae – Thermogravimetric analysis and modelling of the pyrolysis under different temperature conditions. Energy Conversion and Management 2017b; 138:261-272.

Soria-Verdugo A., Morato-Godino A., Garcia-Gutierrez L. M., Garcia-Hernando N. Pyrolysis of sewage sludge in a fixed and a bubbling fluidized bed - Estimation and experimental validation of the pyrolysis time. Energy Conversion and Management 2017c; 144:235-242.

Soria-Verdugo A., Morato-Godino A., García-Gutiérrez L.M., García-Hernando N. Pyrolysis of sewage sludge in a bubbling fluidized bed: determination of the reaction rate, In: 12th International conference on fluidized bed technology (CFB 12), Krakow, Poland; 2017a.

Soustelle M. Handbook of Heterogenous Kinetics. John Wiley & Sons. London, 2010.

Stammbach M.R., Kraaz B., Hagenbucher R., Richarz W. Pyrolysis of sewage sludge in a fluidized bed. Energy and Fuels 1989; 3:255-259.

Strezov V., Moghtaderi B., Lucas J. Thermal study of decomposition of selected biomass samples. Journal of Thermal Analysis and Calorimetry 2003; 72:1041-1048.

Sun Y., Jin B., Wu W., Zuo W., Zhang Y., Zhang Y., Huang Y. Effects of temperature and composite alumina on pyrolysis of sewage sludge. Journal of Environmental Sciences 2015. 30:1-8.

Sun Y., Jin B.S., Huang Y.J., Zuo W., Jia J.Q., Wang Y.Y. Distribution and characteristics of products from pyrolysis of sewage sludge. Advanced Materials Research 2013; 726:2885-2893.

Tan Y.L., Abdullah A.Z., Hammed B.H. Fast pyrolysis of durian (Durio zibethinus L) shell in a drop-fixed bed reactor: Pyrolysis behavior and product analysis. Bioresource Technology 2017; 243:85-92.

Tonbul Y., Saydut A., Yurdako K., Hamamci C. A kinetic investigation on the pyrolysis of Seguruk asphaltite. Journal of Thermal Analysis and Calorimetry 2009; 95:197-202.

Torres C.M., Ríos S.D., Torras C., Salvadó J., Mateo-Sanz J.M., Jiménez L. Sustainability analysis of biodiesel production from Cynara cardunculus crop. Fuel 2013; 111:535-542.

Tsai W.T., Lee M.K., Chang Y.M. Fast pyrolysis of rice husk: product yields and compositions. Bioresource Technology 2007; 98:22-28.

Urych B., Smolinski A. Kinetics of sewage sludge pyrolysis and air gasification of its chars. Energy and Fuels 2016; 30:4869-4878.

Uzun B.B., Pütün A.E., Pütün E. Fast pyrolysis of soybean cake: Product yields and compositions. Bioresource Technology 2006; 97:569-576.

Vand V. A theory of the irreversible electrical resistance changes of metallic films evaporated in vacuum. Proceedings of the Physical Society 1943; 55:222-246.

Várghegyi G., Szabó P., Antal M.J. Kinetics of charcoal devolatilization. Energy and Fuels 2002; 16:724-731.

Villanueva-Chávez J.G., Bizzo W.A. Fluid dynamic modeling of a large bubbling fluidized bed for biomass combustion: Mass transfer in bubbles. Chemical Engineering Science 2019; 196: 414-424.

Wagenaar B.M., Prins W., Swaaij W.P.M. Pyrolysis of biomass in the rotating cone reactor: modelling and experimental justification. Chemical Engineering Science 1994; 49:5109-5126.

Wampler T.P. Applied Pyrolysis Handbook. Marcel Dekker, Inc, Nueva York. 1995.

Wang Q., Wang H., Sun B., Bai J., Guan X. Interactions between oil shale and its semi-coke during co-combustion. Fuel 2009; 88:1520-1529.

Wang X., Deng S., Tan H., Adeosun A., Vujanovic M., Yang F., Duic N. Synergetic effect of sewage sludge and biomass co-pyrolysis: A combined study in thermogravimetric analyzer and a fixed bed reactor. Energy Conversion and Management 2016b; 118:399-405.

Wang X., Zhao B., Yang X. Co-pyrolysis of microalgae and sewage sludge: biocrude assessment and char yield prediction. Energy Conversion and Management 2016a, 117:326-334.

Wanjun T., Cunxin W., Donghua C. Kinetic studies on the pyrolysis of chitin and chitosan. Polymer Degradation and Stability 2005; 87:389-394.

Williams A., Jones J.M., Ma L., Pourkashanian M. Pollutants from the combustion of solid biomass fuels. Progress in Energy and Combustion Science 2012; 38:113-137.

Xiu S., Shahbazi A. Bio-oil production and upgrading research: A review. Renewable and Sustainable Energy Reviews 2012; 16:4406-4414.

Xu R., Ferrante L., Briens C., Berruti F. Flash pyrolysis of grape residues into biofuel in a bubbling fluid bed. Journal of Analytical and Applied Pyrolysis 2009; 86:58-65.

Yaman S. Pyrolysis of biomass to produce fuels and chemical feedstocks. Energy Conversion and Management 2004; 45:651-671.

Yan J.H., Zhu H.M., Jiang X.G., Chi Y., Cen K.F. Analysis of volatile species kinetics during typical medical waste materials pyrolysis using a distributed activation energy model. Journal of Hazardous Materials 2009; 162:646-651.

Yan Q., Toghiani H., Yu F., Cai Z., Zhang J. Effects of pyrolysis conditions on yield of bio-chars from pine chips. Forest Products Journal 2011; 61:367-371.

Yang X., Zhang R., Fu J., Geng S., Cheng J.J., Sun Y. Pyrolysis kinetic and product analysis of different microalgal biomass by distributed activation energy model and pyrolysis-gas chromatography-mass spectrometry. Bioresource Technology 2014; 163:335-342.

Zeng K., Minh D.P., Gauthier D., Weiss-Hortala E., Nzihou A., Flamant G. The effect of temperature and heating rate on char properties obtained from solar pyrolysis of beech wood. Bioresource Technology 2015; 182:114-119.

Zhang H., Degrève J., Baeyens J., Wu S.Y. Powder attrition in gas fluidized beds. Powder Technology 2016; 287:1-11.